er number: : .....
al number: .....

People's Democratic Republic of Algeria

Ministry of Higher Education and Scientific Research

University of El Oued

Faculty of Exact Sciences

Department of Chemistry

Submitted in partial fulfillment of the Requirements for the degree of Professional Master's

Field: Chemistry

Specialization: Analytical Chemistry

Prepared by:

Mennai Kods and Medaoui Latra

THESIS TITLE

Applicability of Gypsum for Enhanced Dye Removal: Structural Characterization, Equilibrium, Kinetics, and Adsorption Mechanism.

Defended on: June 07, 2026

Before the Examination Committee:

Pr. Mahboub Mohammed Sadok	President	El Oued University
Pr. Haddad Larbi	Examiner	El Oued University
Pr. Zobeidi Ammar	Supervisor	El Oued University

Academic year: 2025–2026


بسم الله الرحمن الرحيم

Acknowledgements

In the name of Allah, the Most Gracious, the Most Merciful All praise and gratitude are due to Allah, whom we thank for granting us strength, patience, and guidance throughout the completion of this work. We pray that this effort may be beneficial and blessed. With deep feelings of loyalty and respect, we dedicate our first words to the memory of the late Dr. Atia Djamal, may Allah have mercy upon him. His scientific and human legacy remains alive in our hearts, and his honorable memory and noble contributions will forever be remembered. May Allah reward him abundantly and grant him eternal peace. We would like to express our sincere gratitude to our supervisor, Prof. Zobeidi Ammar, for his valuable guidance, continuous support, and dedicated supervision, which played a significant role in the accomplishment of this thesis. Our heartfelt thanks are also extended to the members of the examination committee, Prof. Haddad Larbi and Prof. Mahboub Mohammed Sadok, for accepting to examine this work and for their valuable academic remarks and contributions. We would also like to express our appreciation to the professors of the Chemistry Department and to the staff and officials of the chemistry laboratories for their cooperation and assistance. Special thanks are addressed to Sheikh Taliba Ali in recognition of his generosity, kindness, and willingness to share his knowledge and guidance without hesitation, as he was a valuable source of support throughout this journey. Finally, we extend our sincere thanks to everyone we have known and to all those who contributed, directly or indirectly, to the completion of this work. We pray for success and blessings for all.

Dedication

Dedication In the name of Allah, the Most Gracious, the Most Merciful. All praise is due to Allah, by whose grace good deeds are accomplished, and who granted me the strength and guidance to complete this humble work. To Him belongs all praise, first and last. I dedicate this humble work ,

the fruit of effort and perseverance,

To myself, who remained patient, worked hard, and never gave up despite all difficulties. I dedicate this achievement as a source of pride for what has been accomplished and as hope for what lies ahead .

To my beloved parents, you are my first support and the source of my strength after Allah. Through your prayers and love, my dreams have grown. May Allah protect you and keep you as a blessing in my life .

To my beloved mothers, you are the warmth of my heart and the sincerity of every prayer. My deepest love and gratitude go to you both. May Allah preserve you and grant me your everlasting satisfaction.

To my dear siblings: ♕ A, M, I, W, H, S, Gh, Y ♕ Thank you for your love and continuous support. I dedicate this work to you as a token of loyalty and appreciation.

To my supervisor, Professor Zobeidi Ammar, with all respect and gratitude, I sincerely thank him for his valuable guidance, patience, and scientific supervision, which greatly contributed to the completion of this work .

And to a person whose presence made this journey different... His sincere support and reassuring presence were woven into the details of this work, easing the difficulties and making this achievement even more meaningful. Destiny willed that this companionship would not remain merely a memory of the road, but would grow into a story adorned with mutual respect and cherished by the most beautiful wishes. Words cannot fully express my loyalty and gratitude to him... ♡ Taha ♡

To my friend and partner in accomplishing this work, ♕ Medaoui Latra ♕, Thank you for sharing both the hardships of the journey and the joy of success. May Allah always keep between us affection, friendship, and success .

To my dear friends, Thank you for your kindness, support, and encouraging words. I wish you all the happiness and success in the world.

M. Kods

Dedication

Dedication To those through whom I rise, and to whom I dedicate the fruit of my perseverance: To my beloved parents, my support and the crown upon my head: You instilled in me the love of knowledge and sacrificed countless nights to see this day come true. Words can never fully express my gratitude for your endless love, support, and prayers, which have always been my source of strength and guidance. Thank you for believing in me and for being the finest example of generosity, patience, and dedication. To my siblings and family: You have always been my safe harbor throughout this journey. Thank you for your constant encouragement, your unwavering support, and for giving me the strength to continue whenever challenges arose. To my esteemed supervisor, Professor Ammar Zobeidi: I extend my sincere appreciation and gratitude for your valuable guidance, continuous support, and academic advice. Your mentorship greatly enriched this work and helped shape it into an achievement of which I am truly proud. My thanks also go to all my respected professors who enlightened my path throughout my academic journey. To the one who holds a special place in my heart: To the companion whose presence accompanied me through long hours of study and research, and who was a constant source of motivation and support, thank you for being there throughout this journey. To my lifelong friend, Mennai Kods: The sister my mother never gave birth to, my companion in life and in this academic journey. Thank you for being the shoulder I could always lean on, for sharing both the hardships and the joys of this experience. This achievement belongs not only to me but also to two souls united by the same dream and aspiration. To my friends and classmates: Thank you for every discussion, every shared experience, and every memory created throughout our university years. Your companionship transformed our academic journey into a beautiful and unforgettable chapter of life. To everyone who shared this journey with me, whether near or far: To every kind soul, every sincere word, and everyone who supported me through actions, encouragement, or prayers, thank you for being part of this accomplishment. Each of you holds a special place in my heart. To every helping hand extended to me along the way: I dedicate to you the fruit of my efforts and this humble achievement.

M. Latra

Abstract

This study investigated the use of waste gypsum (GS) as a low-cost adsorbent for the removal of Crystal Violet (CV) dye from aqueous solutions. The adsorbent was characterized using XRD, FTIR, and SEM-EDX techniques. The characterization results confirmed the crystalline nature of gypsum and the successful adsorption of dye molecules onto its surface. Furthermore, a Box–Behnken Design (BBD) based on Response Surface Methodology (RSM) was employed to evaluate the influence of the main operating parameters on the adsorption performance. The results revealed that the maximum removal efficiency reached 95.30% under the optimum conditions of 2 g adsorbent dosage, pH 10, temperature of 45 °C, and contact time of 25 min. The adsorption kinetics were best described by the pseudo-second-order (PSO) model, while the Freundlich isotherm provided the best fit to the equilibrium data. In contrast, the Langmuir isotherm estimated a maximum monolayer adsorption capacity of 8.43 mg/g at 45 °C. Thermodynamic studies indicated that the adsorption process was spontaneous and endothermic. The proposed adsorption mechanism involved multiple interactions, including electrostatic interactions, n–π interactions, and hydrogen bonding. These findings highlight the potential of GS as an effective and eco-friendly adsorbent for wastewater treatment, contributing to waste valorization and environmental sustainability.

Keywords: Waste gypsum; Crystal Violet dye; Adsorption; Box–Behnken design; Kinetics; Equilibrium isotherms

الملخص :

تندرج هذه الدراسة في إطار استخدام مخلفات جبس (GS) كممتز منخفض التكلفة لإزالة صبغة كريستال البنفسجي (CV)من المحاليل المائية. تم توصيف المادة المازة باستخدام تقنيات XRD ، FTIR و SEM-EDX . أكدت نتائج التوصيف الطبيعة البلورية للجبس ونجاح امتزاز جزيئات الصبغة على سطحه. علاوة على ذلك، تم استخدام تصميم–Box Behnken (BBD)المعتمد على منهجية سطح الاستجابة (RSM) لتقييم تأثير معاملات التشغيل الرئيسية على أداء الامتزاز. أظهرت النتائج أن أقصى كفاءة إزالة بلغت 95.30% تحت الظروف المثلى: كمية المادة المُمتزة 2g ، درجة الحموضة10 = pH ، درجة حرارة 45°C، وزمن تلامس 25 min . تم وصف حركيات الامتزاز بشكل أفضل بنموذج pseudo-second-order (PSO)، بينما قدم نموذج Freundlich أفضل توافق مع بيانات التوازن. في المقابل، قدر نموذج Langmuir سعة امتزاز أحادية الطبقة بحد أقصى 8.43mg/g عند 45 درجة مئوية. أشارت الدراسات الديناميكية الحرارية إلى أن عملية الامتزاز كانت تلقائية وماصة للحرارة. تضمنت آلية الامتزاز المقترحة تفاعلات متعددة، منها التجاذب الإلكتروستاتيكي، وتفاعلاتn–π ، والروابط الهيدروجينية. تُبرز هذه النتائج إمكانات الجبس كمادة ماصة فعالة وصديقة للبيئة لمعالجة مياه الصرف الصحي، مما يُسهم في إعادة تدوير النفايات وتحقيق الاستدامة البيئية.

الكلمات المفتاحية: جبس النفايات؛ صبغة الكريستال البنفسجي؛ الامتزاز؛ تصميم بوكس–بينكن؛ حركية الامتزاز؛ متساويات الحرارة .

Résumé

Cette étude a examiné l'utilisation du gypse résiduaire (GS) comme adsorbant à faible coût pour l'élimination du colorant Cristal Violet (CV) des solutions aqueuses. L'adsorbant a été caractérisé par les techniques XRD, FTIR et SEM-EDX. Les résultats de caractérisation ont confirmé la nature cristalline du gypse et l'adsorption réussie des molécules de colorant à sa surface. De plus, un plan de Box–Behnken (BBD) basé sur la méthodologie des surfaces de réponse (RSM) a été utilisé pour évaluer l'influence des principaux paramètres opératoires sur les performances d'adsorption. Les résultats ont révélé que l'efficacité d'élimination maximale atteignait 95,30 % dans les conditions optimales suivantes : dose d'adsorbant de 2 g, pH 10, température de 45 °C et temps de contact de 25 minutes. La cinétique d'adsorption était mieux décrite par le modèle pseudo-second ordre (PSO), tandis que l'isotherme de Freundlich fournissait le meilleur ajustement aux données d'équilibre. En revanche, l'isotherme de Langmuir a estimé une capacité d'adsorption maximale en monocouche de 8,43 mg/g à 45 °C. Les études thermodynamiques ont indiqué que le processus d'adsorption était spontané et endothermique. Le mécanisme d'adsorption proposé impliquait de multiples interactions, y compris des interactions électrostatiques, des interactions n–π et des liaisons hydrogène. Ces résultats mettent en évidence le potentiel du gypse comme adsorbant efficace et respectueux de l'environnement pour le traitement des eaux usées, contribuant ainsi au recyclage des déchets et à la durabilité environnementale.

Mots-clés : Gypse résiduaire ; Colorant Cristal Violet ; Adsorption ; Plan de Box–Behnken ; Cinétique ; Isotherme d'équilibre.

List of symbols and abbreviations

Symbol	Abbreviations
ΔG°	Change in free energy
ΔH°	Change in enthalpy
ΔS°	Change in entropy
ε	Polani factor
ANOVA	Analysis of variance
BBD	Box Behnken design
C0	Box Behnken design
CCD	Central Composite Design
CV	Crystal Violet
EDX	Energy Dispersive X-ray Spectroscopy
FTIR	Fourier Transform Infrared
GS	Gypsum
K	Number of factors
Kf	Freundlich constant
KL	Langmuir constant
Ks	Equilibrium link constant
MW	Molecular Weight
pH H	ydrogen Potential
PFO	Pseudo First Order
PSO	Pseudo Second Order
q_e	Adsorption capacity at equilibrium
qmax	Maximum adsorption capacity
q°	Adsorption capacity at time t
R	Perfect gas constant
R^2	Linearity factor
RSM	Response Surface Methodology
SEM	Scanning Electron Microscope

t	Time of contact
T	Solution Volume
XRD	X-ray Diffraction
Y	Continuous response

List of tables

List of figures

Table of Contents

Chapter III: Materials and Methods

Chapter IV : Results and Discussion

General Introduction

General Introduction

Among the major sources of water contamination are industrial effluents from textile, paper, leather, plastics, and cosmetics industries [1]. Wastewater volume is forecast to increase by 24% by 2030 (>470 billion m^3) and by 51% by 2050 (~574 billion m^3) [2]. These effluents contain large amounts of synthetic dyes [3], which are widespread pollutants due to their high chemical stability and resistance to degradation. Dyes reduce light penetration, limiting photosynthesis in aquatic ecosystems, and are classified as anionic, cationic, or nonionic[4].

Crystal Violet (CV) is one of the most commonly used cationic dyes in textile dyeing, printing, paper coloration, and ink manufacturing industries. However, its discharge into aquatic environments represents a serious environmental and health concern because of its toxicity, persistence, and low biodegradability, making its removal from wastewater a necessity before discharge into natural water bodies [5].

Several treatment technologies have been developed for the removal of dyes from contaminated wastewater, including chemical oxidation, coagulation flocculation, membrane filtration, biological treatment, photocatalytic degradation, and ion exchange processes [6]. Although some of these techniques are effective, many suffer from high operational costs, complex equipment requirements, or the generation of secondary pollutants that may create additional environmental problems [7]. Consequently, adsorption has gained considerable attention over recent decades as one of the most efficient and practical methods for removing organic contaminants from aqueous solutions. This technique offers several advantages, including operational simplicity, high removal efficiency, and the possibility of using inexpensive and naturally abundant adsorbent materials [8]. In this context, scientific research has increasingly focused on the utilization of naturally available materials as economical and sustainable alternatives to conventional adsorbents. Among these materials, natural gypsum has attracted considerable interest.

Gypsum (GS) is a widely distributed sedimentary mineral primarily composed of hydrated calcium sulfate ($CaSO_4 \cdot 2H_2O$). It is characterized by its natural abundance, low cost, and favorable physicochemical properties, which make it suitable for various environmental applications [9]. Several recent studies have demonstrated the potential of natural gypsum for the removal of different pollutants from aqueous media, including dyes and heavy metals, owing to the presence of active surface sites and its ability to interact with pollutant molecules through various adsorption mechanisms [10].

Previous investigations have also shown that the adsorption performance of gypsum is significantly influenced by operational parameters such as pH, adsorbent dosage, contact time, temperature, and pollutant concentration. Therefore, optimization of these factors is essential to achieve maximum adsorption efficiency [11]. With the growing development of experimental design and process optimization techniques in environmental engineering, Response Surface Methodology (RSM) has become one of the most widely used statistical tools in adsorption studies. This methodology allows the evaluation of both individual and interactive effects of different variables while minimizing the number of experimental runs required to determine optimal operating conditions [12]. Among the available experimental designs, the Box–Behnken Design (BBD) is particularly popular due to its efficiency and reliability in modeling multivariable systems [13].

Considering the urgent need for low-cost and environmentally friendly adsorbents for wastewater treatment, the present study aims to evaluate the applicability of natural gypsum as an adsorbent for the removal of CV dye from aqueous solutions. The adsorbent material was characterized using several analytical techniques, including Xray diffraction (XRD), Fourier-transform infrared spectroscopy (FT-IR), and scanning electron microscopy coupled with energy-dispersive X-ray analysis (SEM–EDX), in order to investigate its crystalline structure, surface properties, and elemental composition. In addition, RSM based on the BBD was employed to investigate and optimize the main operational parameters affecting the adsorption process, namely adsorbent dosage, solution pH, temperature, and contact time. Furthermore, adsorption behavior was evaluated through kinetic, equilibrium, and thermodynamic studies to better understand the nature of the adsorption process and identify the mechanisms governing dye uptake. Based on the physicochemical characterization results, a possible adsorption mechanism of CV dye onto the surface of waste gypsum (GS) was also proposed.

This research is organized into four main chapters:

- Literature Review - Examines recent 15 year studies on natural gypsum as an adsorbent for pollutant removal, highlighting key findings and developments.

- Bibliographic Research- Covers theoretical background: dye classification, adsorption models and mechanisms, properties of natural gypsum, and an overview of RSM for adsorption optimization.

- Materials and Experimental Methods - Describes chemicals, materials, instruments, and the batch adsorption methodology using natural gypsum.

- Results & Discussion - Presents findings with comparative analysis and concludes with key outcomes and future research directions.

- The work concludes with a general summary of key outcomes and recommendations for future work.

Bibliography

[1] R. Connor, The United Nations World Water Development Report 2015: Water for a Sustainable World, vol. 1. Paris, France: UNESCO Publishing, 2015.

[2] A. Kumar, Environmental Toxicology and Ecosystem. Boca Raton, FL, USA: CRC Press, 2022.

[3] H. B. Slama, A. Chenari Bouket, Z. Pourhassan, F. N. Alenezi, A. Silini, H. Cherif-Silini, et al., "Diversity of Synthetic Dyes from Textile Industries, Discharge Impacts and Treatment Methods," Applied Sciences, vol. 11, p. 6255, 2021.

[4] S. S. Affat, "Classifications, Advantages, Disadvantages, Toxicity Effects of Natural and Synthetic Dyes: A Review," University of Thi-Qar Journal of Science, vol. 8, pp. 130–135, 2021.

[5] A. Mittal, J. Mittal, A. Malviya, D. Kaur, and V. Gupta, "Adsorption of Hazardous Dye Crystal Violet from Wastewater by Waste Materials," Journal of Colloid and Interface Science, vol. 343, pp. 463–473, 2010.

[6] S. S. Beulah and K. Muthukumaran, "Methodologies of Removal of Dyes from Wastewater: A Review," International Research Journal of Pure and Applied Chemistry, vol. 21, pp. 68–78, 2020.

[7] V. K. Gupta, "Application of Low-Cost Adsorbents for Dye Removal: A Review," Journal of Environmental Management, vol. 90, pp. 2313–2342, 2009.

[8] G. Crini, "Non-Conventional Low-Cost Adsorbents for Dye Removal: A Review," Bioresource Technology, vol. 97, pp. 1061–1085, 2006. [9] M. J. Hassan, M. F. Islam, N. Akter, M. N. Uddin, A. Y. Abir, S. B. Aoun, et al., "Applicability of Gypsum in Selective Removal of Anionic Dye Molecules from Aqueous Medium," Applied Water Science, vol. 11, p. 7, 2021.

[10] F. Deniz and S. D. Saygideger, "Investigation of Adsorption Characteristics of Basic Red 46 onto Gypsum: Equilibrium, Kinetic and Thermodynamic Studies," Desalination, vol. 262, pp. 161–165, 2010.

[11] S. Karimifard and M. R. A. Moghaddam, "Application of Response Surface Methodology in Physicochemical Removal of Dyes from Wastewater: A Critical Review," Science of the Total Environment, vol. 640, pp. 772–797, 2018.

[12] R. H. Myers and D. C. Montgomery, Response Surface Methodology. London, U.K.: Taylor & Francis, 1996.

[13] D. C. Montgomery, Design and Analysis of Experiments. Hoboken, NJ, USA: John Wiley & Sons, 2017.

Chapter I :
Literature Review

I.1 Background

Water pollution, mainly from textile and dye industries, is a critical global issue. These industries release wastewater containing stable, complex organic dyes that resist biodegradation and conventional treatment. Dyes in water reduce light penetration, disrupt photosynthesis in aquatic plants, and pose toxic and carcinogenic risks to living organisms and humans [1, 2].

In response to these challenges, various techniques (chemical oxidation, precipitation, membrane filtration, biological treatment) have limitations in cost, efficiency, or complexity. Adsorption is superior due to its simplicity, ease of use, and effectiveness even at low pollutant concentrations [3]. Although activated carbon is widely used, its high cost and difficult regeneration have driven the search for lowcost natural alternatives [4].

Gypsum (calcium sulfate dihydrate, **($CaSO_4 \cdot 2H_2O$)** is an abundant, low-cost natural material, particularly in developing countries. Its stable crystalline structure provides active sites for dye molecule interactions [5]. Additionally, gypsum possesses favorable adsorption properties, including porosity and the ability to form weak bonds with pollutants through electrostatic interactions and van der Waals forces [6].

The effectiveness of gypsum as an adsorbent depends on operational factors such as pH, temperature, initial dye concentration, and contact time. These factors directly influence the interaction between the gypsum surface and dye molecules. For instance, pH determines the surface charge of gypsum, thereby affecting electrostatic attraction with dye molecules [7].

Adsorption behavior is analyzed using isotherm models: the Langmuir isotherm (monolayer adsorption on homogeneous surfaces) and the Freundlich isotherm (adsorption on heterogeneous surfaces) [8]. Kinetic studies use pseudo-first-order and pseudo-second-order models to explain adsorption rate, mechanism, and whether the process is governed by physical diffusion or chemical interactions [9]. These models are essential graphical tools for interpreting adsorption behavior and evaluating adsorbent efficiency in applied water treatment studies.

According to data from Science Direct, there has been a significant increase in the number of scientific publications related to the use of gypsum for pollution removal during 2010–2026, with more than 20,000 articles and books published worldwide on adsorption using this material

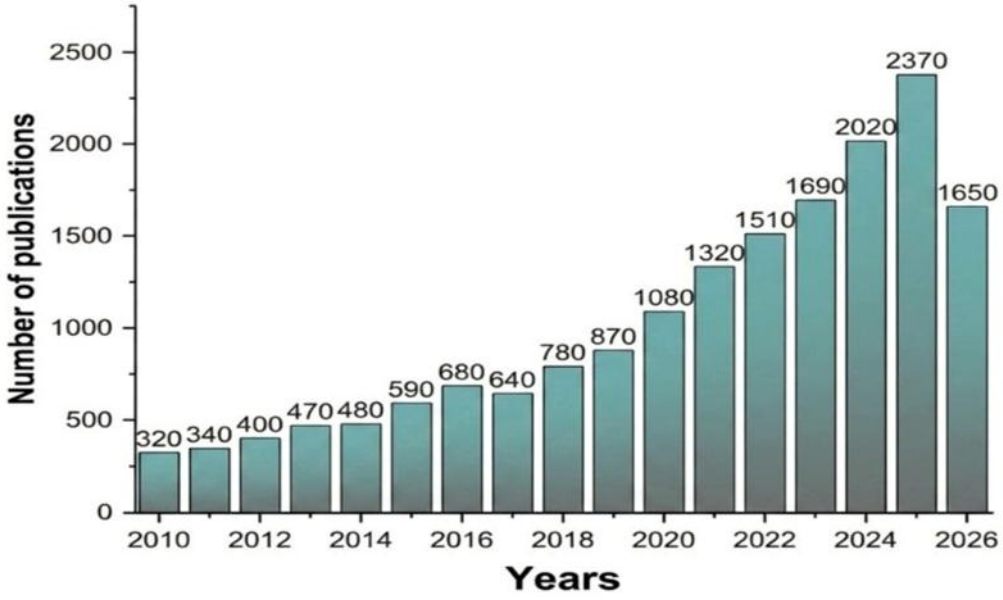

Figure I.1. The number of publications (2010-2026) on gypsum for adsorption applications according to data taken from Web of Science and Scopus-indexed journals.

I.2 Previous Studies

In recent years, increasing attention has been directed toward the use of natural and low-cost materials for the adsorption of organic dyes from wastewater. Among these materials, gypsum has emerged as a promising adsorbent because of its availability, low cost, porous structure, and environmental compatibility. Several scientific studies have investigated the adsorption behavior of different dyes on gypsum under various experimental conditions.

A 2010 study investigated the use of natural gypsum as a low-cost adsorbent for the removal of Basic Red 46 (BR46) dye from aqueous solutions. Adsorption experiments were conducted in batch mode, studying the effect of several factors such as pH, contact time, temperature, and initial dye concentration. The results showed that the best adsorption conditions were at pH = 8, an initial dye concentration of 60 mg/L, a temperature of 50°C, and a contact time of 60 minutes. The kinetic study showed that the adsorption process follows the Pseudo-second-order model, indicating that the adsorption rate depends on the interactions between the dye molecules and the active sites on the gypsum surface. Regarding the isotherm, the adsorption fitted well with the Langmuir model, indicating the formation of a dye monolayer on the adsorbent surface, with a maximum adsorption capacity of about 39.17mg/g. The thermodynamic study also clarified that the adsorption process is spontaneous and feasible through negative Gibbs free energy values, with adsorption improving with increasing temperature, indicating that the procesis endothermic in nature. The results confirmed that

gypsum can represent an effective and economical adsorbent for treating industrial wastewater containing dyes [10].

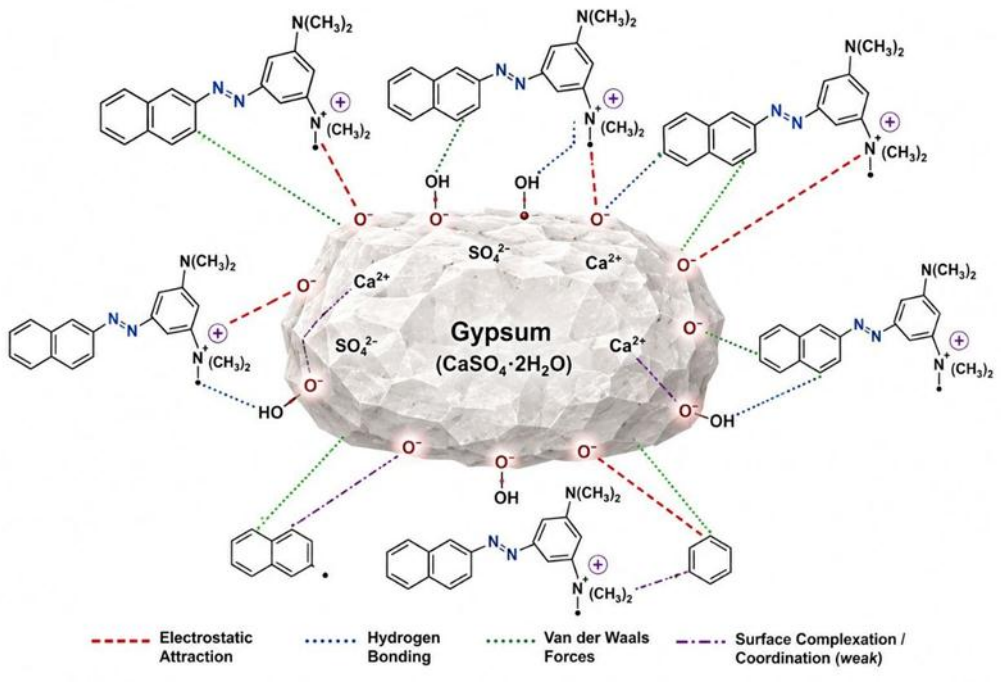

Figure I.2. Adsorption Mechanism of Basic Red 46 Dye on Gypsum Surface ($CaSO_4 \cdot 2H_2O$) [10]

A 2012 Study, Obunwo et al. investigated the adsorption of Reactive Red 1 using gypsum as an adsorbent in batch experiments at ambient temperature. The results showed that the optimum adsorption conditions were pH = 2, contact time of 25–35 min, and adsorbent dosage of 0.8 g using acid-treated gypsum with a particle size of 150 µm. Under these conditions, a removal efficiency of 89.8% was achieved. The study also revealed that the smaller particle size enhanced adsorption due to the larger surface area. The adsorption data fitted both Langmuir and Freundlich isotherm models, indicating favorable adsorption behavior, while the pseudo-second-order kinetic model demonstrated that chemisorption was the controlling mechanism of the process (R2 > 0.99). Thermodynamic parameters and adsorption capacity values were not explicitly reported in the paragraph [11].

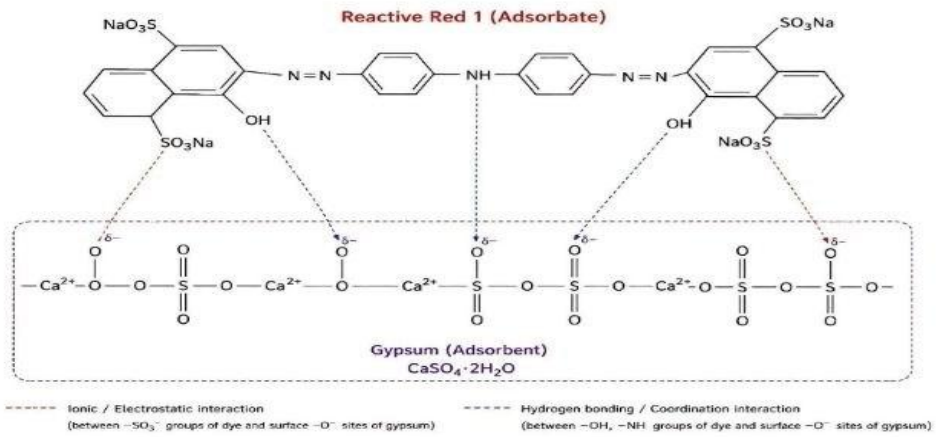

Figure I.3. Schematic representation of the adsorption mechanism of Reactive Red 1 onto gypsum [11]

In a 2013 study, the adsorbent material was gypsum and ceiling tiles, while the adsorbate was formaldehyde gas. The experiments were conducted inside a 48 m^3 stainless steel test chamber under controlled climatic conditions of temperature, humidity, and ventilation, with monitoring of changes in formaldehyde concentrations in the indoor air. The results showed that gypsum boards possess a significant capacity to adsorb formaldehyde and then re-emit it gradually, which directly affects indoor air quality. It was also found that adsorption is affected by humidity, temperature, and air exchange rate, and that the final formaldehyde concentrations result from the cumulative effect of all building materials present inside the room, not from a single material. The study indicated a clear adsorption/desorption phenomenon [12].

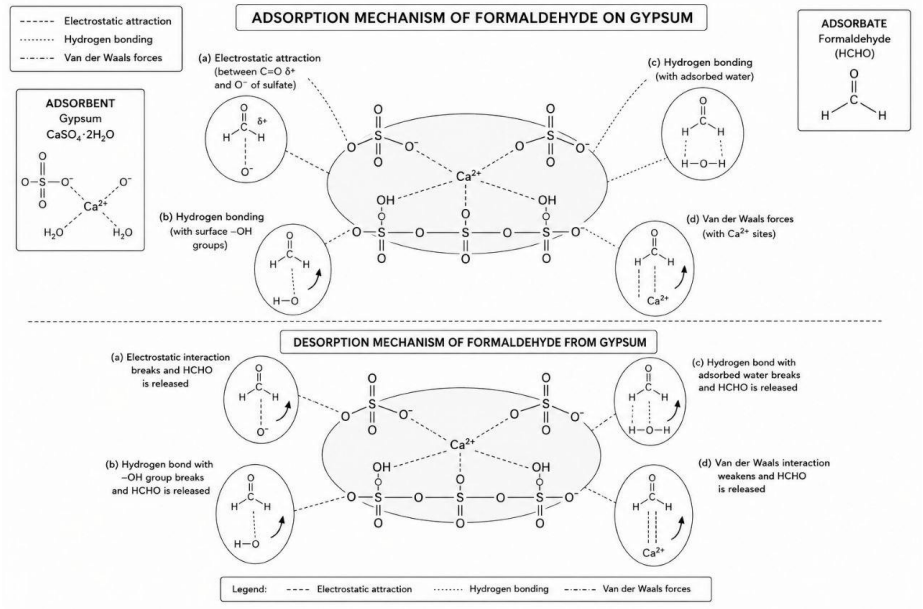

Figure I.4. Schematic Illustration of Formaldehyde Adsorption and Desorption Mechanisms on Gypsum Board [12]

A 2014 study relied on the use of commercial gypsum (CG) and secondary industrial gypsum resulting from the phosphoric acid industry (IG) as an adsorbent for the removal of lead (Pb^{2+}) and cadmium (Cd^{2+}) ions from aqueous solutions. The adsorbates were lead and cadmium, while gypsum in its commercial and industrial forms was used as the adsorbent without complex treatment. Adsorption experiments were conducted under ambient conditions for 24 hours, monitoring the pH change during the reaction. The results showed that lead adsorption was very fast, with more than 99% of Pb^{2+} removed using commercial gypsum, while industrial gypsum achieved significant removal reaching approximately 550 $mg \cdot g^{-1}$ as an adsorption capacity for lead. As for cadmium, the adsorption capacity reached about 144–150 $mg \cdot g^{-1}$ with a removal rate close to 44–46%. The study also indicated that equilibrium was reached after 24 hours for lead and after about 3 hours for cadmium. When Pb^{2+} and Cd^{2+} were present together in the same medium, lead was preferentially adsorbed on the gypsum surface, while cadmium adsorption decreased significantly due to competition for active sites. The study clarified that the removal mechanism mainly relied on surface adsorption with the possibility of surface precipitation of a $PbSO_4$ compound. FTIR analyses also indicated changes in the arrangement of sulfate groups on the gypsum surface after adsorption, but it focused on adsorption capacity, competition between ions, and the fixation mechanism on the gypsum surface [13].

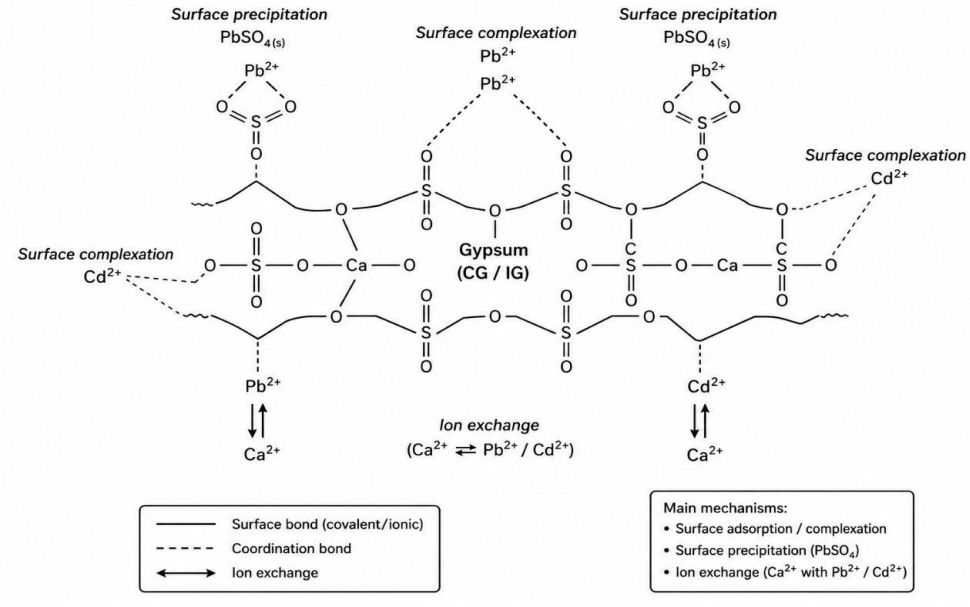

Figure I.5. Proposed Mechanism of Pb^{2+} and Cd^{2+} Adsorption onto Commercial and Industrial Gypsum Surfaces [13]

Meanwhile, a 2015 study used Flue Gas Desulfurization gypsum (FGD Gypsum) as a low-cost adsorbent for the removal of lead Pb(II) and cadmium Cd(II) ions from aqueous solutions. The

adsorbent was prepared by washing, drying, and grinding the gypsum to obtain a fine powder. TCLP toxicity tests showed that the gypsum is relatively safe and can be reused environmentally. The study demonstrated that the adsorption process was significantly related to pH, with the best adsorption efficiency achieved at pH ranging from 5 to 7 for both metals. The results also showed that the adsorption of Pb(II) and Cd(II) followed the Pseudo-second-order kinetic model, indicating that surface chemical interaction controls the adsorption process, noting that lead had a higher adsorption rate than cadmium. As for the isotherm, the results fitted well with the Langmuir model, indicating the formation of a monolayer of ions on the gypsum surface. The study confirmed that the adsorption process is spontaneous and thermodynamically favorable, with thermodynamic parameters showing that increasing temperature increases removal efficiency, meaning the process is endothermic and occurs spontaneously. The adsorbent also recorded high adsorption capacities compared to some artificially prepared materials, highlighting the effectiveness of FGD gypsum as an economical and effective material for treating water contaminated with heavy metals [14].

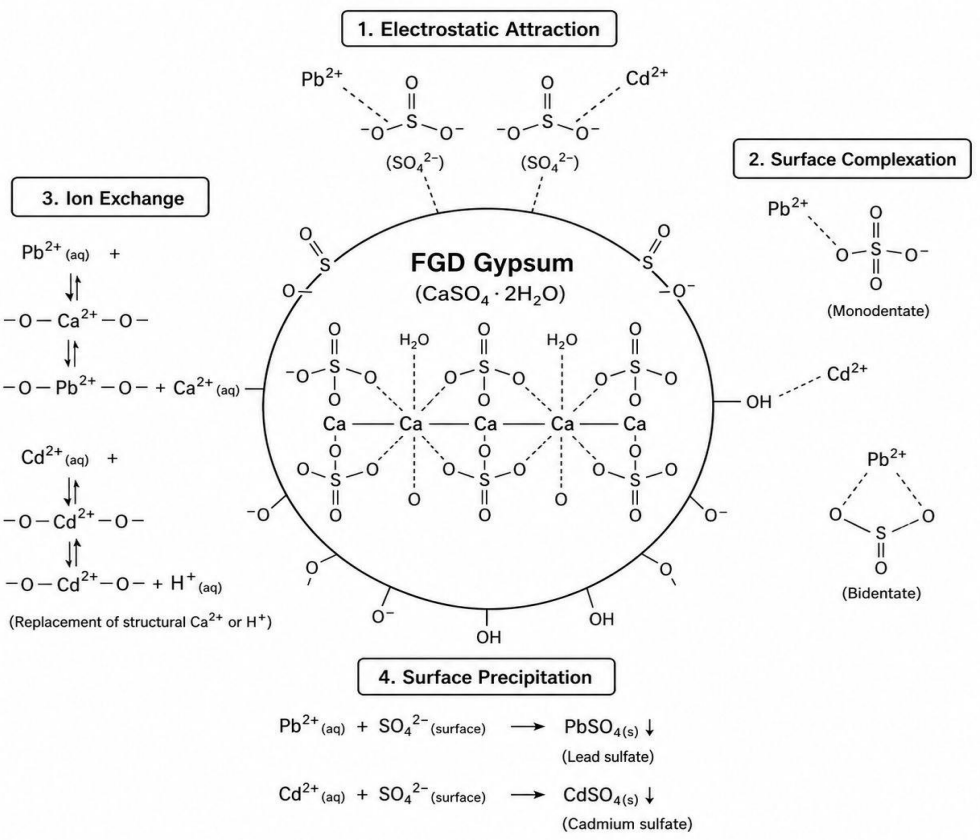

Figure I.6. Schematic Illustration of Pb(II) and Cd(II) Adsorption Mechanisms on FGD Gypsum ($CaSO_4 \cdot 2H_2O$) [14]

A 2017 Study Wenyi et al. investigated the removal of Disperse Blue 165 from aqueous solutions using chitosan and phosphogypsum as low-cost adsorbents. The results showed that the

optimum contact time was 60 min for chitosan and 30 min for phosphogypsum. The adsorption data fitted the Langmuir isotherm model, with maximum adsorption capacities of 103.09 mg/g for chitosan and 6.79 mg/g for phosphogypsum. The kinetic study revealed that the adsorption process followed the pseudo-first-order model. Ther-modynamic parameters were also evaluated. The findings demonstrated that chitosan was more efficient, whereas phosphogypsum represented an economical alternative for textile wastewater treatment [15].

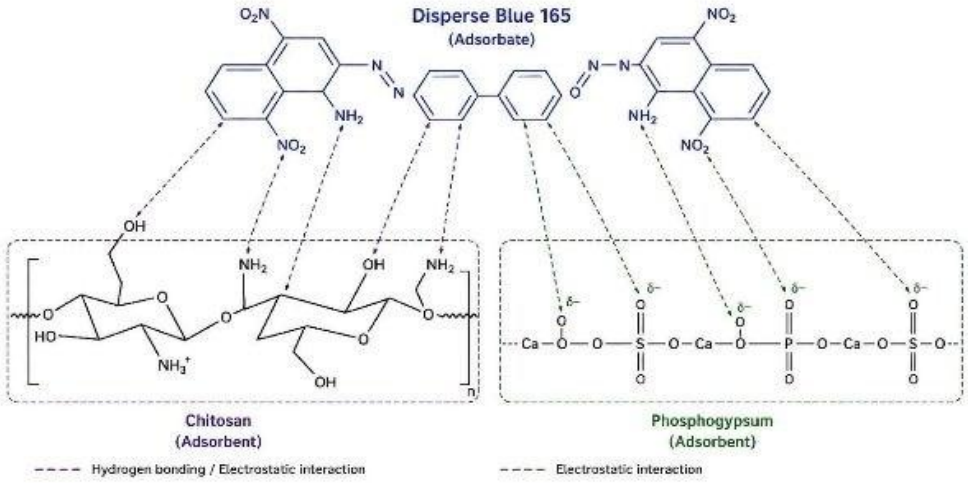

Figure I.7. Schematic representation of the adsorption mechanism of Disperse Blue 165 onto chitosan and phosphogypsum [15]

In a 2018 study, the use of Flue Gas Desulfurization gypsum (FGD gypsum) was explored as a low-cost adsorbent for the removal of silicates from wastewater resulting from the scheelite mineral flotation process. The adsorbent was FGD gypsum rich in calcium sulfate dihydrate ($CaSO_4 \cdot 2H_2O$), while the adsorbate was silicate ions present in the flotation water with an initial silicon concentration of approximately 2650 mg/L. The results showed that the best conditions were achieved at a gypsum dose exceeding 20 g/L and when lowering the pH value to about 10, where the silicate removal efficiency reached about 95%. The study demonstrated that the reaction was very fast, with the maximum reaction rate reached within 60 seconds and the equilibrium state reached after about 240 seconds, indicating rapid adsorption/precipitation kinetics. Microscopic analyses and SEM-EDS measurements also clarified that silicate removal occurred primarily through the formation of a calcium silicate precipitate. The study confirmed a high removal efficiency with a low treatment cost of about 0.18/m^3 [16].

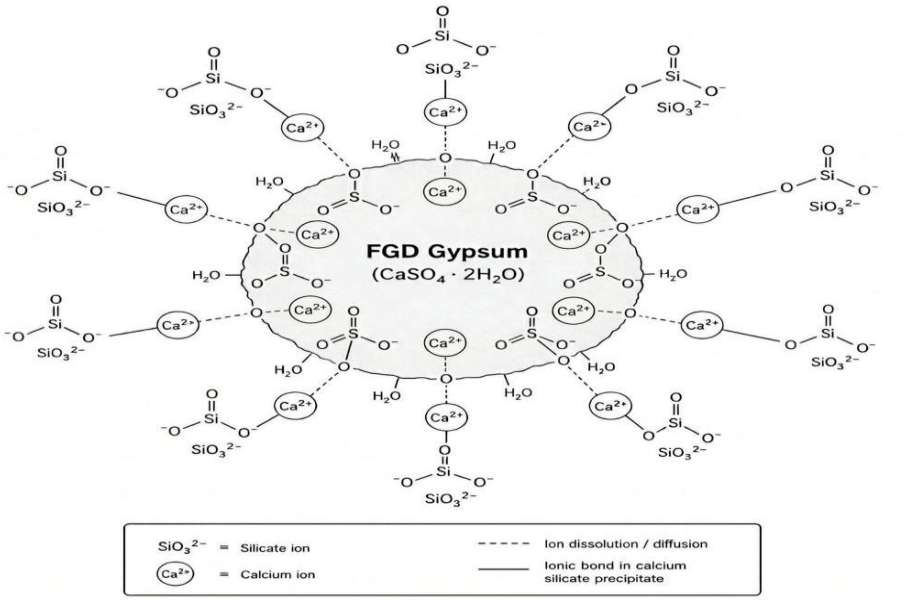

Figure I.8. Schematic Illustration of Silicate Removal Mechanism by FGD Gypsum ($CaSO_4 \cdot 2H_2O$) [16]

In this 2019 study, Flue Gas Desulfurization Gypsum (FGD Gypsum) was used as a low-cost adsorbent for removing fluoride ions from simulated industrial aqueous solutions. The adsorbent was desulfurization gypsum resulting from SO_2 removal plants, while the adsorbate was fluoride ions (F^-) present in a simulated solution with an initial concentration of about 109 mg/L. The results showed that the optimal pH range was between 5 and 11, because a strongly acidic medium reduces the formation of calcium fluoride, while a highly alkaline medium hinders the release of Ca^{2+} from the gypsum. The study also indicated that increasing the gypsum dose improved fluoride removal, with the fluoride concentration dropping from 109 mg/L to 7.3 mg/L, achieving a removal rate of 93.31%. The kinetic study showed that the removal process aligns with the Pseudo-second-order kinetic model, indicating that the process mainly depends on chemical reaction and precipitation. The isotherm was more associated with the calcium fluoride formation reaction than with traditional surface adsorption, with a theoretical removal capacity of about 96.9 mg/g when using 1 g/L of gypsum. Through thermodynamic analysis, the study confirmed that the conversion of calcium sulfate to calcium fluoride is a spontaneously feasible reaction at pH > 5. XRD, FTIR, and SEM-EDS analyses also clarified that the primary removal mechanism involves the release of calcium ions from gypsum and their subsequent union with fluoride to form a CaF_2 precipitate on the adsorbent surface [17].

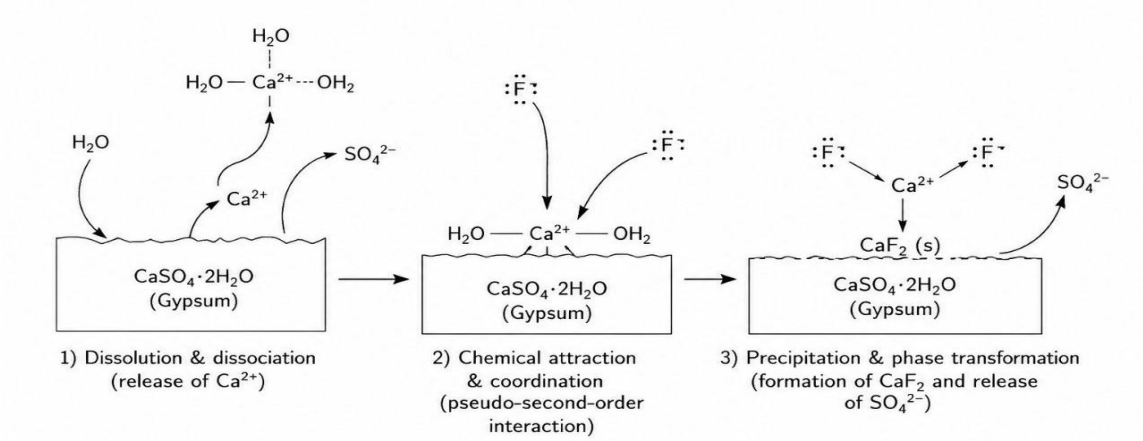

Figure I.9. Mechanism of Fluoride Removal by Flue Gas Desulfurization Gypsum (FGD Gypsum) through Calcium Release and Calcium Fluoride (CaF_2) Precipitation [17]

As for a 2020 study, it relied on preparing a solid adsorbent from Flue Gas Desulfurization Gypsum (FGDG) modified with two diamines (DMAEE and PEHA) for CO_2 adsorption. The presence of crystallization water in gypsum significantly increased adsorption capacity and breakthrough time. Optimal performance was achieved using a mixture of both amines due to synergistic effects. The adsorbent showed excellent stability, with only 1.86% loss in capacity after 12 cycles. The Avrami model best described the kinetics, while the Redlich–Peterson model fitted the isotherm data. Thermodynamic analysis indicated chemisorption as the main mechanism. The study concluded that modified industrial gypsum is a low-cost and effective alternative to traditional porous supports like MCM-41 and ZSM-5 for CO_2 removal [18].

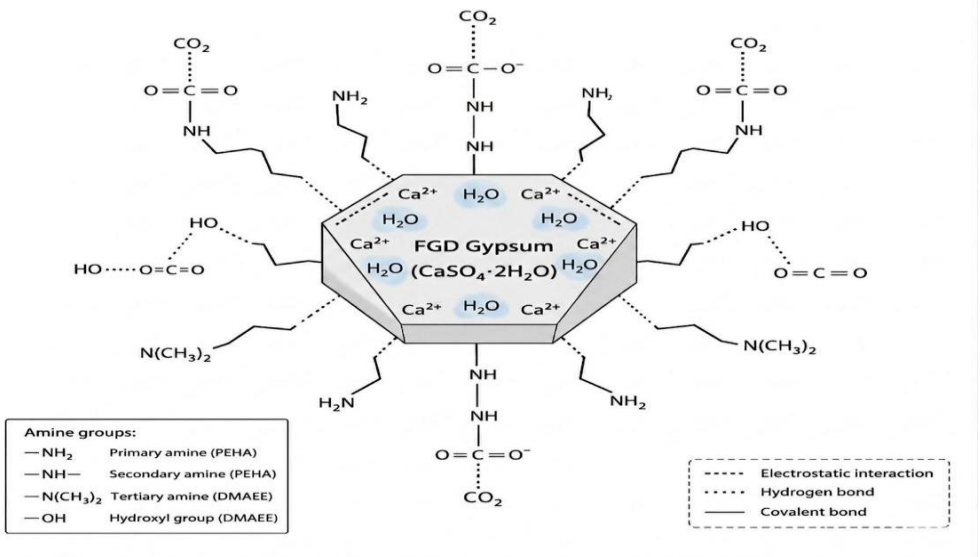

Figure I.10. Schematic Illustration of CO_2 Adsorption Mechanism on Bi-Amine Modified FGD Gypsum ($CaSO_4 \cdot 2H_2O$) [18]

In 2022, a study used thermally treated Titanium Gypsum (TiG) co-pyrolyzed with waste sludge as an adsorbent for phosphate removal from water. The adsorbent was prepared by co-calcination

in a nitrogen atmosphere at temperatures ranging between 400–850 °C, where the results showed a significant improvement in phosphate removal efficiency compared to raw gypsum, with the formation of active sites such as CaO and $Ca(OH)_2$. The study indicated that the adsorption process follows chemical adsorption (Chemisorption), while the isotherm aligned with monolayer adsorption and surface precipitation of the mineral Brushite. The thermodynamic study did not mention detailed values for ΔG°,ΔH°, or ΔS°. The adsorption capacity ranged between 70–160 mg/g, whereas it was less than 10 mg/g for raw gypsum [19].

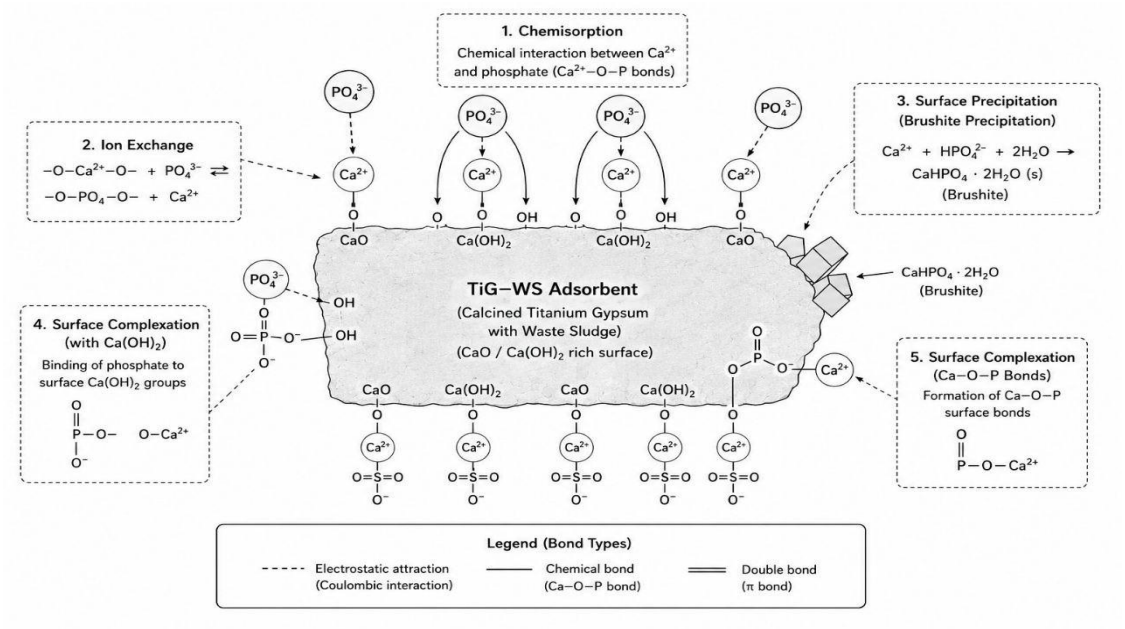

Figure I.11. Proposed phosphate adsorption mechanism gathering the four main stages on calcined titanium gypsum adsorbent [19]

A 2023 study prepared a self-supporting adsorbent from Desulfurization Gypsum and aluminate cement, supported by layered double hydroxides (LDHs), for fluoride ion removal from aqueous solutions. Optimal conditions were near-neutral pH, with efficiency increasing with contact time and adsorbent dose. The material showed high fluoride removal due to aluminum and calcium-rich active sites. Kinetics followed the pseudo-second-order model, indicating chemisorption, while the Langmuir isotherm suggested monolayer formation. The process was spontaneous and thermodynamically favorable. The adsorption mechanism involved ion exchange with LDH anions, chemical precipitation, and surface bonding with calcium and aluminum. The adsorbent demonstrated good capacity, confirming its effectiveness for fluoride-contaminated water treatment [20].

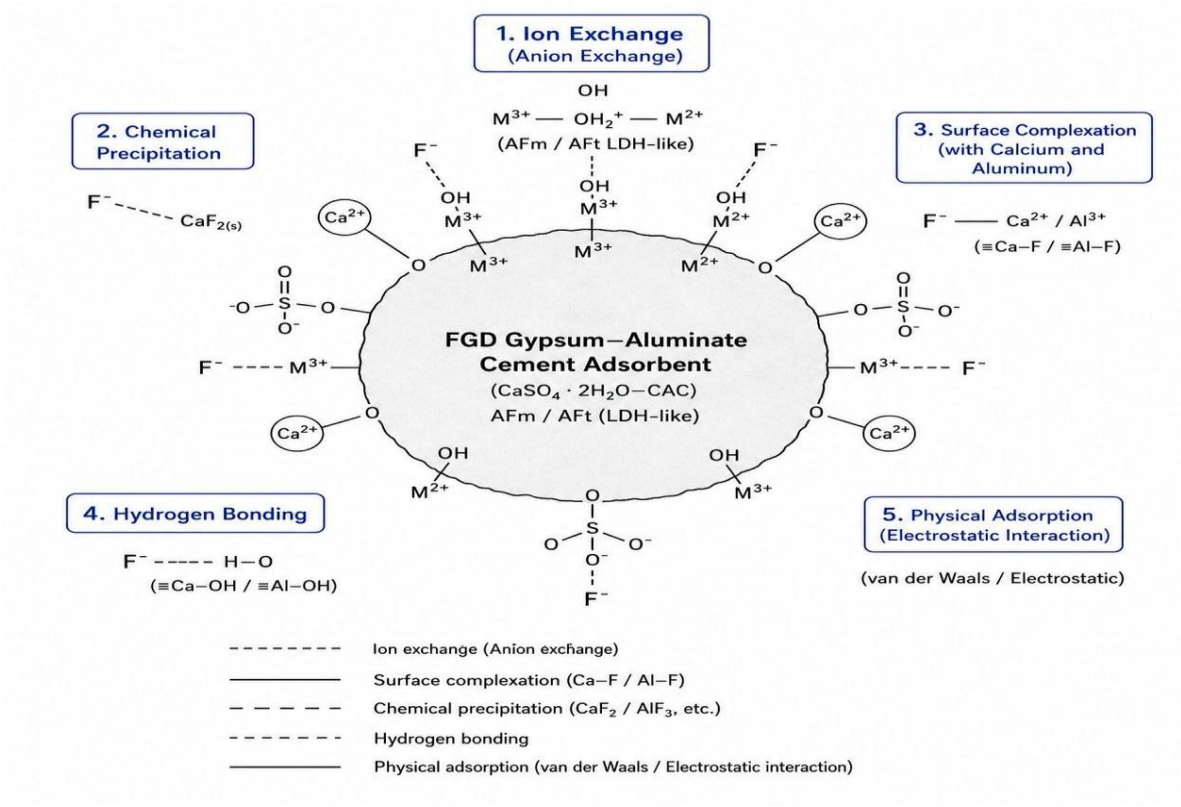

Figure I.12. Proposed fluoride adsorption mechanism gathering the five main stages on gypsum–aluminate cement adsorbent [20]

A 2024 study prepared a magnetic adsorbent from industrial Titanium Gypsum (TiG) and corncobs via co-pyrolysis to remove Pb(II) and Cd(II) from water. Raw gypsum alone showed weak Cd removal (<15%) but reduced Pb to <4 mg/L. After modification with corncobs, the magnetic adsorbent GC10 achieved >99% removal of both metals within a very short time. Optimal conditions used GC10 (Ms = 6.3 emu/g) with initial metal concentrations of 10–400 mg/L. Kinetics were extremely fast, with the kinetic constant increasing 218-fold for Cd and 9-fold for Pb compared to raw gypsum, indicating chemisorption. The main removal mechanisms were surface precipitation forming PbS, CdS, and $PbSO_4$, along with complexation with iron oxides. Magnetic iron oxides and calcium sulfide enhanced adsorption and enabled easy magnetic separation. The study confirmed that this material, derived from industrial and agricultural waste, is an effective and sustainable adsorbent for heavy metal removal from water [21].

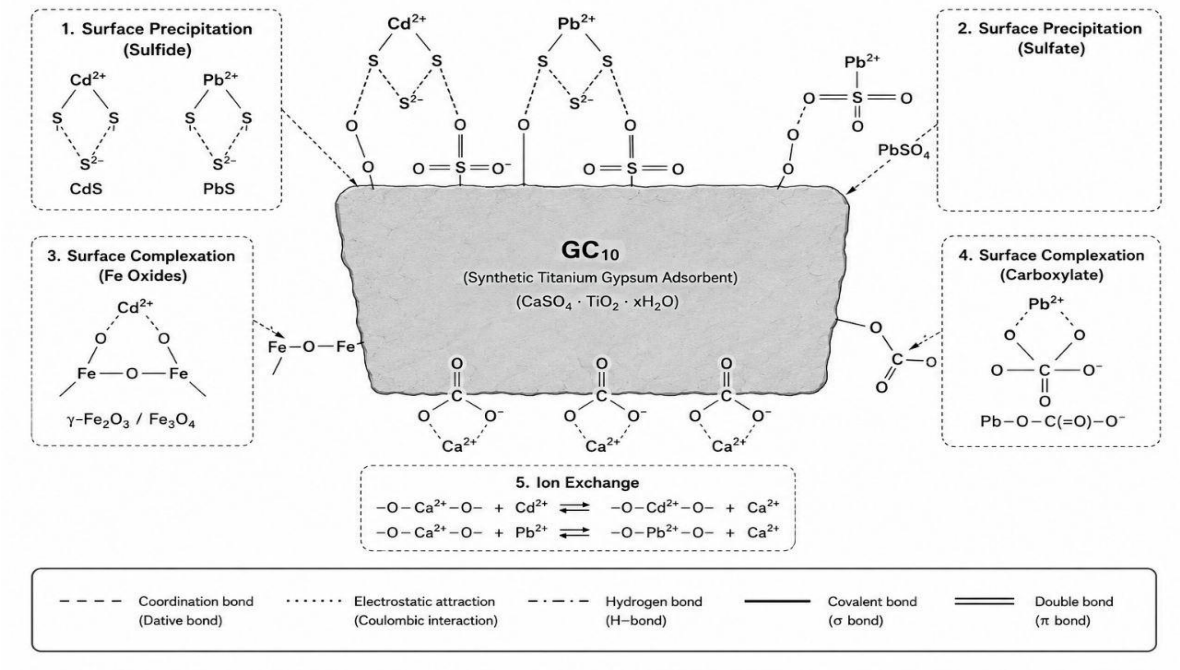

Figure I.13. Proposed adsorption mechanism gathering the five main stages for Pb(II) and Cd(II) removal on magnetic gypsum-based adsorbent GC10 [21]

In this 2025 study, industrial titanium-containing gypsum waste (Titanium Gypsum, TiG) was recycled to prepare an adsorbent for cadmium Cd(II), which, after saturation with cadmium, was then converted into a photocatalyst for removing antibiotics from water under LED irradiation. The GC_{10} adsorbent was prepared through a copyrolysis process of gypsum and corncob waste and was then used for the adsorption of cadmium ions Cd(II) from an aqueous solution. Subsequently, a hydrothermal treatment was performed to obtain the GC_{10}-Cd-H photocatalyst composed primarily of CdS and TiO_2. The adsorbate in the photocatalytic treatment phase was the antibiotic sulfamethazine (SMT). The results showed that the optimal removal conditions were at pH = 3 and under a wavelength of 365 nm using LED, where the SMT removal rate reached about 99.7%. The study also indicated that the presence of humic acids (HA) enhanced the photocatalytic performance of the catalyst. The cadmium loading capacity on the adsorbent material reached about 190 mg/g, indicating a high adsorption efficiency for cadmium before converting the material into a photocatalyst. The study indicated that the removal mechanism relied on the synergistic interaction between CdS and TiO_2 and the presence of sulfur vacancies that improved the separation of electron-hole pairs. The main active species responsible for the photocatalytic degradation were positive holes (h^+) and free radicals •OH and $•O^-$. The study focused primarily on photocatalysis rather than isotherm and thermodynamics; therefore, no isotherm models or thermodynamic parameters were mentioned in detail. However, the initial cadmium adsorption was based on the formation of a CdS precipitate

on the material's surface [22].

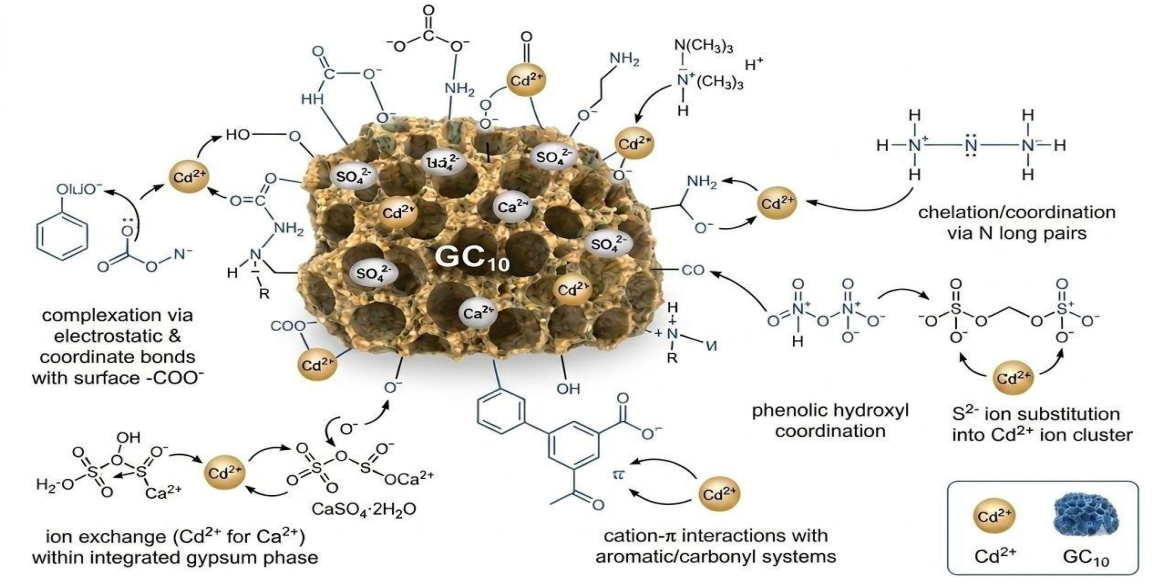

Figure I.14. Schematic illustration of the proposed adsorption mechanisms of Cd(II) onto the GC adsorbent [22]

Bibliography

[1] E. Forgacs, T. Cserháti, and G. Oros, "Removal of Synthetic Dyes from Wastewaters: A Review," Environment International, vol. 30, pp. 953–971, 2004.

[2] T. Robinson, G. McMullan, R. Marchant, and P. Nigam, "Remediation of Dyes in Textile Effluent: A Critical Review on Current Treatment Technologies with a Proposed Alternative," Bioresource Technology, vol. 77, pp. 247–255, 2001.

[3] G. Crini, "Non-Conventional Low-Cost Adsorbents for Dye Removal: A Review," Bioresource Technology, vol. 97, pp. 1061–1085, 2006.

[4] V. K. Gupta, "Application of Low-Cost Adsorbents for Dye Removal: A Review," Journal of Environmental Management, vol. 90, pp. 2313–2342, 2009.

[5] K. Vasiliauskiene and A. Eisinas, "Hydration Properties of Mayenite and Gypsum Mixture," in FIM 2022, 2022.

[6] S. Babel and T. A. Kurniawan, "Low-Cost Adsorbents for Heavy Metals Uptake from Contaminated Water: A Review," Journal of Hazardous Materials, vol. 97, pp. 219–243, 2003.

[7] K. Y. Foo and B. H. Hameed, "Insights into the Modeling of Adsorption Isotherm Systems," Chemical Engineering Journal, vol. 156, pp. 2–10, 2010.

[8] I. Langmuir, "The Adsorption of Gases on Plane Surfaces of Glass, Mica and Platinum," Journal of the American Chemical Society, vol. 40, pp. 1361–1403, 1918.

[9] Y.-S. Ho and G. McKay, "Pseudo-Second-Order Model for Sorption Processes," Process Biochemistry, vol. 34, pp. 451–465, 1999.

[10] F. Deniz and S. D. Saygideger, "Investigation of Adsorption Characteristics of Basic Red 46 onto Gypsum," Desalination, vol. 262, pp. 161–165, 2010.

[11] C. Obunwo, I. Ubong, and G. Orgu, "Removal of Reactive Red 1 Dye from Aqueous Solution Using Gypsum," International Journal of Biological and Chemical Sciences, vol. 6, pp. 2202–2210, 2012.

[12] J. Gunschera, S. Mentese, T. Salthammer, and J. R. Andersen, "Impact of Building Materials on Indoor Formaldehyde Levels," Building and Environment, vol. 64, pp. 138–145, 2013.

[13] M. Raii, D. P. Minh, F. J. E. Sanz, and A. Nzihou, "Lead and Cadmium Removal from Aqueous Solution Using an Industrial Gypsum By-Product," Procedia Engineering, vol. 83, pp. 415–422, 2014.

[14] Y. Y. Yan, Y. Bo, et al., "Recycling Flue Gas Desulphurization (FGD) Gypsum for Removal of Pb(II) and Cd(II) from Wastewater," 2015.

[15] J. Mouldar et al., "Isotherm, Kinetic and Thermodynamic Studies on the Adsorption Behavior of Disperse Blue 165 Dye onto Chitosan and Phosphogypsum," Global Journal of Engineering Science and Research Management, vol. 4, pp. 69–78, 2017.

[16] J. Kang et al., "Utilisation of FGD Gypsum for Silicate Removal from Scheelite Flotation Wastewater," Chemical Engineering Journal, vol. 341, pp. 272–279, 2018.

[17] J. Kang et al., "Efficient Utilisation of Flue Gas Desulfurization Gypsum as a Potential Material for Fluoride Removal," Science of the Total Environment, vol. 649, pp. 344–352, 2019.

[18] J. Chang et al., "Enhanced CO_2 Adsorption Capacity of Bi-Amine Co-Tethered Flue Gas Desulfurization Gypsum with Water of Hydration," Journal of CO_2 Utilization, vol. 35, pp. 115–125, 2020.

[19] Y. Yang, L. Kou, Q. Fan, J. Wang, and K. Jiang, "Synthesis of an Efficient Adsorbent from Titanium Gypsum for Phosphate Removal," Journal of Environmental Chemical Engineering, vol. 10, p. 107920, 2022.

[20] X. Song, M. Sun, J. He, and L. Wang, "Fluoride Ion Adsorption Effect and Adsorption Mechanism of Self-Supported Adsorbent Materials Based on Desulfurization Gypsum–Aluminate Cement," Journal of Renewable Materials, vol. 11, 2023.

[21] Y. Yang, T. Han, and J. Wang, "Ultrafast and Highly Efficient Cd(II) and Pb(II) Removal by Magnetic Adsorbents Derived from Gypsum and Corncob," Ecotoxicology and Environmental Safety, vol. 275, p. 116265, 2024.

[22] J. Wang, T. Han, K. He, Q. Li, and Y. Yang, "Recycling of a Gypsum Waste-Derived Cd(II) Adsorbent into Photocatalysts for Antibiotic Removal under LED Irradiation," Chemical Engineering Journal, p. 166907, 2025.

Chapter II:
Bibliographic Synthesis

Part I: Dyes and Water Pollution

I.1 Water Pollution

Water contamination increased from local to regional to global as industrialization proceeded. Industrial, agricultural, and residential activities pollute much water. The industry uses a lot of water, yet a lot of it is dumped into the environment contaminated with waste, chemicals, and heavy metals. About 85% of industry water is released as waste [1].

I.2 Definition

Water pollution refers to the deterioration of the natural properties of water due to human activity, resulting in physical, chemical, or biological changes. The presence of this disturbs the living circumstances and equilibrium of the aquatic ecosystem, hence affecting the usability of water [2,3].

I.3 Different Types of Pollution

I.3.1 According to the origin of the pollutants

According to the origin of the pollutants, four categories of pollution can be distinguished: domestic and urban, industrial, agricultural [3, 4]

- Domestic and urban pollution: residential areas are the source of domestic and urban pollutants, which is usually transported through the sanitation system to the treatment facility. Feces, organic chemicals, mineral salts including nitrogen and phosphorus, and detergents are common in domestic pollution [5].
- Industrial pollution: Industrial wastewater comes from factories, containing diverse toxins from cooling, cleaning, extraction, and dissolution processes [6]. Includes organic fats, hydrocarbons, metals, acids, chemicals, and radioactive materials [5,7]
- Agricultural pollution: Caused by crop cultivation and farming, mainly from mineral salts (N, K, P) and chemicals (pesticides, herbicides) [5]. Herbicides and insecticides accumulate in soils, groundwater, and the food chain. Some rivers exceed 50 mg/L nitrates. Excess fertilizers contaminate soil and water [3].

I.3.2 According to the nature of pollutants

Depending on the nature of pollutants, there are different types of pollution: physical, chemical and biological [3,7].

- Physical pollution: This form of contamination is known as physical alteration of millet due to numerous sources. The subject can be categorized into three distinct classes: mechanical, thermal, and radioactive [7-9].

- Chemical pollution: Chemical contaminants in water harm plants, animals, and humans. These contaminants are abundant in nature and can harm humans and the environment. Nitrates, phosphates, detergents, phytosanitary products (pesticides), chlorinated solvents, heavy metals (lead, nickel, mercury, chromium), colors, and mineral products are known effluent pollutants. These examples show organic, mineral, and metallic chemical contaminants [8,10].

Biological pollution: Biological contamination includes all organic matter that undergoes bacterial fermentation, leading to significant contamination of water by pathogens such as bacteria, viruses, parasites, fungi, and algae. These microorganisms reduce water usability due to their harmful effects [11].

I.4 Dyes

I.4.1 An overview of the use of dye

The word dye is from Middle English ”deie” and from Old English ”dag” and ”dah”. The first known use of the word dye was before the 12th century [12]. Archaeological evidence shows that dyeing practices have existed since the dawn of human society. A timeline of key historical milestones related to dyestuffs is presented in Figure II.1 [13].

Notably, colored clothing and madder dye remnants were discovered in the ruins of the Indus Valley Civilization (2600–1900 BC). Earliest dyestuff use was documented in China. Spain's El Castillo cave paintings date back ~40,000 years. Colored flax fiber from Georgia (~34,000 BC) may be the oldest found [14]. In 1188, various painters' guilds were established in major European towns. By the mid-12th century, over 200 tailors, clothiers, and painters were officially registered in Florence. Several kings took action to protect traders and goods [15]. The 19th-century rise of synthetic dyes was driven by chemistry, industry, and economic demands. Early attempts failed due to poor lightfastness. In 1856, William Henry Perkin accidentally isolated a violet dye while trying to synthesize quinine for malaria treatment. He named it "mauve," which became popular among royalty and launched a new industry [16]. The dye industry thrived into the early 20th century, leading to the first Color Index in 1924, which listed over 1,200 synthetic and natural dyes. In 2014, more than 500,000 tonnes of pigments were produced globally, with the textile industry using half [17]. A 2016 report stated that over 50,000 tons of synthetic dyes are invented annually, and up to 10% of these dyes enter water bodies [10]. In light of current data, the size of the global market for dyes was estimated to reach $33.2 billion USD in the year 2021.27,000 unique goods are listed in the colour index TM fewer than 13,000 common names and traits. (According to projections, the money made via the production of pigments and dyes. On 2023, the amount at Romania is around $65.1 a million [18].

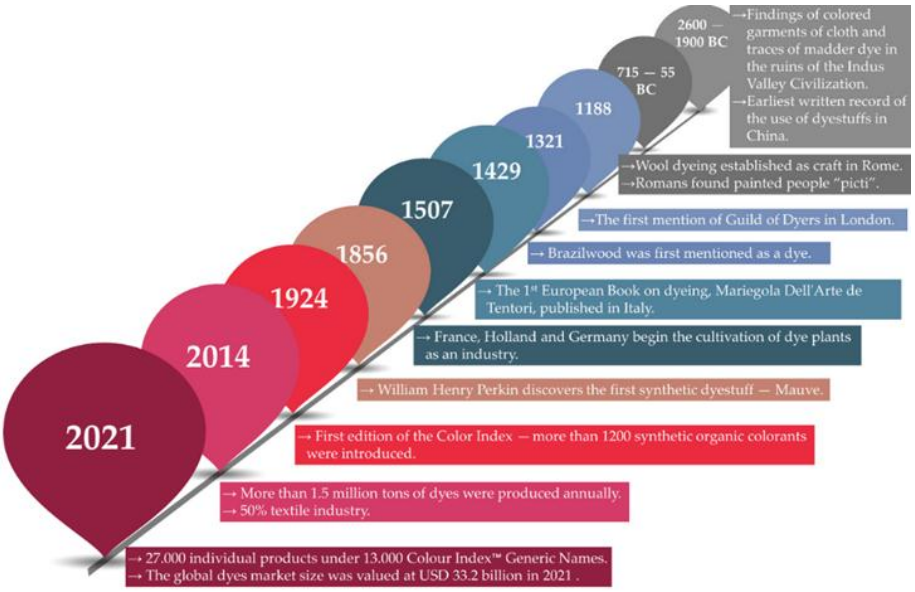

Figure II.1. A timeline of the invention, use, and interesting information regarding dyes [13].

I.4.2 Definition of Dyes

Dyes are coloring chemical compounds used in many industries such as textiles, printing, cosmetics, and food to impart different colors to materials [19]. Dyes are defined as chromophoric substances that have the ability to interact or bind chemically or physically with surfaces, thereby allowing the color to be fixed onto the material to be dyed. The appearance of color in these compounds is related to their ability to absorb specific wavelengths of visible light (from 380 to 750 nm) due to the presence of conjugated systems of electrons in their molecular structure [20]. In short, a dye is defined as a product capable of permanently dyeing a material. It has groups that impart color, called chromophores, and groups that allow it to be fixed, called auxochromes [21].

I.4.3 Chemical Structure of Dyes

Dyes are large aromatic molecules with linked rings that enable resonance and color transfer. Color arises from resonance structures that shift absorption bands into the visible spectrum. A dye contains two essential components: chromophore, auxochrome [21]. Chromophores include aromatic rings (benzene, naphthalene, anthracene) and radicals such as azo (–N=N–), carbonyl (=C=O), carbon (=C=C=C=), carbon-nitrogen, nitroso (–N=O), nitro (–NO2), and sulfur groups [12]. Auxochromes, also known as binding affinity groups, can be amine (-NHX2), hydroxyl (-OH), carboxyl groups (-COOH), aldehydes (-CHO), sulfonic acid (-SO3H) or their derivatives [22].

I.4.4 Classification of Dyes

As the quantity and variety of dyes has increased throughout history, it has become essential to classify them. There are several different classifications, based on their structure, source, color,

solubility and application methods. Basically, the most common classification is based on their chemical structure and application [23]. Figure II.2 combines the grouping by ionic nature (particle charge upon dissolution in aqueous medium) with the application. Accordingly, we can speak of non-ionic and ionic dyes; the latter being cationic and anionic in nature. They are classified according to the method of application as reactive, direct and acid (anionic dyes), basic (cationic dyes), or disperse and or vat and disperse (dyes that are not ionic) [24,25].

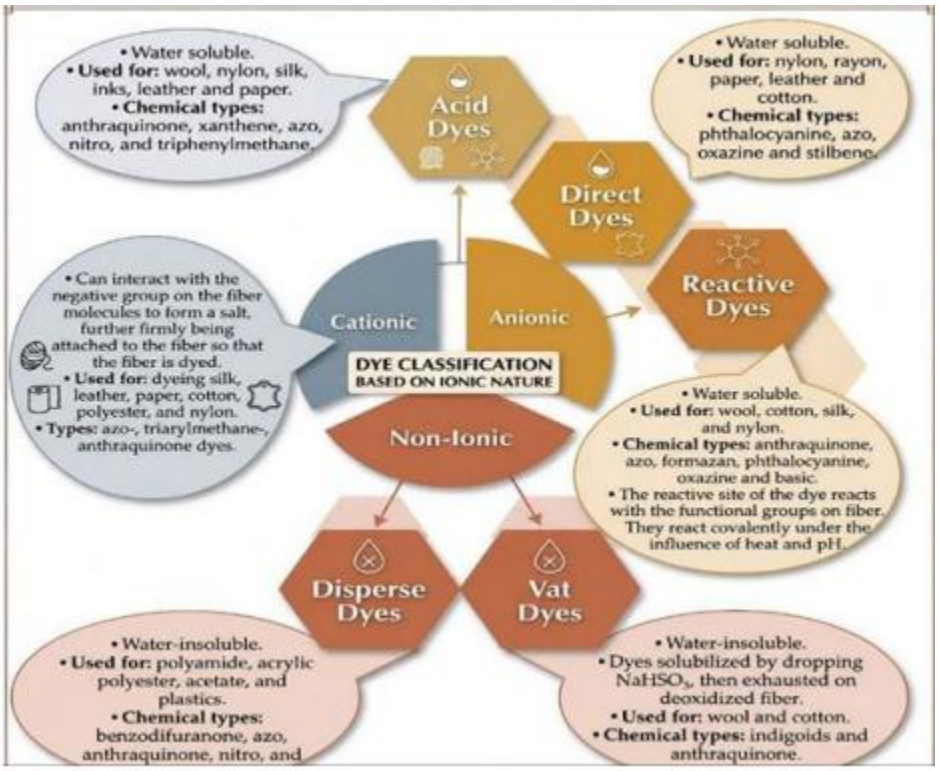

Figure II.2. Classifying dyes according to their ionic structure [24].

I.4.5 Uses of dyes

The main areas of application for dyes are as follows:

- Textile industry.
- Plastics and construction coatings industry.
- Food industry (food colorants).
- Cosmetics industry.

Printing (ink and paper) [26]

I.4.6 Dyes toxicity

The toxicity of dyes stems from the ignorance of researchers or users regarding their chemical structures, which vary from one type to another, as well as the instructions for use during operation [27].

- **Toxicity on human health:**

- Causing skin irritation and eczematous dermatitis.
- Allergic reactions.
- Development of cancer and urinary tumors, especially benign and malignant bladder tumors.
- Asthma and rhinitis.
- Gastrointestinal disorders: painful digestion, nausea, diarrhea; and may cause irritation of the skin, pulmonary and ocular mucous membranes, and especially cancer [28].

- **Toxicity on aquatic environments**

It leads to significant disruptions in various natural mechanisms present in [29]:

- Plants (reduction of the self-purification capacity of watercourses, inhibition of aquatic plant growth, etc.).
- Animals (destruction of certain fish species and microorganisms, etc.).

I.4.6. Current dye removal treatment techniques

Different methods for managing effluents that contain dye contaminants have been applied. Most of these techniques have negative limitations that hinder their use, as some are economically costly or produce toxic waste [30, 31].

The most important methods used for treating polluted water include:

- Sedimentation
- Filtration
- Photocatalysis
- Ion exchange
- Adsorption

It has been found that adsorption is better than the other techniques for water reuse in terms of initial cost, design flexibility and simplicity, ease of operation, and insensitivity to toxic pollutants. Moreover, adsorption does not produce harmful substances [32]

Part II: Adsorption

II.1 Definition of the Adsorption Phenomenon

The term adsorption was first proposed by Kayser in 1881, aiming to distinguish between gas condensation on a surface and gas adsorption, which is a process where gas molecules penetrate into the bulk material. In 1909, M.C. Bain proposed the term ”desorption,” which refers to both the phenomenon of adsorption and desorption [33]. Adsorption refers to the attraction of adsorbate molecules toward the surface of the adsorbent material. In other words, it is a surface phenomenon whereby a multi-component fluid mixture (gaseous or liquid) is attracted to the surface of a solid adsorbent material, forming bonds or interactions between them that are either physical or chemical [34].

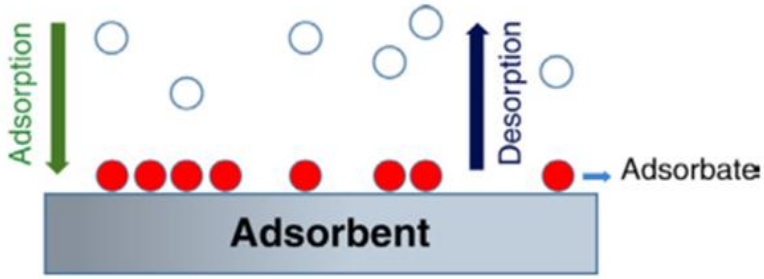

Figure II.3. Diagrammatic Illustration of Desorption and Adsorption Mechanisms [35]

II.2 Classification of Adsorption

Adsorption is classified into two main types based on the forces binding adsorbate to the adsorbent surface, which depend on the adsorbent’s nature and electronic surface activity [36].

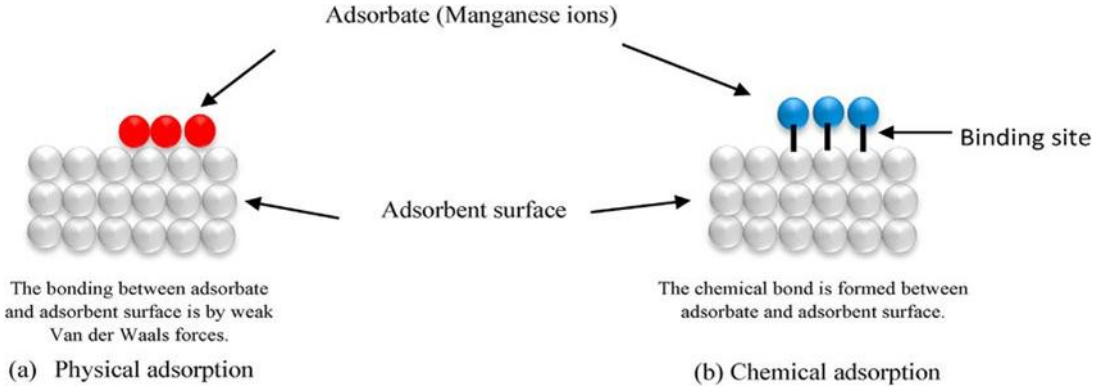

Figure II.4. Types of adsorption bonding

- **Physisorption (physical adsorption):** The interactions between the molecules and the solid matter are characterised by Van der Waals forces. The phenomenon originates from the lack of symmetry among the atoms present on the surface of the material [38].

- **Chemisorption (chemical adsorption):** The process involves true chemical bonds (covalent or ionic), making it highly specific to certain surfaces. It occurs at high temperatures, with efficiency increasing as temperature rises. It forms only a monolayer, is often irreversible, and has high activation energy [39].

Table II.1. Analytical comparison of the two adsorption processes [40]

Properties	Physisorption	Chemisorption
Bonds	Van Der Waals	Chemical
Process temperature	Relatively low	Higher
Adsorption thermal energy	1 to 10 kcal·mol−1	> 10 kcal·mol−1
Desorption process	Easy	Difficult
Kinetics	Very fast	Slow
Layer formation	Multilayers	Monolayer
Reversibility	Reversible	Irreversible

II.3 Factors Affecting the Adsorption Phenomenon

The efficiency of liquid-phase adsorption, and therefore the optimal operation of the water treatment process, depends on several parameters. The sorption performance, as illustrated in Figure II.5, is influenced by physico-chemical factors such as the adsorbent/adsorptive interaction, the surface chemistry and pore structure of the adsorbent, particle size, nature of the adsorbent, presence of other ions in the aqueous solution, pH, temperature, pressure, and contact time. The properties of the adsorbate, its molecular weight, molecular structure, molecular size, and polarity should also be taken into account [25,41].

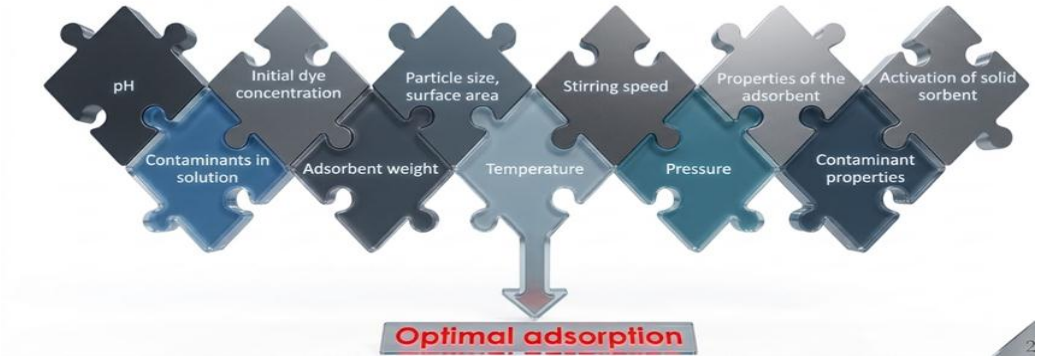

Figure II.5. Factors affecting adsorption process [41].

II.4 Adsorption Isotherms (Isotherm Models)

An adsorption isotherm is defined as the relationship at equilibrium between the concentration of the solute remaining in solution and its concentration adsorbed on the surface of the adsorbent

material [42]. To calculate the amount of adsorbed substance, the following general expression is used:

$$q_e = \frac{(C_0 - C_e)V}{m} \qquad (II.1)$$

The dye removal percentage R (%)

$$R(\%) = \frac{(C_0 - C_e)}{C_0} \qquad (II.2)$$

Where:

q_e = amount adsorbed at equilibrium (mg/g),

C_0 = initial concentration (mg/L),

C_e = equilibrium concentration (mg/L),

m = mass of adsorbent (g),

V = volume of solution (L).

II.5 Adsorption Kinetics

The adsorption kinetics, expressed in terms of the solute retention rate as a function of contact time, is one of the most important characteristics defining the efficiency of an adsorption process [44]. The speed at which thermodynamic equilibrium is reached depends on the diffusion rate of the adsorbate and the adsorbate-adsorbent interaction [45]. Adsorption kinetics generally follow pseudo-first-order or pseudo-second-order models."

II.5.1 Pseudo-first-order model

The first-order kinetic model known by the Lagergren equation [46] is based on the assumption that the rate of retention of a solute over time is proportional to the difference between the amount adsorbed at equilibrium and the amount adsorbed at a given time t, namely:

$$\frac{dq_t}{dt} = K_1(q_e - q_t) \qquad (II.3)$$

The variables q_e, t, and K_1 represent the amount of adsorbate at equilibrium per gramme of adsorbent (mg g^{-1}), contact time (min), and adsorption rate constant for the first order (min^{-1}), respectively. Equation (1) is integrated, giving:

$$\ln(q_e - q_t) = \ln q_e - K_1 t \qquad (II.4)$$

Pseudo-second-order model

The pseudo-second-order kinetic model or the Ho and McKay model [47, 48] can be expressed by the equation:

$$\frac{dq_t}{dt} = K_1(q_e - q_t)^2 \qquad (II.5)$$

The integration of equation **(II.5)** gives:

$$\frac{t}{q_t} = \frac{1}{K_2 q_e^2} + \frac{t}{q_e} \qquad \textbf{(II.6)}$$

While, K_2 being the rate constant for adsorption for the pseudo-second-order ($g.mol^{-1}.min^{-1}$), and q_e is the amount of adsorbate at equilibrium per gram of adsorbent (mg. g^{-1}).

II.6 Modeling of Adsorption Isotherms

Advanced adsorption isotherm models, including Langmuir, Freundlich, and Temkin, provide comprehensive insights into the interactions between adsorbent surfaces and molecules to be adsorbed. Following sections provide concise explanations of these isotherm models.

II.6.1 Langmuir isotherm

Irving Langmuir introduced the adsorption concept in 1932 [49]. The main isotherm model assumptions are: adsorption occurs at adsorbent media surface binding sites, adsorption of all surface adsorbent sites are same, the surface a monolayer of adsorbed molecules covers the adsorbent, and adsorbed molecules on the adsorbent do not interact.

The Langmuir adsorption model equation (II. 7):

$$\frac{C_e}{q_e} = \frac{1}{q_{max} \times K_L} + \frac{C_e}{q_{max}} \qquad \text{(II. 7)}$$

While: C_e (mg. L^{-1}), q_e (mg. g^{-1}) represent the equilibrium concentration and the actual amount of adsorbed molecules on the adsorbent surface, q_{max} denotes maximal adsorption capacity (mg. g^{-1}) and K_L represents Langmuir constant (L mg^{-1}).

The Langmuir constant K_L is given by the following equation:

$$K_L = \frac{q_{max}}{c_e(q_{max} - q_e)} \qquad \text{(II.8)}$$

This model is characterized by the equilibrium parameter R_L:

$$R_L = \frac{1}{1 + K_L . C_0} \qquad \text{(II.9)}$$

Where: $R_L = R_0$: The adsorption is irreversible, $0 < R_L < 1$: The adsorption process is favorable, $R_L = 1$: The adsorption is linear, and $R_L > 1$: The adsorption process is unfavorable

II.6.2 Freundlich isotherm

The Freundlich isotherm model [50] is a method employed to describe the adsorption of molecules on the adsorbent surface by considering the multilayer and heterogeneous composition. Eq. (II.10) illustrates this concept.

$$\ln q_e = \ln K_f + \frac{1}{n} \ln C_e \qquad \text{(II.10)}$$

The variable q_m (mg. g^{-1}) represents the number of molecules adsorbing onto the adsorbent surface

at any particular time. C_e (mg. L^{-1}) represents equilibrium concentration, while n and K_f represent Freundlich constant and exposure, respectively. K_f (mg. g^{-1}) measures the adsorbent's capacity to adsorb the adsorbate, while n characterises surface heterogeneity and molecule dispersion. A higher n indicates that molecules are adsorbed favourably onto the adsorbent. Increased n indicates higher adsorption intensity.

The adsorption intensity can be interpreted based on the value of n:

- If n<1, the adsorption is considered chemical
- If n>1, the adsorption is considered physical

II.6.3 Temkin isotherm

One further adsorption isotherm was proposed by Temkin and Pyzhev in 1940 [51, 52]. This model analyses the impact of adsorption heat, which exhibits a linear reduction as the covering of the adsorbed molecules layer increases. The reduction of the adsorption heat is attributed to the interactions among the molecules that have been adsorbed on the surface.

The Temkin adsorption isotherm is specified by the equation (II. 11):

$$q_e = \frac{R.T}{b_T} \ln K_T + \frac{R.T}{b_T} \ln C_e \qquad \text{(II. 11)}$$

Where, T: temperature (K), R: ideal gas constant (8.314 $J.mol^{-1}. K^{-1}$), b_T: Adsorption intensity and heat of adsorption ($J. mol^{-1}$), and K_T: Temkin constant (L/mg).

II.7 Adsorption Thermodynamics

The thermodynamic study reflects the feasibility and spontaneous nature of the adsorption process. The thermodynamic study includes the Gibbs free energy (ΔG°), the change in enthalpy (ΔH°), and the change in entropy (ΔS°), which can be estimated from the equilibrium constants at different temperatures. To estimate the change in the free energy of the reaction, the adsorption is given by [53] :

$$\Delta G° = -RTLn\, K_d \qquad \text{(II. 12)}$$

$$K_d = \frac{q_e}{C_e} \qquad \text{(II. 13)}$$

$$\mathbf{LnK_d} = \frac{\mathbf{\Delta S°}}{\mathbf{R}} - \frac{\mathbf{\Delta H°}}{\mathbf{RT}} \qquad \text{(II. 14)}$$

While, K_d: equilibrium constant, ΔH°: enthalpy (J/mole), ΔS°: the change in Entropy (J/mole. K), ΔG°: Gibbs free energy (J/mole).

II.8 Adsorption Mechanism

The adsorption mechanism can be summarized in four steps: (1) diffusion of adsorbate to the region near the adsorbent surface, (2) external diffusion through a liquid film, (3) internal diffusion inside pores, (4) adsorption onto active sites [36,54].

- **First step:** Diffusion of the adsorbate from the liquid phase to the region near the surface of the adsorbent material (very fast stage).

- **Second step**: External diffusion of the particles, i.e., transfer of the adsorbate through a liquid film towards the surface of the adsorbent material (fast stage).

- **Third step**: Internal diffusion within the particles through the transfer of the substance inside the porous structure of the external surface of the particles towards the active sites (slow stage).

- **Fourth step**: The adsorption phenomenon upon contact with the active sites (very fast stage).

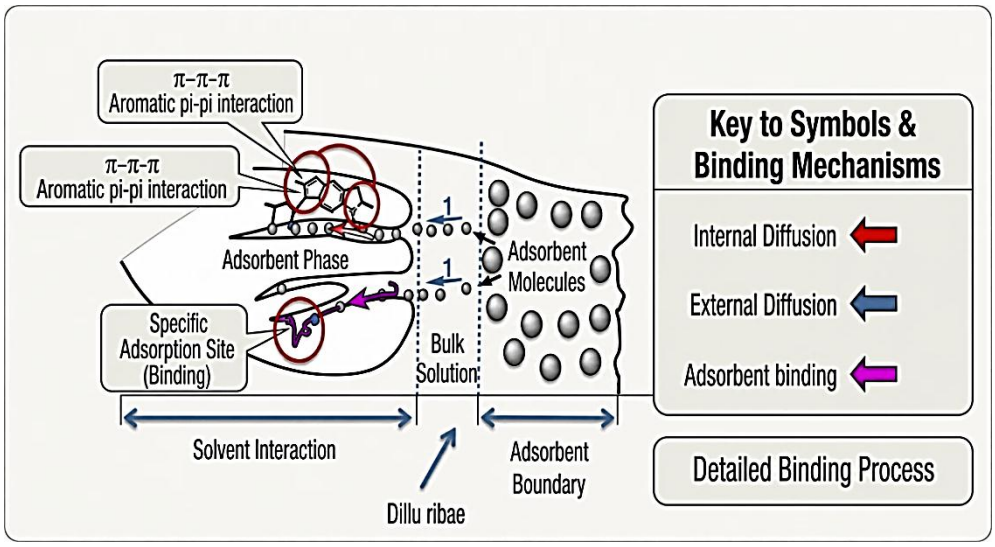

Figure II.6. Schematic diagram illustrating the steps of the adsorption mechanism [55] .

Part III: Gypsum

III.1 A Brief History of Gypsum

Archaeological evidence shows gypsum use dating back nearly 9,000 years in Anatolia and Syria, employed by ancient civilizations such as the Sumerians, Assyrians, Egyptians, Greeks, and Romans for construction and decoration; Egyptians used alabaster (a gypsum type) in Tutankhamun's tomb and coated pyramid walls over 5,000 years ago, Assyrians created winged bull statues now in the British Museum, Greeks made coins and small dishes from gypsum, and in Algeria, the 3rd-century BC Berber mausoleum Imdghas (Madghis) stands as North Africa's oldest royal tomb. Europeans advanced gypsum artistry in the 16th century with the Vatican's Loggia and France's Fontainebleau palace, while at the 1893 World's Columbian Exposition in America, gypsum-decorated buildings led to European craftsmen being brought in to teach their skill [56] .

III.2 Definition of Gypsum

Gypsum is chemically defined as calcium sulfate dihydrate, with the chemical formula ($CaSO_4 \cdot 2H_2O$). It is a sulfur-rich mineral widely found in the Earth's crust and is classified among evaporite sedimentary rocks. Gypsum naturally contains calcium sulfate ($CaSO_4$) at approximately 79.1% by weight and crystal water at approximately 20.9% [57]. It forms in thick layers from saline water evaporation in shallow seabeds and expands upon absorbing water, creating folded layers. Gypsum is fine-grained, becomes powder when heated, and is the basis for Plaster of Paris and stucco. Its specific density ranges from 2.1 to 4.2 depending on purity, and while its crystals are transparent to radiation under microscope, to the naked eye it appears white, yellow, gray, or pink due to impurities [58] .

III.3 Components and Structure of Gypsum

Gypsum is considered a natural material composed primarily of calcium sulfate ($CaSO_4$), along with varying proportions of water, calcium carbonate ($CaCO_3$), and silica or sand (SiO_2), depending on the geological location from which the deposits are extracted [59].

Gypsum crystallizes in the monoclinic system. Its structure consists of alternating layers, where calcium ions (Ca^{2+}) and sulfate groups (SO_4^{-2}) are strongly connected through ionic and covalent bonds forming rigid layers, while water molecules are located between these layers and are held together by weak hydrogen bonds. This layered structure explains the ease of cleavage of gypsum and its sensitivity to physical conditions,providing important surface areas for surface reactions [60].

III.4. Types and Sources of Gypsum

Gypsum can be classified according to its origin and formation process into two main categories, each with distinct physical and chemical properties relevant to environmental and treatment applications:

III.4.1. Natural gypsum

Natural gypsum is extracted directly from mines or quarries. It is formed through the evaporation of seawater in shallow basins over geological time periods. It typically exhibits a stable crystalline structure and a purity ranging from 80% to 95%. It may contain natural impurities such as carbonates (calcite), clays, or metal oxides, which may influence its properties [58]. Gypsum occurs in nature in several forms: Gypsite (a fine-grained, impure deposit containing clay or sand), Selenite (transparent, well-formed crystals), Alabaster (fine-grained blocks used for carving and decoration), Satinspar (a fibrous, highly fractured type with a thermal luster), and Desert Rose (crystals resembling roses, formed in sandy or clayey soils in desert areas) [61].

III.4.2. Synthetic Gypsum (Synthetic/Chemical Gypsum):

Synthetic gypsum is a by- product of industrial chemical processes and is produced in large quantities in industrial areas. It is classified according to its production process into:

- **Phosphogypsum:** A major by-product obtained during the production of phosphoric acid from phosphate rock. It is characterized by fine particle size and relatively acidic nature, making it an important material for environmental studies.
- **Flue Gas Desulfurization (FGD) Gypsum:** Produced from the desulfurization of flue gases in coal-fired power plants to reduce sulfur emissions. It is characterized by very high chemical purity.
- **Fluorogypsum:** A by-product of hydrofluoric acid production. It exhibits unique surface properties that make it a promising material for use as an effective adsorbent [35].

III.5. Gypsum Preparation

III.5.1. Traditional Method:

Gypsum is prepared using the traditional method through **four simple stages**: **Crushing** (breaking large blocks into smaller pieces), then **Cooking** in a primitive kiln using wood, followed by **Grinding** into a fine powder, and finally **Sieving** to separate large particles. This method is among the oldest used for preparing gypsum due to its simplicity and efficiency in producing a powder that meets the basic requirements for various applications [58].

Figure II.7. Stages of preparing gypsum powder using the traditional method [55] .

III.5.2. Modern Method:

The modern production of natural gypsum involves five main stages [62]: **crushing** (two-stage industrial crushing), **extraction** (washing, sieving, and drying), **calcination** (heating to ~130 °C to produce hemihydrate, $CaSO_4 \cdot ½H_2O$), grinding, and final testing/packaging (checking setting time, purity, flexural resistance, and impurities). Two types of hemihydrate are obtained: **alpha gypsum (α)** (formed under high pressure, denser crystals, slower setting, requires more water) and **beta gypsum (β)** (formed under milder conditions, faster setting, widely used industrially).

$$CaSO_4 \cdot 2H_2O + \text{heat} = CaSO_4.\frac{1}{2}H_2O + \frac{3}{2}H_2O$$

Grinding, after calcination, the gypsum is ground in specialized mills to achieve the required fineness. **Packaging and Testing**, the resulting powder is then tested for setting time, purity, flexural resistance, and impurity levels before being packaged. These tests ensure quality classification according to approved standards. Additionally, industrial gypsum can be produced as a by-product, either via organic acid reactions (e.g., oxalic acid reacting with calcium oxalate and sulfuric acid) or through flue gas desulfurization (FGD), where calcium hydroxide absorbs SO_2 and is oxidized to form calcium sulfate ($CaSO_4$).

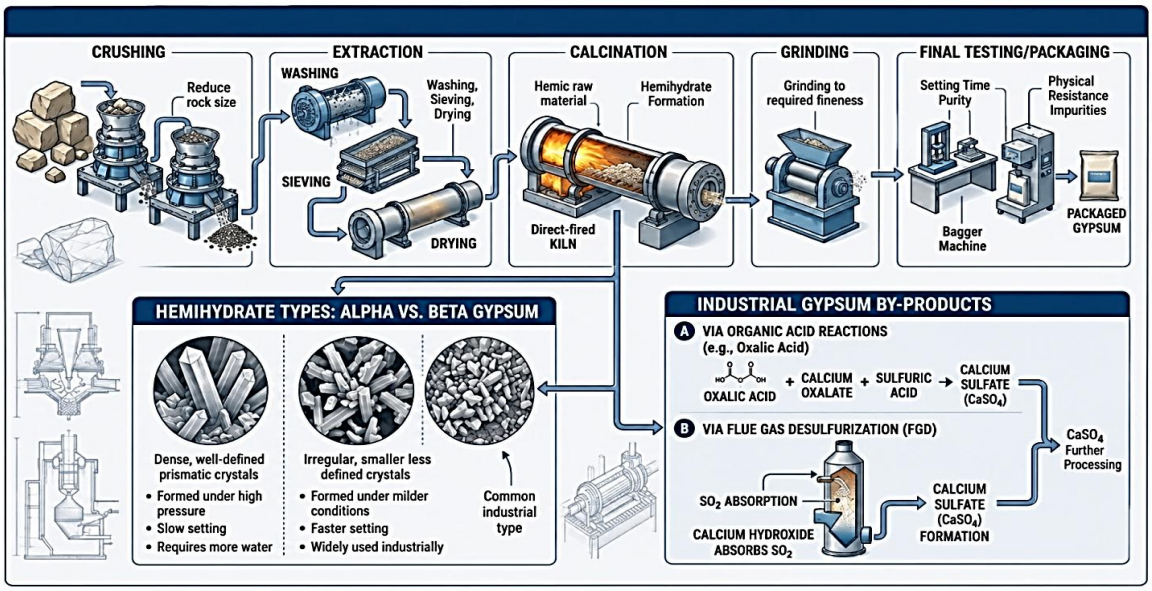

Figure II.8. Simplified modern gypsum production[62].

III.6. Physicochemical Characterization and Surface Dynamics of Gypsum

The efficiency of gypsum in adsorption processes depends on several structural and chemical properties[58, 63]:

- Surface Area and Porosity: Gypsum contains micropores and micro-cracks that increase its specific surface area, providing active sites for the adsorption of organic molecules.
- Point of Zero Charge (pHPZC): The point of zero charge (pHPZC) is the pH value at which the surface charge of gypsum becomes neutral. When the solution pH is higher than pHPZC, the surface becomes negatively charged, creating strong electrostatic attraction with positively charged (cationic) pollutants.
- Stability and Solubility: Gypsum exhibits low solubility in aqueous media (approximately 2.1 mg/L), which provides dynamic stability and prevents the adsorbent from disintegration during contact with solutions [36].

III.7. Surface Structure and Functional Groups of Gypsum

The surface of gypsum contains active chemical groups that act as binding centers for physicochemical interactions [64]:

- **Surface hydroxyl groups (–OH):** These groups form when the mineral interacts with water and act as sites for hydrogen bonding with organic pollutants.
- **Sulfate groups (SO_4^{2-}):** These ions provide high electron density on the surface, facilitating electrostatic interactions with positively charged pollutants.

- **Active sites:** The surface contains micro-defects and crystal imperfections with high surface energy, making them favorable sites for rapid adsorption of organic molecules.

III.8. Environmental Role of Gypsum in Wastewater Treatment

Gypsum is classified as a low-cost natural adsorbent, and its main applications include [65]:

- **Removal of organic pollutants and dyes:** Gypsum helps purify water from complex organic compounds due to its porous structure, where micro-cracks provide suitable geometrical sites for trapping large dye molecules [66].
- **Heavy metal adsorption and ion exchange:** Gypsum can remove heavy metal ions such as lead and cadmium through ion exchange with calcium ions (Ca^{2+}) or through surface precipitation within pores [67].
- **Sustainability and circular economy:** The environmental value of gypsum lies in its ability to recycle industrial waste (such as synthetic gypsum) into a water purification material, reducing costs compared to conventional adsorbents [68].
-

Part IV: Optimization Methods

IV.1. Introduction:

Given rapid development in industrial and scientific fields, it has become necessary to adopt systematic methods that help improve processes and understand the impact of various factors on their outputs. Studying complex systems involving multiple interacting variables requires analytical tools capable of reducing experimental effort while ensuring result accuracy. In this context, modern statistical methodologies concerned with experimental design and systematic data analysis have emerged, allowing the extraction of approximate models that represent the behavior of the phenomena under study. These methods also help reduce the number of required experiments, save time and cost, while maintaining the quality of outcome prediction. Among these methods, the Response Surface Methodology (RSM) has emerged as one of the most important tools used in process optimization, enabling researchers to study the effect of multiple factors simultaneously and analyze their interactions within an organized experimental framework, which has made it widely used in various scientific and engineering applications [69, 70].

IV.2. Concept and Principle of Response Surface Methodology (RSM)

- Response Surface Methodology (RSM) is a set of statistical and mathematical techniques used for modeling and optimizing scientific experiments. This methodology aims to analyze the relationship between various variables that affect a specific response variable, and to determine the optimal values of these variables that lead to improving the desired response [71]. RSM relies on designing systematic experiments by changing the values of the variables and measuring the response, then analyzing the data using statistical techniques to estimate the relationship between the variables and the response, and to determine.
- the optimal values of the variables to achieve the desired response [72].

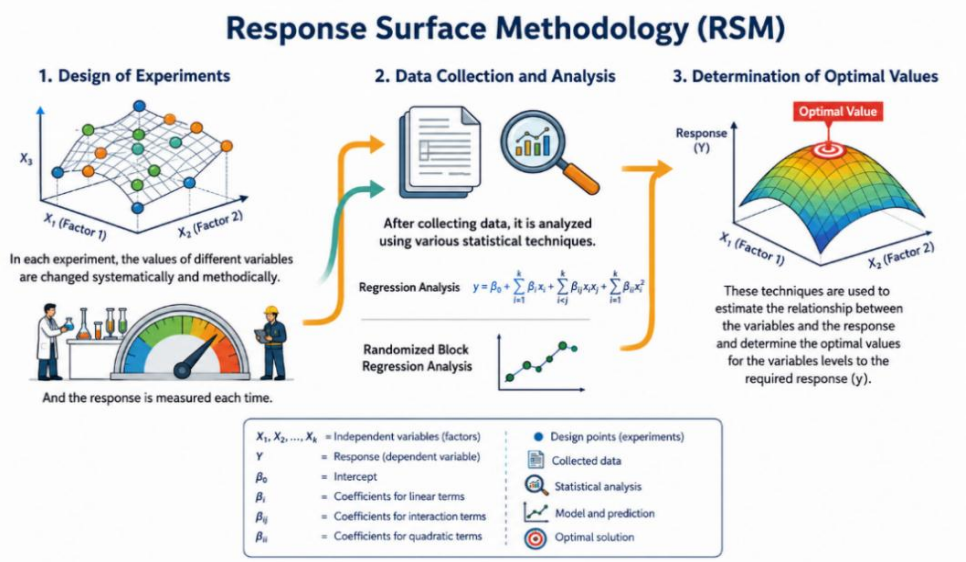

Figure II.9. Principle of Surface Response Methodology (RSM) [55] .

IV.3. Modeling steps using RSM

IV.3.1. Experimental design of RSM

To obtain a good experimental design, it is recommended to minimize the number of experiments as much as possible in order to reduce computational requirements, delays, and experimental costs. This also allows for a reduction in the variance of the coefficients of the mathematical model used, which will make the obtained response surfaces more accurate. We must determine the most appropriate experimental design to obtain the desired experiments. The designs used within the framework of RSM studies are quadratic designs such as the Central Composite Design (**CCD**) or the Box–Behnken Design (**BBD**) [73].

IV.3.2. Modeling of RSM

When using RSM, we try to relate the continuous response Y (Optimizing) to a number of factors affecting the response process (K) using a linear regression model, which can be written as follows [64]:

$$Y=f_B\ (X_1, X_2\text{……..}X_k) \qquad \text{(II.15)}$$

Although the exact form of the response function f_B is unknown, experimentation reveals it. A good approximation can be obtained using a polynomial. In the case of two factors, the linear regression model takes the form:

$$Y = \beta_0 + \sum_{i=1}^{k} \beta_i \chi_i + \sum_{i=1}^{k} \beta_{ii} \chi_i^2 + \sum_{i=1}^{k} \sum_{j=1}^{k} \beta_{ij} \chi_i \chi_j + \varepsilon \qquad \text{(II.16)}$$

Where: The indices i and j are used to represent the variable count, β_0 is the constant coefficient, β_i, β_{ii}, and β_{ij} represent the linear, quadratic, and interaction coefficients, respectively. ε indicates random error. The values χ_i and χ_j correspond to the response and the coded values of the independent factors (-1, 0, +1).

IV.3.3. Analysis of variance:

Analysis of variance, usually abbreviated as ANOVA. In general, in terms of regression, the principle of analysis of variance is to divide the total variance into a factorial component related to the regression equation or the model used and a residual component. The factorial and residual components are represented mathematically by mean squares, i.e., variances. The advantage of analysis of variance is the ability to absolutely test the effect of factors on differences in a given response [74].

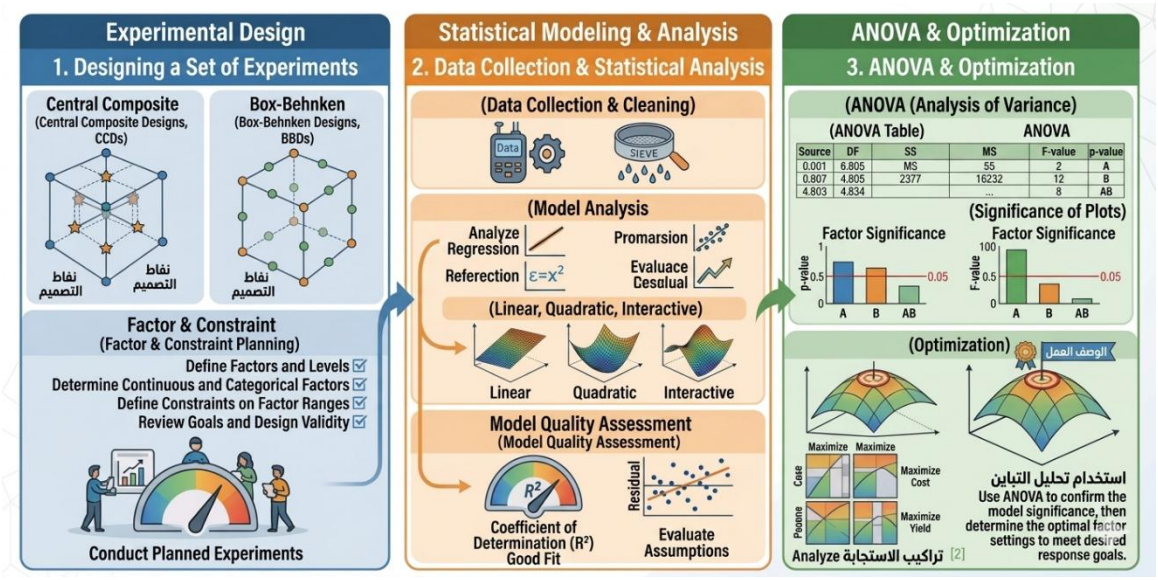

Figure II.10. Stages of the Response Surface Methodology [55] .

IV.4. Types of designs:

There are several types of designs for Response Surface Methodology (RSM), among which the common designs include:

IV.4.1. Central Composite Design (CCD):

This design is denoted as CCD and was introduced by Box and Wilson in 1951.

It is the most commonly used design for building second-order models. Many modifications have been made to develop it due to its characteristics, and it has numerous applications in the scientific field. This design combines a full factorial design or a fractional factorial design with additional starting points and at least one point at the center of the experimental domain [75].

IV.4.2. Box–Behnken Design (BBD):

This design was developed by Box and Behnken. This design presents three levels (+1, 0, -1) for each variable, which are equally spaced. All points except the central ones lie at the midpoints of the edges of a cube within a circle of radius (1). Therefore, this design is symmetric and rotatable. Additionally, this design does not contain any points at the vertices of the cube or at the upper and lower boundaries of each variable [76].

The BBD generally has better advantages compared to CCD, especially when the number of variables is small, as it requires the smallest number of experiments for the same phenomenon under study, as shown in the table below.

Create Response Surface Design - Display Available Designs

Available Response Surface Designs (with Number of Runs)

Design		Factors								
		2	3	4	5	6	7	8	9	10
Central Composite full	unblocked	13	20	31	52	90	152			
	blocked	14	20	30	54	90	160			
Central Composite half	unblocked				32	53	88	154		
	blocked				33	54	90	160		
Central composite quarter	unblocked							90	156	
	blocked							90	160	
Central Composite eighth	unblocked									158
	blocked									160
Box-Behnken	unblocked		15	27	46	54	62		130	170
	blocked			27	46	54	62		130	170

Help OK

Figure II.11. BBD vs. CCD for three variables by (Design-Expert 13).

The BBD is a popular experimental design used in RSM for optimizing processes and studying the relationships between factors and responses. This is the model adopted in this study**.**

IV.5. Advantages and disadvantages of the Box-Behnken design

IV.5.1. Advantages of the Box-Behnken design [77 ,76]:

- It is considered less expensive compared to other designs.

- It contains fewer design points.

- The BBD does not contain axial points, thus ensuring that all design points lie within the experimental space.

- It is more economical and efficient in terms of the number of experiments required.

- The BBD ensures that not all factors are set at their extreme levels simultaneously.

- It is useful for avoiding experiments that would be conducted under difficult conditions which might produce undesirable results.

- This design requires a smaller number of experiments compared to full or fractional factorial designs.

IV.5.2. Disadvantages of the Box-Behnken design [76]:

- It is not effective in cases where we wish to know extreme responses.

- It is not suitable for sequential experiments.

IV.6. Applications of RSM [78]:

Response Surface Methodology can be used in many applications, such as:

- Production processes and product quality improvement.

- Improving the efficiency of industrial processes.

- Improving agricultural and environmental processes.

- Improving the engineering design of products, devices, and systems.

- Using the BBD in simulations.

- Chromatographic analysis using the BBD to optimize chromatographic conditions

Bibliography

[1] D. Gupta, "The Importance of Water Resources," in Int. Conf. Water and Environment, Dublin, 1992.

[2] L. R. Berg, P. H. Raven, and D. M. Hassenzahl, Environnement. De Boeck Supérieur, 2009.

[3] C. Brémaud et al., "Alimentation, Santé, Qualité de l'Environnement," Educagri, 2006.

[4] É. Gilli, C. Mangan, and J. Mudry, Hydrogéologie. Dunod, 2008.

[5] C. Faurie et al., Ecologie. Tec & Doc, 2011.

[6] D. Gaujous, La Pollution des Milieux Aquatiques. Lavoisier, 1995.

[7] F. Ramade, Introduction à l'Écochimie. Lavoisier, 2011.

[8] P. Goudet and A. Kowalski, Physique et Chimie. Educagri, 2011.

[9] J. M. Stellman, Encyclopédie de Sécurité, vol. 2. ILO, 2000.

[10] G. Crini, A. J. Montiel, and P.-M. Badot, Traitement des Eaux Industrielles. Presses Univ. Franche-Comté, 2007.

[11] S. Baumont et al., "Réutilisation des Eaux Usées Épurées," ORS IdF, 2014.

[12] E. Rápó and S. Tonk, "Molecules," vol. 26, p. 5419, 2021.

[13] Y. Zhang, "Reduction of Water Footprint in Textile Dyeing," UPC, 2022.

[14] R. Eszter, "Removal of micro-pollutants from wastewater by bioremediation". Diss. Magyar Agrár-és Élettudományi Egyetem, 2022.

[15] Z. B. Bouabidi et al., Chemical Engineering Journal, vol. 334, pp. 837–844, 2018.

[16] R. Kant, Natural Science, vol. 4, pp. 22–26, 2012.

[17] P. K. Yeow et al., Biointerface Research in Applied Chemistry, vol. 11, pp. 8218–8232, 2021.

[18] S. De Gisi et al., Sustainable Materials and Technologies, vol. 9, pp. 10–40, 2016.

[19] S. El Harfi and A. El Harfi, Applied Journal of Environmental Engineering Science, vol. 3, pp. 311–320, 2017.

[20] E. O. Alegbe and T. O. Uthman, Heliyon, vol. 10, 2024.

[21] S. Benkhaya et al., Inorganic Chemistry Communications, vol. 115, p. 107891, 2020.

[22] M. H. R. Khudhair, Heliyon, 2019.

[23] D. Bhardwaj and N. Bharadvaja, Journal of Water Process Engineering, vol. 41, p. 102080, 2021.

[24] A. Gürses et al., Dyes and Pigments, pp. 31–45, 2016.

[25] M. T. Yagub et al., Advances in Colloid and Interface Science, vol. 209, pp. 172–184, 2014.

[26] M. Crepy, Documents pour le Médecin du Travail, pp. 565–576, 2004.

[27] A. Boulal and B. Mustapha, Master's thesis, Univ. Oran, 2014.

[28] I. Belbachir, Ph.D. dissertation, Univ. Tlemcen.

[29] G. Samira, Master's thesis, Univ. Badji Mokhtar, 2015.

[30] L. Tang et al., Chemical Engineering Journal, vol. 336, pp. 160–169, 2018.

[31] A. Zobeidi and A. A. Bebba, Research Journal of Pharmaceutical, Biological and Chemical Sciences, vol. 6, pp. 1097–1102, 2015.

[32] M. Rafatullah et al., Journal of Hazardous Materials, vol. 177, pp. 70–80, 2010.

[33] I. Gaballah and G. Kilbertus, Journal of Geochemical Exploration, vol. 62, pp. 241–286, 1998.

[34] N. An et al., Journal of Environmental Management, vol. 305, p. 114390, 2022.

[35] R. Kecili and C. M. Hussain, "Nanomaterials in Chromatography," in Nanomaterials in Chromatography. Elsevier, 2018, pp. 89–115.

[36] M. Alaqarbeh, RHAZES, vol. 13, pp. 43–51, 2021.

[37] N. N. Rudi et al., Heliyon, vol. 6, 2020.

[38] N. Sedira, Master's thesis, Univ. Souk-Ahras, 2013.

[39] G. N. White et al., Clays and Clay Minerals, vol. 40, pp. 555–560, 1992.

[40] M. Abbas, "Valorisation du noyau d'abricot," 2015.

[41] M. A. M. Razi et al., MATEC Web of Conferences, 2017, p. 06015.

[42] N. Sedira, Master's thesis, Univ. Souk-Ahras, 2013.

[43] R. D. Noble and P. A. Terry, Principles of Chemical Separations. CUP, 2004.

[44] K. A. Krishnan and T. Anirudhan, Water SA, vol. 29, pp. 147–156, 2003.

[45] O. Bouras, Ph.D. dissertation, Limoges, 2003.

[46] Y. S, Ho. "Citation review of Lagergren kinetic rate equation on adsorption reactions." Scientometrics 59.1 171-177, 2004.

[47] Y. Ho and G. McKay, Adsorption Science & Technology, vol. 16, pp. 243–255, 1998.

[48] Y.-S. Ho, Water Research, vol. 40, pp. 119–125, 2006.

[49] I. Langmuir, Journal of the American Chemical Society, vol. 40, pp. 1361–1403, 1918.

[50] H. Freundlich, Zeitschrift für Physikalische Chemie, vol. 57, pp. 385–470, 1907.

[51] M. J. Temkin and V. Pyzhev, 1940.

[52] M. Temkin, Acta Physiochimica URSS, vol. 12, pp. 327–356, 1940.

[53] A. Miraoui, and M.A. Didi. "Thorium (IV) sorption onto sodium bentonite and magnetic bentonite." Eur. Chem. Bull 4.11, 512-521,2015.

[54] N. A. Rosli et al., Journal of Engineering Research, vol. 13, pp. 433–444, 2025.

[55] OpenAI. DALL-E 3. (v. 3.0). (2025). OpenAI. Accessed: Jun. 01, 2026. [Online]. Available:

[56] D. M. Rachal et al., Geoarchaeology, vol. 41, p. e70059, 2026.

[57] A. Lancia et al., "Gypsum," in Kirk-Othmer Encyclopedia of Chemical Technology, pp. 1–22, 2000.

[58] C. Wu et al., Molecules, vol. 31, p. 484, 2026.

[59] M. Singh, Gypsum & Gypsum Products. CRC, 2022.

[60] K. Vasiliauskiene and A. Eisinas, "Hydration Properties of Mayenite and Gypsum Mixture," in FIM 2022.

[61] U. G. S. Kansas, Special Report on Gypsum, vol. 5, 1899.

[62] M. Golež et al., Journal of Cultural Heritage, vol. 32, pp. 38–43, 2018.

[63] F. Teng et al., Journal of Physical Chemistry C, vol. 115, pp. 17485–17494, 2011.

[64] Y.-F. Guan et al., Nature Communications, vol. 16, p. 713, 2025.

[65] H. Wu et al., Science of the Total Environment, vol. 691, pp. 9–15, 2019.

[66] M. J. Hassan et al., Applied Water Science, vol. 11, p. 7, 2021.

[67] J. Lefers et al., Water Research, vol. 21, pp. 1345–1354, 1987.

[68] A. Jiménez-Rivero and J. García-Navarro, Journal of Cleaner Production, vol. 167, pp. 1335–1344, 2017.

[69] D. C. Montgomery, Design and Analysis of Experiments. Wiley, 2017.

[70] L. C. Onyiah, Design and Analysis of Experiments. CRC, 2008.

[71] C. M. Anderson-Cook, Journal of the American Statistical Association, vol. 97, p. 1216, 2002.

[72] A. I. Khuri, Response Surface Methodology. World Scientific, 2006.

[73] A. I. Khuri and S. Mukhopadhyay, WIREs Computational Statistics, vol. 2, pp. 128–149, 2010.

[74] A. B. Naik and A. C. Reddy, Thermal Science and Engineering Progress, vol. 8, pp. 327–339, 2018.

[75] J. Li et al., Applied Microbiology and Biotechnology, vol. 74, pp. 563–571, 2007.

[76] M. Kousha et al., Chemical Engineering Journal, vol. 179, pp. 158–168, 2012.

[77] L. Wu et al., Expert Systems with Applications, vol. 39, pp. 8059–8065, 2012.

[78] M. Yolmeh and S. M. Jafari, Food and Bioprocess Technology, vol. 10, pp. 413–433, 2017.

Chapter III:

Materials and Methods

III.1 Introduction:

The Tow laboratories where all of the experiments for this research project were carried out were the pedagogical laboratory in the Department of Chemistry, University of El-Oued, and the Laboratory of Applied Chemistry and Environment, University of El-Oued. There are four main sections of this chapter that the following can be used to summarize. The initial step involves the practical steps followed for sample preparation of gypsum (GS), as a low-cost natural adsorbent. In the second section, four different dyes (cationic: Crystal Violet; anionic: Remazol Brilliant, Evans Blue, and Red.MX.5B) were used. Crystal Violet (CV) was selected as a model dye due to its textile use and high water stability, but its high stability in water raises environmental and health concerns. CV was then used for the rest of the study to investigate its removal from aqueous solution using gypsum (GS). About the third section, it briefly explains the instruments: The techniques used in this work include fourier transform infrared (FTIR), X-ray diffraction (XRD), analysis scanning electron microscopy (SEM)/energy-dispersive X-ray (EDX) analysis, and pHpzc. The fourth section provides an illustration of how to use the BBD by studying the effects of adsorbent dosage, solution pH, contact time, and temperature. Additionally, equilibrium data were analyzed by Langmuir, Freundlich, and Temkin isotherm models. Kinetic data were evaluated by pseudo-first-order and pseudo-second-order. Thermodynamic parameters (ΔG°, ΔH°, and ΔS°) were also determined to better understand the adsorption mechanism and determine the ideal operation parameters.

III.2 Adsorbent material and dye solution

In this study, waste gypsum ($CaSO_4 \cdot 2H_2O$) sample was collected from Bayada, El-Oued Southeast Algeria. Glassware was initially soaked in dilute HNO3 (10 % v/v) and washed with distilled water before use. The chemical reagents used included sodium hydroxide (NaOH), HCl (hydrochloric acid), and sodium chloride (NaCl) of a high purity grade were bought from Merck, which was used without further purification. Similarly, the following dyes were purchased from Sigma-Aldrich: Crystal Violet, Remazol Brilliant, Evans Blue, and Red.MX.5B. The dye stock solution was prepared by dissolving accurately weighted amounts of dye into 500 mL distilled water and the experimental solutions were obtained by diluting the stock solution to the required concentrations. All of the chemicals and reagents utilized in the research were of analytical grade and didn't require any additional purification.

III.3 Preparation of Gypsum

A considerable quantity of waste gypsum was collected from an old demolished wall located in a residential neighborhood in the municipality of Bayadha, El-Oued, in eastern Algeria, at coordinates 33°24′31″ N and 6°54′51.012″ E (Figure III.1). After collection, the material was homogenized through proportional blending to obtain a homogeneous composite sample with standardized mass. The resulting sample then underwent a simple preliminary preparation process, including crushing the gypsum using a laboratory mortar, followed by sieving to achieve a uniform particle size, without any prior chemical or thermal treatment. Finally, the prepared sample was stored in clean, dry containers until its use in the adsorption experiments Figure III.2 .

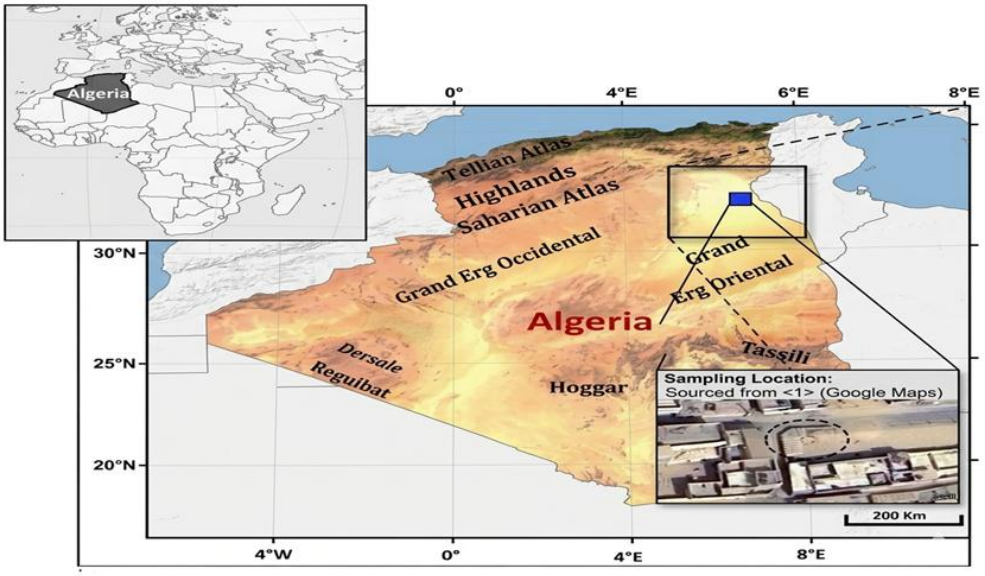

Figure III.1. Map of Algeria indicating the precise sampling location in the El-Oued district.

Figure III.2. Stages of preparing a natural confinement sample within the laboratory.

III.4 Material Analysis and Characterization Tools

The effect of modification on the surface properties of gypsum (GS) was analysed using various characterization tools, including XRD, FTIR, and SEM-EDX, and pHpzc. A brief description of these tools is discussed below.

III.4.1 X-ray Diffraction (XRD)

X-ray diffraction is one of the most important techniques used for characterizing crystalline materials and studying their structural and compositional properties. It is based on analyzing the diffraction of incident X-rays on the crystal planes of the material. The main objective of this technique is to accurately determine the crystal structure of powder samples and study their structural and compositional properties [1]

Analysis is performed using an XRD device equipped with Cu-Kα radiation, with diffraction patterns recorded within a range of angles at room temperature. The waste gypsum sample used in this study was employed to study its crystalline and structural properties.

Figure III.3. A Photographic Image of X-ray diffractometer

III.4.2 Fourier Transform Infrared Spectroscopy (FTIR)

FTIR spectroscopy is widely used for characterizing and studying chemical materials, as it enables the identification of the chemical structure of simple molecules and the detection of functional groups in organic compounds, in addition to providing precise information about the nature of chemical bonds within the material [2].In this work, an FTIR device of type (Agilent Technologies Cray 630 FTIR) was used to record the infrared spectra of samples before and after the adsorption process, with the aim of monitoring chemical changes and identifying functional groups present on the material's surface. Measurements were carried out within a wavenumber range between 4000 and 400 cm−1.

Figure III.4. A Photographic Image of FTIR Spectroscopy Instrument.

The study included the analysis of two different samples: the first was waste gypsum subjected to grinding and sieving to obtain homogeneous particles, while the second was gypsum after the adsorption of CV dye on its surface. After the adsorption process, the sample was dried at 105 °C to remove moisture and residual solution, then the samples were placed in special tubes in preparation for FTIR analysis and studying the changes that occurred on the gypsum surface due to adsorption.

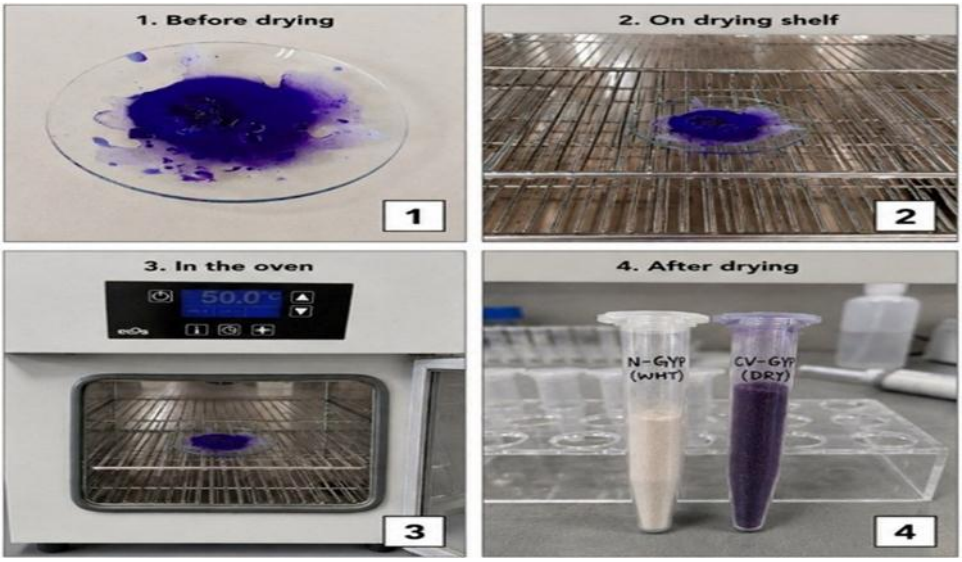

Figure III.5. Stages of preparing and drying gypsum samples prior to characterization processes.

III.4.3 Scanning Electron Microscopy (SEM-EDX)

SEM and EDX are key techniques for material characterization at the microscopic level. SEM directs a high-energy electron beam onto the sample surface, generating signals that produce high-resolution images of surface morphology, particle shape, and topography. Its main objective is to study surface structure and morphological changes [3]. EDX analyzes the characteristic X-rays emitted from chemical elements in the sample under electron

bombardment, determining elemental types and their percentages. Its main objective is elemental analysis and identifying chemical composition [4].

Combining SEM/EDX provides simultaneous morphological and compositional information, making them a powerful tool. In this work, these techniques were used to analyze gypsum before and after CV dye adsorption to track surface changes in shape, structure, and elemental composition, thereby explaining the adsorption mechanism and linking it to physical and chemical changes on the surface.

Figure III.6. A Photographic Image of SEM/EDX System.

III.4.4 Point of Zero Charge (pHpzc)

The effect of pH was evaluated by determining the point of zero charge (pHpzc), which is defined as the pH value at which the net charge of the adsorbent surface is zero. The method followed was based on the procedure described in reference [5, 6].

A series of beakers were prepared, where 0.3 g of gypsum (adsorbent) was added to 50 mL of sodium chloride (NaCl) solution at 0.1 M concentration. The initial pH was then adjusted within the range of 3 to 11 using sodium hydroxide (NaOH 0.1N) and hydrochloric acid (HCl 0.1N) solutions. Afterwards, the samples were placed on a magnetic stirrer and left for 24 hours to ensure equilibrium was reached. After the reaction period, the final pH values of each sample were measured, and by comparing the initial and final values, the pHpzc of the studied gypsum was determined.

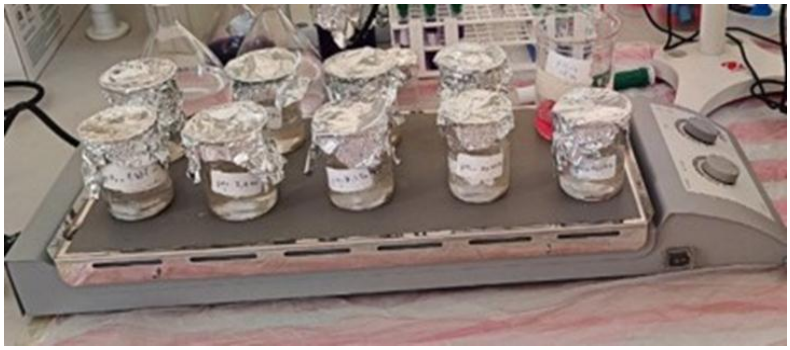

Figure III.7. Experimental setup for determining the pHpzc of the gypsum surface.

III.5 Selection of the Dyes:

A pretreatment study was carried out to determine which types of dyes the GS was effective on. Optimization studies were then carried out on the dye with the highest removal among four different anionic and cationic dyes under the same adsorption conditions. We used four different dyes (cationic: Crystal Violet; anionic: Remazol Brilliant, Evans Blue, and Red.MX.5B).

We conducted experiments on each dye. Adsorption experiment sets were prepared for each dye at 50 ppm concentrations. In these experiments 0.7g GS was added and mixed continuously on an orbital shaker at 250 rpm for 20 minutes of contact time. Following the adsorption experiments, the influent and effluent concentrations were measured using a UV–vis spectrophotometer (DLAB SP-V1100), and the removal efficiencies were calculated.

As a result of the preliminary adsorption experiments, higher removal efficiency was obtained for CV dye compared to the other dyes used in this study. Therefore, CV dye was selected as a model dye due to its textile use and high water stability, which raises environmental and health concerns. This dye was chosen for optimization experiments of adsorption conditions.

Table III.1. Percentage of dye removal by gypsum (GS)

Dye	Dye Removal (%)
Remazol Brilliant	26.56
Evans bleu	73.46
Red.MX.5B	20.22
Crystal Violet	82.38

Crystal Violet is characterized by physical and chemical properties shown in Table III.2.

Table III.2. Physicochemical Properties of CV dye [7]

Name	**Molecular formula**	**MW(g.mol^{-1})**	**Nature**	**λ_{max}(nm)**
CV	$C_{25}H_{30}ClN_3$	407.99	Cationic	590

Figure III.8. Crystal Violet dye (CV) used in the study.

III.5.1 Determination of Maximum Wavelength (λmax) of CV Dye

The maximum absorption wavelength (λmax) of CV dye was determined for use in spectral analyses. A stock solution of the dye (1000 mg/L) was prepared, and a diluted solution was then prepared using distilled water. The absorption spectrum was recorded using a UV-Vis spectrophotometer, and the results showed that λmax ≈ 590 nm.

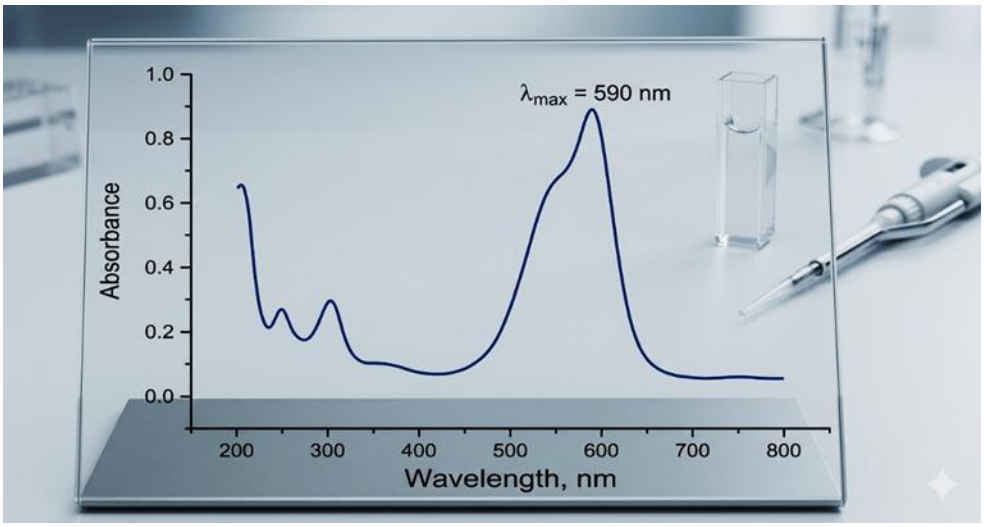

Figure III.9. Absorption spectrum of Crystal Violet dye in the UV-Visible range.

This wavelength was adopted in all subsequent spectral measurements of the studied solutions in order to obtain the best accuracy and sensitivity during analysis.

III.5.2. Determination of the Calibration Curve for CV dye

To construct the calibration curve, a series of standard solutions (5-50 mg/L) were prepared starting from the stock solution (1000 mg/L) by performing serial dilutions. After wards, the absorbance of each solution was measured using a UV-Vis spectrophotometer at the maximum wavelength (λmax = 590 nm). Then the calibration curve was plotted by representing the absorbance as a function of concentration, to extract the characteristic linear equation of the dye as follows: **Y = aX + b**

Where: Y: Represents absorbance (A), X: Represents concentration [C], a, b: Equation coefficients

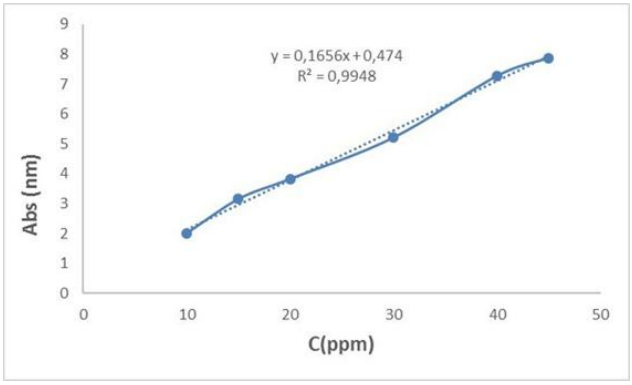

Figure III.10. Calibration curve for Crystal Violet dye (CV).

III.6 Design of experiment

The RSM Design-Expert is a specific functionality present in the Design-Expert program developed by Stat-Ease. It emphasizes RSM for process optimization. It facilitates investigators in designing experiments, fitting response surface models, and effectively analyzing data [8]. In this work, the Design Expert 13.0 software was used as a statistical tool for designing the experiments and performing statistical analysis. RSM-BBD was applied for optimizing and studying the impact of four adsorption key factors, such as GS dosage, solution pH, contact time, and temperature, on the CV dye. Table III.3 presents the levels of independent adsorption key factors applied in BBD model. A quadratic equation was adopted to predict the CV dye removal.

besides experimental data analysis as Equation (III.1) mentioned in the chapter (II).

$$Y = \beta_0 + \sum_{i=1}^{k} \beta_i X_i + \sum_{i=1}^{k} \beta_i X^2{}_i + \sum_{i=1}^{k} \sum_{j=1}^{k} \beta_{ij} X_i X_j + \varepsilon \qquad (\text{III.1})$$

Where, Y is the predicted response (CV dyes decolourization), k is the number of variables, i and j are the variable indices, β0 is the constant coefficient, βi and βii are linear and quadratic

coefficients, βij is the interaction coefficient, and E is a random error. Xi and Xj are the response and coded values for independent factors (-1, 0, and +1), respectively. Positive coefficients show synergy, while negative ones indicate antagonism between variables.

Table III.3. Factors and their levels used in the experimental design.

Codes	Factor	Low (-1)	Medium (0)	High (+1)
A	Adsorbent dose (g)	1	1.5	2
B	pH	4	7	10
C	Contact time (min)	5	25	45
D	Temperature (°C)	30	45	60

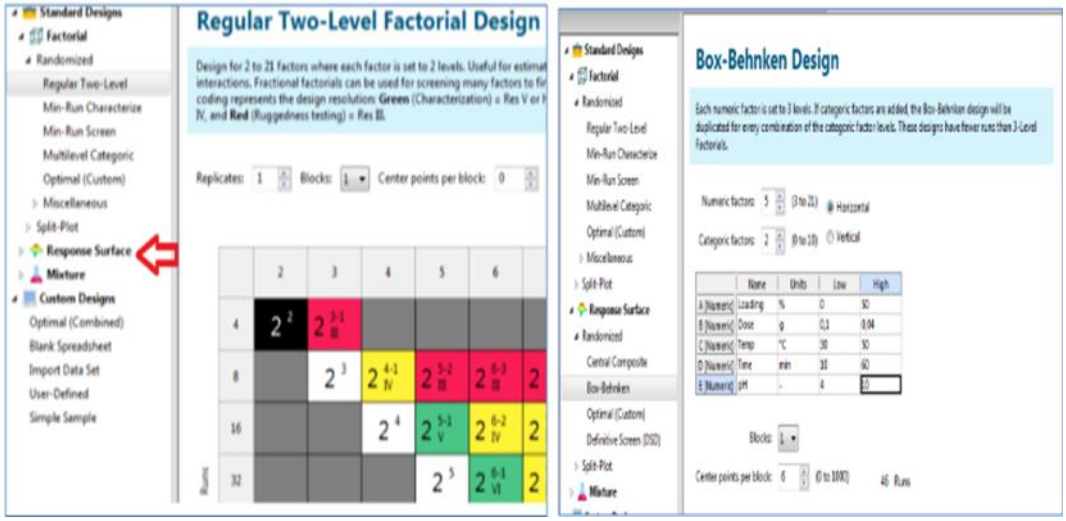

Figure III.11. The Response Surface Methodology (RSM) software

Using analysis of variance (ANOVA), researchers evaluated the accuracy of the model by calculating the coefficients, which included p-value, F-value, determination coefficient (R^2), predicted determination coefficient (R^2 pred), adjusted determination coefficient (R^2 adj), acceptable precision, degree of freedom (DF), and standard deviation [9]. These factors were essential in assessing the precision of both empirical data and the theoretical framework. The researchers utilized a dependable second-order quadratic model equation to forecast optimal values and investigate the interrelationships among the components. The optimal factor values were achieved by utilizing the regression equation, counter-response surface map, and imposing restrictions on the levels of variables. An initial set of tests was performed to detect extreme values of variables.

III.7 Batch Adsorption Studies

Adsorption studies of CV dye pollutants on GS were carried out under the same working conditions. According to BBD, a total of 29 experimental (runs) were conducted to optimize and analyze the effects of four key variables A: GS dosage (1 to 2 g), B: pH levels ranging (4 to 10) C: contact time (5 to 45 min), D: temperatures ranging (30 to 60 °C), and which were adjusted by HCl and NaOH (0.1 M). The outcomes of these 29 runs for both CV dye removals are detailed in Table III.4

A specified quantity of adsorbent was taken in a set of Erlenmeyer flasks (250 mL) containing

100 mL of dye solution before being placed in an shaking water bath incubator (Memmert WNB 29) and set with 110 rpm, the mixture was separated using a centrifuge (SCILOGEX SCI 412) at 4500 rpm for 10 minutes. Finally, the concentrations of CV dye was calculated by UV-Vis spectroscopy (DLAB SP-V1100) at λmax = 590 nm. The CV dye removal percentage (R%), and the adsorption capacity (qe, mg/g) of both dyes at various time intervals are calculated by Eqs. (III.2) and (III.3), respectively.

$$R(\%) = \frac{C_0 - C_e}{C_0} \times 100 \qquad \text{(III.2)}$$

$$q_e = \frac{V}{W}(C_0 - C_e) \qquad \text{(III.3)}$$

Where:C0: Initial concentration of CV dye in solution (mg/L), Ce: Residual dye concentration at equilibrium (mg/L), V: Volume of dye solution used (L), and W: Mass of waste gypsum used (g)

Figure III.12. Photographs of the equipment used for dye adsorption experiments: (a) UV-Visible (UV-Vis) spectrophotometer, (b) shaking water bath, and (c) centrifuge.

Table III.4. The 4 varibles BBD matrix and experimental data for CV dye removal.

Run	A:Adsorbent dose (g)	B:pH	C: Time (min)	D: Temp. (°C)	CV removal (%)
1	1	7	25	60	71.75
2	2	7	25	60	87.11
3	1.5	10	25	30	90.49
4	2	7	25	30	88.26
5	2	4	25	45	78.03
6	1	4	25	45	44.26
7	1.5	7	25	45	72.86
8	1.5	7	25	45	72.86
9	1	7	45	45	84.72
10	1.5	7	5	30	67.28
11	1.5	4	45	45	72.83
12	1	7	5	45	56.77
13	1.5	4	25	60	65.68
14	2	10	25	45	95.30
15	1.5	10	25	60	90.30
16	1	7	25	30	62.78
17	1.5	4	25	30	64.03
18	1.5	7	25	45	72.86
19	1.5	7	25	45	72.86
20	1	10	25	45	80.33
21	1.5	10	45	45	94.61
22	1.5	7	5	60	76.83
23	1.5	7	45	30	80.99
24	1.5	7	45	60	82.06
25	1.5	10	5	45	88.22
26	2	7	45	45	94.34
27	1.5	4	5	45	57.48
28	1.5	7	25	45	72.86
29	2	7	5	45	88.03

III.8 Adsorption Kinetics

Kinetic models are used to understand the behavior of the adsorption process and to determine the rate of interaction of the adsorbate with the adsorbent surface. The most commonly used models are the Pseudo-First-Order (PFO) and the Pseudo-Second-Order (PSO) models.

III.8.1 Pseudo-First-Order Model

The linear equation (III.4), PFO kinetic models are defined by the following equations:

$$\ln(q_e - q_t) = \ln q_e - K_1 t \qquad \text{(III.4)}$$

The PSO kinetic model for adsorption is expressed as a plot of $\frac{t}{q_t}$ vs t. The qe (cal) (mg/g) parameter can be obtained from the intercept, and The k_2 ($g \cdot mol^{-1} \cdot min^{-1}$) the rate constant of adsorption according PSO from slope

III.8.2 Pseudo-Second-Order Model

The linear equation (III.5), PSO kinetic models are defined by the following equations:

$$\frac{t}{q_t} = \frac{1}{K_2 q_e^2} + \frac{t}{q_e} \qquad \text{(III.5)}$$

The PSO kinetic model for adsorption is expressed as a plot of $\frac{t}{q_t}$ vs t. The qe (cal) (mg/g) parameter can be obtained from the intercept, and the k_2 ($g \cdot mol^{-1} \cdot min^{-1}$) the rate constant of adsorption according PSO from slope.

III.9 Adsorption Isotherms

Adsorption isotherms explain the interaction between adsorbate with adsorbent, where it describes the interaction on how the dye molecules distribute between the bulk dye solution and the solid adsorbent once the system attended equilibrium state.

The linear Freundlich isotherm, Langmuir and Temkin can be obtained from the equilibrium data. [10].

The Freundlich model is an empirical model that accounts for the heterogeneity of adsorption energies on the surface of the adsorbent. Its linear form is given by the following equation (III.6) [11]:

$$\ln q_e = \ln K_f + \frac{1}{n} \ln C_e \quad \text{(III.6)}$$

When plot of ln qe versus ln Ce, a straight line is obtained, and its slope is a measure of the adsorption intensity (n), while the intercept of Kf represents the adsorption capacity.

The Langmuir model is the most commonly used equation, and the linearized form is written as follows equation (III.7) [12]:

$$\frac{C_e}{q_e} = \frac{1}{q_{max} \times K_L} + \frac{C_e}{q_{max}} \quad \text{(III.7)}$$

Hence, a straight line with a slope $\frac{\mathbf{1}}{\boldsymbol{K_L \times q_{max}}}$ and an intercept as $\frac{\mathbf{1}}{\boldsymbol{K_L \times q_{max}}}$ can be obtained by plotting Ce/qe versus Ce

The Temkin model assumes that the adsorption energy of all molecules decreases linearly with increasing surface coverage. The Temkin model can be described by the following linear equation (III.8) [13]:

$$q_e = \frac{RT}{b} \ln K_T + \frac{RT}{b} \ln C_e \quad \text{(III.8)}$$

The equilibrium binding constant (K_T) can be obtained by plotting (K_T) versus $\ln C_e$ which yields a linear relationship. The slope of the resulting straight line corresponds to $\frac{RT}{b}$, while the intercept $\ln C_e$. From these values, the Temkin parameters the heat-related constant (b) and the equilibrium binding constant (KT) can be calculated.

III.10 Adsorption Thermodynamics

The adsorption behavior of CV dye onto GS was evaluated through thermodynamic analysis. Key parameters including the standard Gibbs free energy change (ΔG°), standard enthalpy change (ΔH°), and standard entropy change (ΔS°) were determined to elucidate the nature of the adsorption process. Adsorption experiments were conducted at temperatures ranging from 30°C to 60°C using a shaking water bath.

$$\ln K_d = \frac{\Delta S}{R} - \frac{\Delta H}{RT} \quad \text{(III.9)}$$

$$K_d = \frac{(C_i - C_t)}{C_t} \frac{V}{W} \quad \text{(III.10)}$$

$$\Delta G° = \Delta H° - T\Delta S° \quad \text{(III.11)}$$

The thermodynamic parameters ΔH° (enthalpy change) and ΔS° (entropy change) were determined from the linear van't Hoff plot of ln K_d versus $\left(\frac{1}{T}\right)$, where the slope corresponds to $\left(\frac{-\Delta H^{\circ}}{R}\right)$ and the intercept equals $\left(\frac{\Delta S^{\circ}}{R}\right)$

III.11 Regeneration and Reuse of Waste Gypsum

After completing the adsorption experiments, the waste gypsum loaded with CV dye was separated from the solution by centrifugation, discarding the liquid phase and retaining the solid precipitate. The saturated samples were then collected and subjected to a drying process. The reuse study was based on the optimal conditions previously obtained from the adsorption experiments, namely: adsorbent mass of 2 g, initial dye concentration of 25 ppm, pH = 10, temperature of 45°C, and contact time of 25 min. To regenerate the adsorbent material, the saturated gypsum was washed using a 1 M hydrochloric acid solution several consecutive times until a clear washing solution was obtained, indicating the removal of the majority of adsorbed dye molecules. Afterwards, the sample was washed with distilled water until reaching a near-neutral pH (pH 7), and then dried again [14].

The regenerated adsorbent material was reused in a second adsorption cycle under the same previous optimal experimental conditions, following the same separation and regeneration steps after each adsorption cycle.

Bibliography

[1] F. J. Muhana, B. I. El-Eswed, and F. I. Khalili, Desalination and Water Treatment, vol. 87, pp. 292–305, 2017.

[2] A. H. Jawad et al., Journal of Polymers and the Environment, vol. 30, pp. 2759–2773, 2022.

[3] J. I. Goldstein et al., Scanning Electron Microscopy and X-Ray Microanalysis. Springer, 2017.

[4] E. R. Levin, Scanning Electron Microscopy, 1986.

[5] B. M. Babić et al., Carbon, vol. 37, pp. 477–481, 1999.

[6] R. Mecheri et al., Materials, vol. 16, p. 4082, 2023.

[7] J. Y. Tong, "Batch Study and Experimental Design," UTAR, 2024.

[8] N. Malekjani and S. M. Jafari, "Math. Stat. Appl. Food Eng.," in Math. Stat. Appl. Food Eng. CRC, 2020, pp. 181–203.

[9] S. Zhu et al., NeuroReport, vol. 25, pp. 1151–1155, 2014.

[10] N. Ayawei, A. N. Ebelegi, and D. Wankasi, Journal of Chemistry, vol. 2017, p. 3039817, 2017.

[11] Y. A. E. H. Ali et al., Journal of Molecular Liquids, vol. 399, p. 124435, 2024.

[12] S. Banerjee et al., Journal of Molecular Liquids, vol. 213, pp. 162–172, 2016.

[13] E. Dundar, "Modélisation par la Théorie du Potentiel," Univ. Québec, 2014.

[14] G. Crini, Bioresource Technology, vol. 97, pp. 1061–1085, 2006.

Chapter IV :

Results and Discussion

IV.1 Introduction

In this chapter, the physicochemical properties of waste gypsum (GS) as an adsorbent are presented and discussed. These properties were investigated to evaluate its efficiency in removing CV dye from aqueous solutions. This study is part of the ongoing search for effective and environmentally friendly adsorbent materials for the treatment of dye contaminated wastewater. The factors affecting the adsorption process were also analyzed using the Box-Behnken design (BBD) to determine the optimal conditions for achieving the highest possible removal yield. In addition, the study addressed the kinetic and thermodynamic aspects of the adsorption process, along with the adsorption isotherm models, to understand the nature and mechanism of interaction of the dye with the GS surface.

IV.2 Results and characterization of the material

IV.2.1 X-ray diffraction analysis (XRD)

The XRD analysis was performed on the waste gypsum (GS) sample used as a starting material in this study to determine its crystalline structure. The diffraction pattern showed sharp reflection peaks of high intensity, indicating the good crystalline nature of the sample [1]. The main peaks of waste gypsum (GS) ($CaSO_4 \cdot 2H_2O$) were identified at diffraction angles (2θ) of 11.6°, 20.7°, 23.4°, 27.0°, and 29.2°, corresponding to the crystallographic planes (020), (021), (040), (041), and (131), respectively. These results are in good agreement with the standard diffraction card data from the ICDD database (Card No. 33-0311) [2].

The absence of additional peaks with significant intensity or broad background indicates that the sample possesses a high degree of crystallinity, with very minor possible mineral impurities, which enhances the reliability of subsequent results in comparative analyses of thermally or chemically treated samples [3].

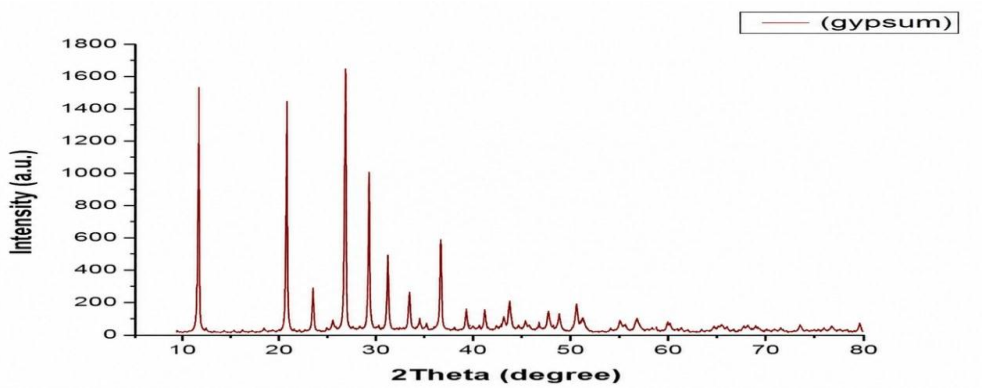

Figure IV.1. XRD pattern of waste gypsum (GS).

IV.2.2 Fourier Transform Infrared Spectroscopy (FTIR)

The FTIR analysis is one of the most important spectroscopic techniques used to identify functional groups and chemical bonds in materials, by measuring the absorption of characteristic vibrations of each chemical bond. This analysis is also widely used to study surface changes of materials before and after the adsorption process, as a shift in peak positions or a change in their intensity is evidence of an interaction between the adsorbed molecules and the active sites on the material surface [4].

By comparing The FTIR spectrum of GS **Figure IV.2**, several changes were observed confirming the success of the adsorption process. In the region 3200–3600 cm^{-1}, a broad band appears corresponding to O–H stretching vibrations, which became broader after adsorption, indicating the involvement of hydrogen bonds between the gypsum surface and CV dye molecules [5]. A band around 1620 cm^{-1} is also observed, mainly attributed to the bending vibrations of water molecules adsorbed within the gypsum structure, with a possible weak contribution from the aromatic C=C vibrations of the dye. A slight change in the intensity of this band was observed after adsorption, indicating that the surface environment of the material is affected by the presence of adsorbed molecules [6].

In the region 1000–1200 cm^{-1}, characteristic peaks appear for the stretching vibrations of sulfate groups (SO_4^{2-}) specific to the gypsum structure. A decrease in the intensity of these peaks with a slight shift was observed after adsorption, indicating surface interactions between the active sites on the gypsum surface and the positively charged dye molecules [7].

Furthermore, the slight changes recorded below 800 cm^{-1} indicate surface disturbances resulting from the immobilization of dye molecules on the material surface without any noticeable change in the basic crystalline structure of GS [8].

Overall, the FTIR results confirm that the adsorption of CV dye onto gypsum occurs mainly through electrostatic interactions, hydrogen bonds, and surface interactions between the functional groups of gypsum and the dye molecules, without significant structural change in the adsorbent, indicating that the adsorption process was essentially surface-based.

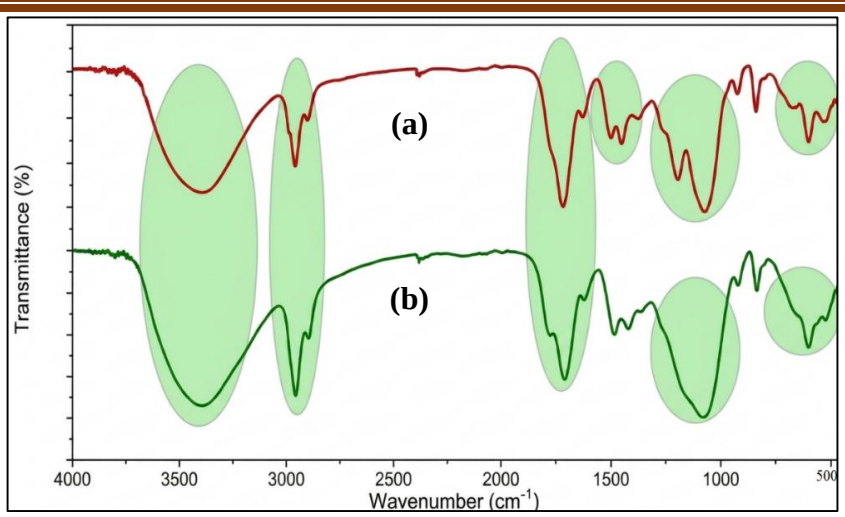

Figure IV.2. FTIR spectra of (a) waste gypsum (GS), and (b) (GS-CV) after adsorption of CV dye.

IV.2.3 Scanning Electron Microscopy with Energy Dispersive X-ray Spectroscopy (SEM-EDX)

The morphological structure of GS was examined by SEM-EDX analysis in Figure (IV.3) show a clear change in the surface morphology of the gypsum sample before and after CV dye adsorption. In Figure IV.3.a1 , the GS surface appears composed of platelet particles with a relatively smooth surface and regular structure, while Figure IV.3.b1 , shows deposits and fine particles covering the material surface, as indicated by arrows, demonstrating the attachment of dye molecules to the active sites of the GS surface after the adsorption process [9].

The results of EDX elemental analysis, shown in Figure IV.3,a2,b2 reveal a noticeable change in the surface chemical composition after adsorption. Spectrum IV.3,a2 shows the basic elements characteristic of gypsum: oxygen (O), calcium (Ca), sulfur (S), and carbon (C). Meanwhile, spectrum IV.3,b2 shows the appearance of signals for nitrogen (N) and chlorine (Cl), along with an increase in carbon percentage, elements associated with the chemical structure of CV dye. This change in elemental composition is clear evidence of the successful adsorption of the dye onto the GS surface [10]. The recorded changes in weight concentrations of the elements indicate a transition of the GS surface from an initially nearly pure state to a surface covered with adsorbed organic molecules, reflecting surface interactions between dye molecules and active sites of the adsorbent [11].

These results are consistent with the previous FTIR data, supporting the proposed adsorption mechanism and confirming the effectiveness of GS in removing CV dye from the aqueous medium.

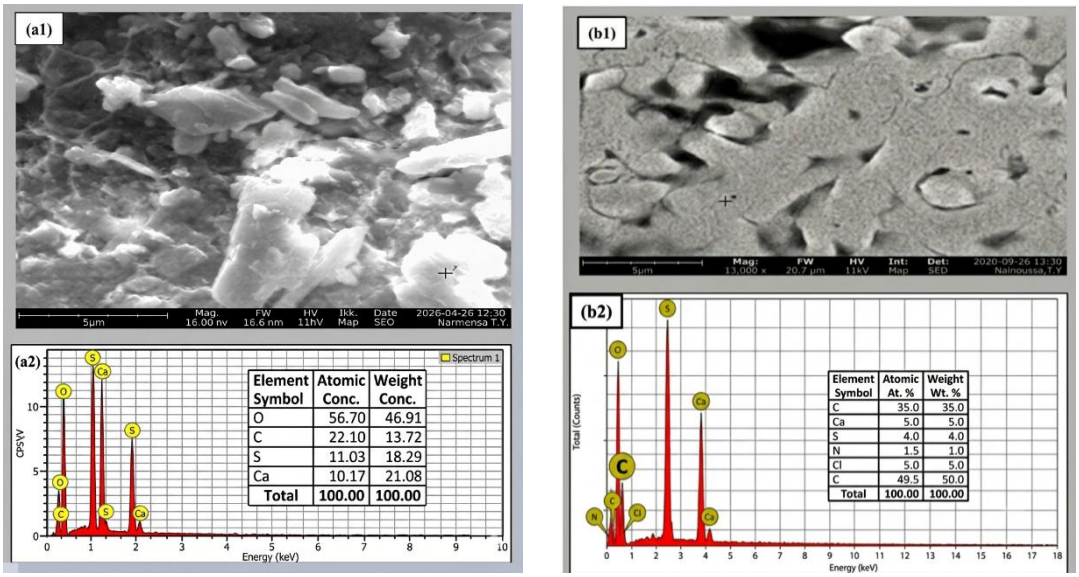

Figure IV.3. SEM images of (a) GS, and (b) GS after adsorption of CV dye

IV.2.4. Point of Zero Charge (pHpzc)

The point of zero charge is one of the fundamental physical and chemical properties used in the characterization of adsorbent materials, as it represents the pH value at which the net surface charge of the material is zero due to the balance of positive and negative charges on the surface [12].

The results showed that the pH_{pzc} value for GS surface is 6.87. This value indicates

that the nature of the surface charge of the material changes depending on the solution medium as follows:

At pH values below 6.87 (pH < 6.87), the medium is rich in hydrogen ions, leading to protonation of the functional groups on the gypsum surface, thus the surface acquires a positive charge. In this case, electrostatic repulsion occurs between the material surface and cationic dyes such as Crystal Violet, limiting the adsorption efficiency.

At pH values above 6.87 (pH > 6.87), the concentration of hydroxide ions in the medium increases, leading to deprotonation of the surface and its acquisition of a negative charge. As a result, the electrostatic attraction forces between the negatively charged surface and the positively charged dye are enhanced, which contributes to increasing the adsorption efficiency. This result indicates that GS surface shows greater effectiveness in removing cationic dyes in neutral and alkaline media, which is consistent with the known behavior of adsorption processes based on electrostatic interactions [13].

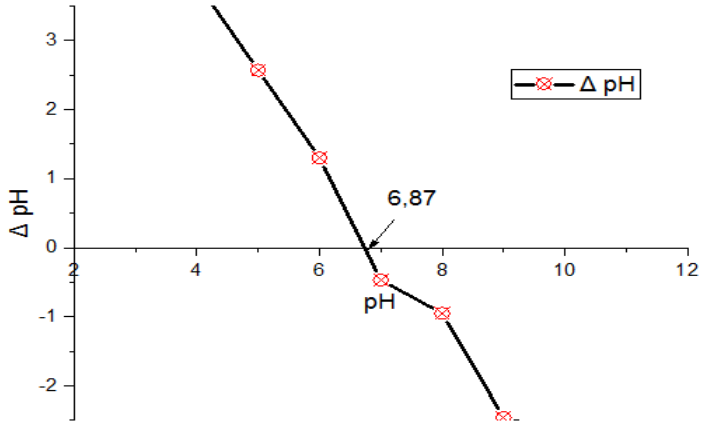

Figure IV.4. pH_{pzc} of GS

IV.3 Optimization using (BBD-RSM) design

Table (III.4) (refer to previous chapter) shows that BBD included 29 laboratory experiments, and it was adopted to study the individual and interaction effects of different factors on the removal efficiency of CV dye as a response variable. The independent factors studied were adsorbent dosage (A), solution pH (B), contact time (D), and temperature (C). The results showed that the highest removal efficiency (95.30%) was obtained from run 2 under the following conditions: adsorbent dose (A: 2 g), solution pH (B: 10), contact time (D: 25 min), and temperature (C: 45°C).

IV.3.1 Model fitting and statistical analysis

The significance of the developed mathematical model for CV removal was evaluated using analysis of variance (ANOVA) **Table.IV.1.** The results showed that the model F-value was 39.79 with a p-value < 0.0001, indicating that the model is statistically significant and that the probability of this effect being due to noise is less than 0.01% [14].

The linear terms showed that dosage (A), pH (B), and contact time (C) each have a significant effect on the removal yield at a significance level < 0.05, while temperature (D) did not show a significant individual effect within the studied range [14, 15].

Regarding interaction effects, it was found that the interactions AB and AC have a significant effect on the response, while the other binary interactions (AD, BC, BD, CD) were not statistically significant, indicating that the effect of dosage is influenced by both pH and contact time [15].

The quadratic terms showed that A^2 and C^2 have a significant effect, indicating a nonlinear relationship between these variables and dye removal efficiency, a common feature in RSM models [15]. Based on the statistical results, the reduced mathematical model can be expressed by the following equation:

$$\textbf{CV removal (\%)} = +72.86+10.87A+13.07B+6.24C-4.70AB-5.41AC+2.42A^2+3.98C^2 \quad \text{(IV.1)}$$

The fit statistics showed that the coefficient of determination value was: $R^2 = 0.9755$ indicating that the model explains 97.55% of the variations occurring in the adsorption process, reflecting a high goodness of fit of the mathematical model [14].The closeness between Adjusted $R^2 = 0.9510$ and Predicted $R^2 = 0.8588$ (difference < 0.2) indicates good agreement between predicted and adjusted values, confirming the model's ability to predict experimental results with acceptable accuracy [15]

Table.IV.1. Analysis of variance (ANOVA) for CV dye removal (%)

Source	Sum of Squares	df	Mean Square	F-value	p-value
Model	4369.16	14	312.08	39.79	<0.0001
A-Dose	1418.32	1	1418.32	180.85	<0.0001
B-pH	2052.51	1	2052.51	261.72	<0.0001
C-Time	468.00	1	468.00	59.67	<0.0001
D-Temp	33.00	1	33.00	4.21	0.0594
AB	88.36	1	88.36	11.27	0.0047
AC	117.07	1	117.07	14.93	0.0017
AD	25.60	1	25.60	3.26	0.0923
BC	20.07	1	20.07	2.56	0.1320
BD	0.8464	1	0.8464	0.1079	0.7474
CD	17.98	1	17.98	2.29	0.1523
A^2	38.20	1	38.20	4.87	0.0445
B^2	8.75	1	8.75	1.12	0.3086
C^2	103.09	1	103.09	13.15	0.0028
D^2	23.70	1	23.70	3.02	0.1040
Residual	109.80	14	7.84		
Lack of Fit	109.80	10	10.98		
Pure Error	0.0000	4	0.0000		
Cor Total	4478.95	28			

Diagnostic plots of RSM can also be used to evaluate the adequacy of the statistical model used in the study of CV adsorption onto GS, by analyzing the distribution of residuals and

studying the relationship between actual and predicted removal efficiency. **Figure IV.5** shows the normal probability plot of residuals and the plot of the relationship between predicted and actual values for CV dye removal using GS.

The normal probability plot **Figure IV.5.a** of residuals shows that most points are distributed near the straight line, indicating that the residuals follow a normal distribution and that experimental errors are independent and random, confirming the validity of the statistical assumptions of the mathematical model [15].

The predicted vs. actual plot **Figure IV.5.b** shows a clear agreement between experimental results and values predicted by the model, as most points are concentrated near the straight line, indicating good agreement between actual and predicted values, and confirming the high predictive efficiency of the statistical model used to describe the adsorption process of CV dye onto GS [16].

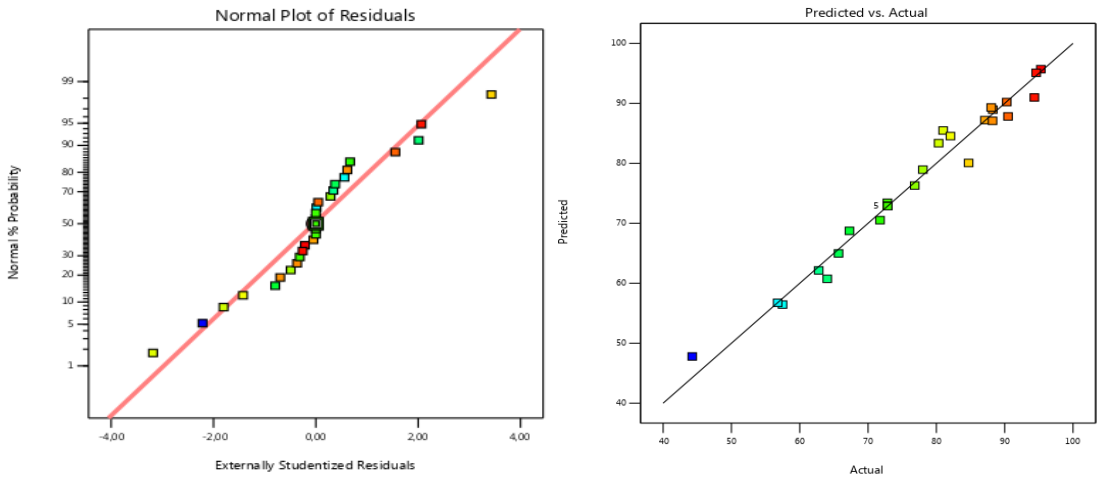

Figure IV.5. (a) Normal probability plot of residuals for CV dye removal, (b) plot of the relationship between the predicted and actual values of CV removal (%).

Plotting the response surface graphs for CV dye removal allowed us to demonstrate how the individual parameters affected the response (R1) while keeping the other variables at their mean values **Figure IV.6** . These plots allow the determination of the individual effect of each factor and the sensitivity of the response to its change, and also help to understand the behavior of the adsorption process within the RSM model.

From the plot for dosage (A: dose), it was observed that increasing the gypsum amount from 1 to 2 g led to a clear increase in the response value, as the dye removal percentage gradually increased with increasing dosage. This indicates that the dosage has a positive effect on the adsorption process. This behavior can be explained by the increase in the number of

active sites and surface area available for the adsorption of CV dye molecules when the adsorbent amount is increased, leading to enhanced dye removal from the solution.

Regarding the effect of pH (B: pH), the curves show that increasing the pH from 4 to 10 led to a significant increase in the response, indicating a positive effect of this factor. This is because CV is a cationic dye, so increasing the pH reduces the concentration of H^+ ions on the gypsum surface, increasing the negative charge of the surface and enhancing the electrostatic attraction forces between the adsorbent surface and the positively charged dye molecules [17].

For contact time (C: Time), it is observed that the response gradually increases with increasing time from 5 to 45 minutes, but this effect appears less severe compared to dosage and pH. This indicates that increasing the contact time allows for greater interaction between the dye molecules and the active sites on the gypsum surface, gradually raising the amount of adsorbed dye until approaching equilibrium. The limited slope of the curve may indicate that a large part of the adsorption occurs during the initial stages of the process, and then the adsorption rate becomes slower over time due to the decrease in available sites [18].

Regarding the effect of temperature (D: Temp), the plot shows that increasing the temperature from 30 to 60 °C resulted in only a slight increase in the response, indicating that the temperature effect was limited compared to the other factors. This can be explained by the fact that raising the temperature may improve the movement of dye molecules and their transport towards the gypsum surface, but the adsorption process here does not appear to be highly dependent on temperature within the studied thermal range.

Conversely, all plots demonstrate that the factors are involved in multiple interactions, suggesting that the effect of any given factor within the mathematical model is not solely attributable to its individual contribution but is also contingent upon its synergistic or antagonistic interplay with other variables.Therefore, the interpretation of these curves must take into account the results of binary interactions and the statistical model equation referred to in **equation (IV.1)** .The upward trend of most curves corresponds to the signs of the positive coefficients in the mathematical equation of the model, confirming a positive effect of dosage, pH, contact time, and temperature on the removal percentage of CV dye using natural gypsum, albeit with different intensities of each factor

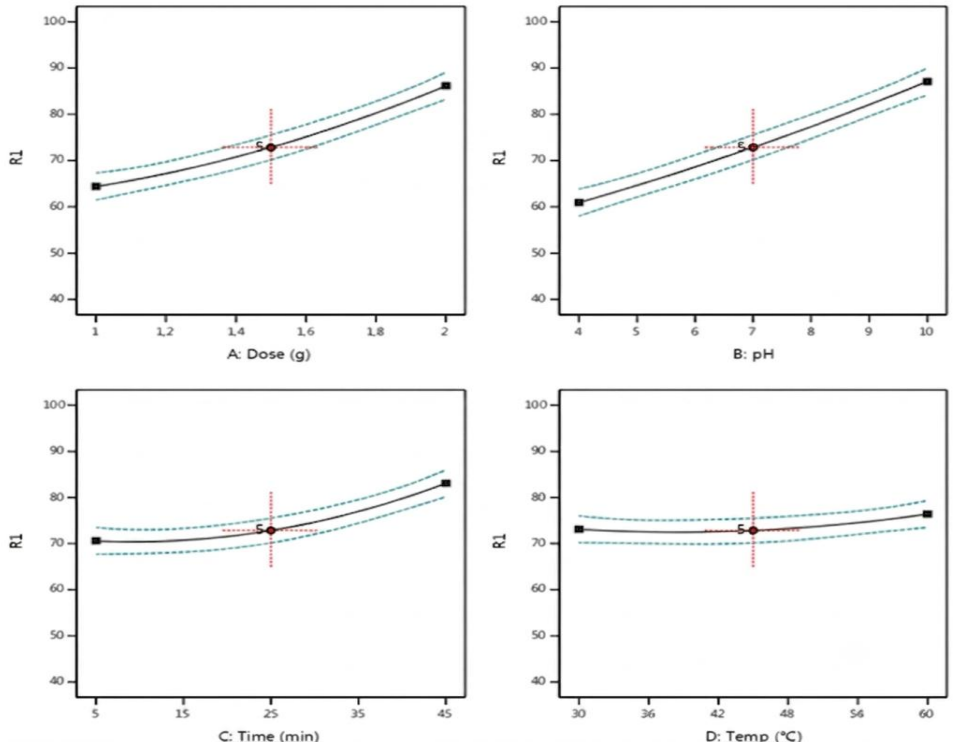

Figure IV.6. Influence of the main working parameters on CV dye adsorption process.

IV.3.2 Statistically significant interactions for CV dye removal

Figure (IV.7) shows the three-dimensional (3D) response surface plot illustrating the effect of the interaction between adsorbent dosage (A: dose) and pH (B: pH) on the removal of CV dye using natural gypsum. This interaction showed considerable statistical significance ($p = 0.0047$), indicating a significant effect of the interaction between the two factors on the response (R1), where the other operating factors were fixed at their mean values during the study.

The results show that the removal percentage increases with increasing both dosage and pH, with the lowest values recorded at low dosages and acidic medium, while it increases significantly at high dosages and alkaline medium. The effect of dosage is explained by the increase in the number of active sites and surface area available for adsorption [19], while the effect of pH is attributed to the reduced competition with H^+ ions and the increase in the negative charge on the gypsum surface, which enhances electrostatic attraction with the cationic dye [17]. The surface plot also indicates a positive synergy between dosage and pH, which is reflected in improved removal efficiency without sharp drop regions. This mechanism aligns with findings by M .J. Hassan et *al*. (2021), who reported similar behavior in dye adsorption using gypsum [10].

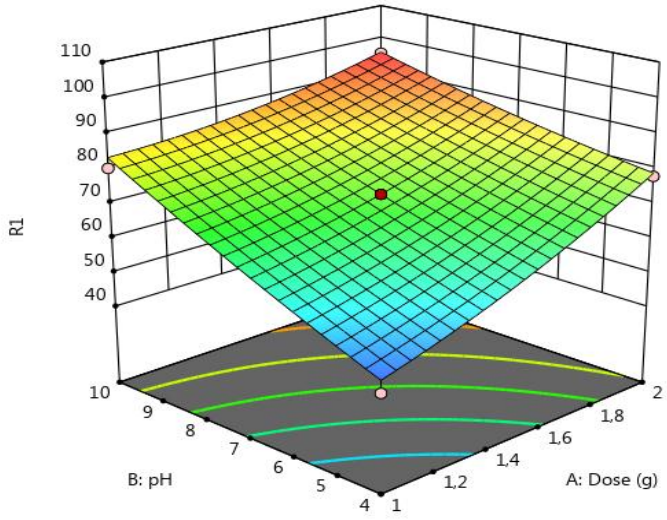

Figure IV.7. 3D response surface plot of CV removal showing interaction between adsorbent dose and pH.

Figure (IV.8) shows the three-dimensional (3D) response surface plot illustrating the effect of the interaction between adsorbent dosage (A: Dose) and contact time (C: Time) on the removal efficiency of CV dye. Statistical analysis showed that this interaction has high significance ($p = 0.0017$), indicating a clear synergistic effect between the two variables in the adsorption process.

The results indicate that the removal efficiency gradually increases with increasing both adsorbent dosage and contact time, where the lowest removal percentages were recorded at the lowest dosage and shortest contact time, while the highest removal efficiency was achieved at high dosages (2 g) and longer contact time (45 min).

The positive effect of contact time is attributed to providing sufficient time for dye molecules to transfer from the solution to the active sites on the adsorbent surface, as the adsorption process goes through several stages including surface diffusion then intra-particle diffusion until equilibrium is reached [20]. Moreover, increasing the adsorbent dosage provides a larger number of active sites, enhancing the adsorption capacity and raising the removal efficiency [21].

This behavior agrees with many previous studies that confirmed that the interaction between contact time and adsorbent dosage is one of the fundamental factors in improving the removal of organic pollutants in batch systems [22].

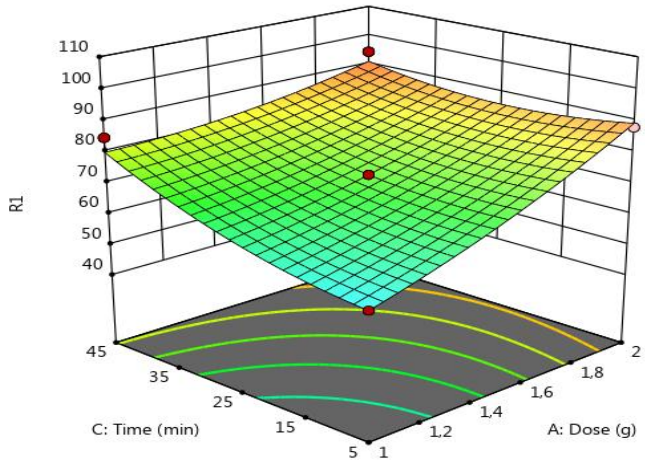

Figure IV.8. 3D response surface plot of CV removal showing interaction between adsorbent dose and time.

IV.4 Effect of initial dye (CV) concentration as a function of contact time

The effect of initial CV dye concentration and contact time on adsorption equilibrium was investigated. The adsorption capacity, qt (mg/g), as a function of contact time at various initial CV dye concentrations (25, 50, 100, 150, 200, and 250 mg/L) was examined, as depicted in figure (IV.9). During these experiments, other optimum factors were kept constant: adsorbent dose = 2 g, solution pH = 10, and temperature = 45 °C. It was observed from figure (IV.9) that the quantity of CV dye molecules adsorbed onto the surface of the GS increased from 0.5 to 4.31 mg/g as the initial CV dye concentration increased from 25 to 250 mg/L. This can be attributed to the higher concentration gradient, which provides a driving force to move the CV dye toward active adsorption sites [23]

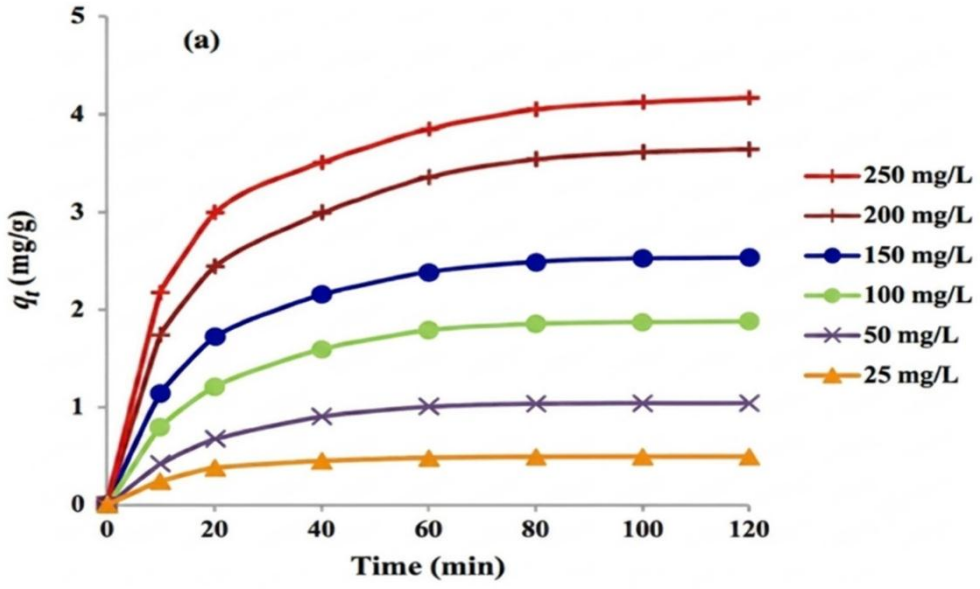

Figure IV.9. Effect of initial CV concentration on adsorption using GS

IV.5 Adsorption kinetics

Adsorption kinetics was studied by applying the pseudo-first-order (PFO), and pseudo-second-order (PSO) models [24, 25]. The results showed that the coefficient of determination (R^2) values for the pseudo-second-order model were significantly higher (ranging between 0.983 and 0.996) compared to the pseudo-first-order model, indicating that the PSO model

is the most suitable for describing the adsorption kinetics. As explained by Ho and McKay [18], the good agreement of the data with this model supports the hypothesis that chemisorption is the rate-limiting step of the process.

Table IV.2 also shows a strong agreement between the experimental adsorption capacity values **($q_{e,exp}$)** and the theoretically calculated values **($q_{e,cal}$)** for the pseudo-second-order model, confirming the accuracy of this model in representing the kinetic behavior of the adsorption process. On the other hand, a decrease in the rate constant (k_2) was observed with increasing initial concentration of the adsorbate. This behavior is attributed to the increased competition for available active sites on the adsorbent surface at high concentrations, leading to a decrease in the apparent adsorption rate, which is consistent with theories related to adsorption kinetics. This result reflects that the CV dye uptake on the GS surface is governed by chemisorption phenomenon [26].

Table IV.2. Kinetic models of adsorption process

Concentration (mg/L)	$q_{e\ exp}$ (mg/g)	Pseudo-first-order			Pseudo-second-order		
		$q_{e\ cal}$ (mg/g)	K_1 (1/min)	R^2	$q_{e\ cal}$ (mg/g)	K_2*10^{-2} (g/mg.min)	R^2
25	0,50	0,20	0,0377	0,7806	0,54	0,26590	0,995
50	1,05	0,31	0,0275	0,969	1,08	0,15870	0,996
100	1,94	1,58	0,0704	0,9217	1,88	0,05347	0,9917
150	2,72	2,38	0,1168	0,87	2,62	0,09093	0,9944
200	3,64	3,04	0,0341	0,9388	3,56	0,01608	0,9958
250	4,31	3,44	0,0912	0,9034	4,17	0,02319	0,983

IV.6 Adsorption isotherm

Adsorption data were analyzed using Freundlich [27], Langmuir [28], and Temkin [29] models in order to determine the model best fitting the experimental results and to un- derstand the nature of adsorption on the adsorbent surface.

The results showed that the Freundlich model is the best in describing the adsorption process, recording the highest coefficient of determination R^2 = 0.9932 values **Table IV.3** and **Figure IV.10**, indicating that adsorption occurs on a heterogeneous surface and in a multilayered manner [28, 30]. The value of n=1.47 indicates that the adsorption process is favorable and effective [30], while the value of K_f=0.23 reflects the adsorption capacity of the adsorbent.

The Langmuir model gave an R^2=0.9268, indicating that the monolayer adsorption hypothesis does not fully represent the system, while the maximum adsorption capacity q_{max}=8.43 mg/g, representing the maximum amount that can be adsorbed to form a monolayer on the surface [28].

The Temkin model recorded R^2=0.946, indicating interactions between the surface and the adsorbate [29], and the value of b_T=23.75 J/mol indicates that the heat of adsorption gradually decreases with increasing surface coverage [30].

Table IV.3. Langmuir, Freundlich, and Temkin isotherm models for CV adsorption GS at 45 °C.

Adsorption isotherm	Parameter	Value
Langmuir	q_{max} (mg/g)	8.43
	K_L (L/mg)	0.01
	R^2	0.9268
Freundlich	K_f (mg/g) $(L/mg)^{1/n}$	0.23
	n	1.47
	R^2	0.9932
Temkin	K_T (L/mg)	2.12
	b_T (J/mol)	23.75
	R^2	0.9461

Overall, the results confirm that the Freundlich model [27] is the most suitable for describing the adsorption process in this study, which is consistent with interpretations from modern isotherm models [30, 31]

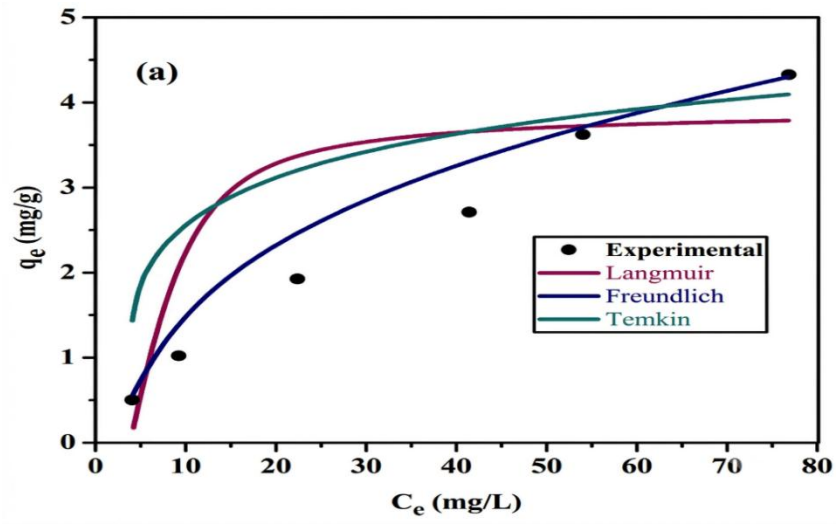

Figure IV. 10. Adsorption isotherms of CV by GS (dosage 2 g, pH of solution 10, temperature 45°C, agitation speed = 100 strokes/min, and volume of solution =100 mL).

The adsorption capacity of CV dye by GS was compared with other various chitosan composite materials as given in **Table IV.4** From, it can be deduced that the GS was a potential and effective bioadsorbent for removal of CV dye from aqueous environment.

Table IV.4 Comparison of the adsorption capacity of GS towards CV with several adsorbents.

Adsorbents	q_{max} **(mg/g)**	**References**
Waste gypsum	8.43	Present work
Peanut Husk	20.95	[32]
Phosphogypsum	63	[33]
Naturel Polysaccharide	32	[34]
Carbon from Onion Waste (non-activated)	8.7	[35]
Neem Sawdust	4.44	[36]

IV.7 Thermodynamics of adsorption

Adsorption thermodynamic parameters are executed to study the adsorption process of CV dye onto the GS surface in terms of feasibility and spontaneity, in addition to estimate the degree of randomness at the interface of CV dye with GS surface. Adsorption thermodynamic

parameters including Gibbs free energy change (ΔG°), entropy change (ΔS°), and enthalpy change (ΔH°) to understand the nature of the adsorption process, its spontaneity, and the effect of temperature. The values of thermodynamic parameters (ΔH° and ΔS°) were calculated from plotting ln k_d against 1/T **Figure.IV.11** , where the slope and intercept represent ΔH° and ΔS°, respectively.

According to obtained results in **Table IV.5** The results showed that the values of ΔG° were negative at all temperatures, ranging between (–7.20 kJ/mol and –11.02 kJ/mol), indicating that the adsorption process is spontaneous and thermodynamically favorable [37].It was also observed that the values became more negative as the temperature increased (from 303.15 K to 333.15 K), indicating an improvement in adsorption efficiency with increasing temperature and increased affinity of the adsorbate towards the adsorbent surface [31].

Furthermore, the positive value of enthalpy ΔH°=33.43 kJ/mol confirms that the adsorption process is endothermic, i.e., increasing the temperature contributes to increasing the adsorption rate and improving the surface interaction with the adsorbed molecules [37].

The positive value of entropy ΔS° = 0.134 kJ/mol.K indicates an increase in randomness at the solid solution interface during the adsorption process, reflecting a good affinity between the surface and the adsorbate [31].

In addition, the increase in ln K_d values (from 2.857 to 3.981) with increasing temperature confirms the increased stability and effectiveness of the adsorption process, which is consistent with the typical behavior of endothermic adsorption processes [38]. Overall, it can be concluded that the adsorption process was spontaneous and endothermic, and was accompanied by an increase in randomness at the interface, indicating improved interaction between the adsorbate and the adsorbent surface with increasing temperature [31].

Table IV.5. Thermodynamic parameters for the adsorption of CV dye by GS

T(k)	Ln K_d	ΔG^o (kJ/mol)	ΔH^o (kJ/mol)	ΔS^o (kJ/mol K)
303,15	2.857	-7.20	33.43	0.134
313.15	3.265	-8.50		
318.15	3.949	-10.60		
333.15	3.981	-11.02		

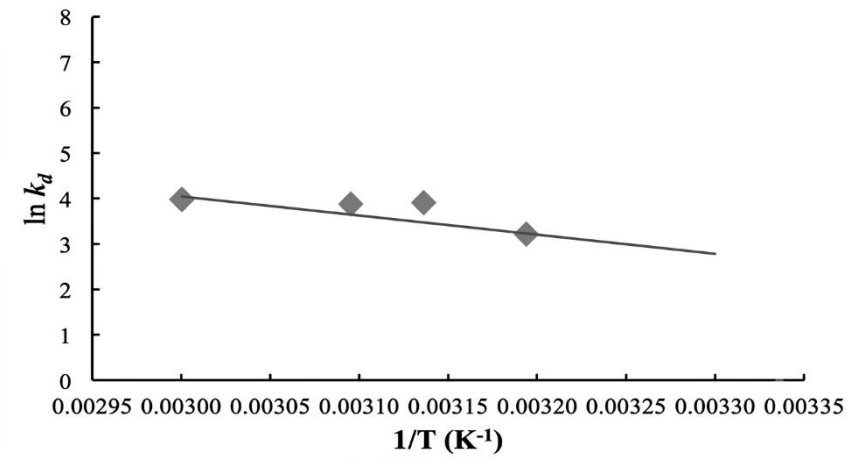

Figure.IV.11. Van't Hoff plot for CV adsorption onto GS (dosage 2 g, pH of solution 10, temperature 45°C, agitation speed = 100 strokes/min, and volume of solution =100 mL).

IV.8 Adsorption mechanisms

Adsorption mechanism of CV dye on GS surface by different types of interactions is shown in **Figure IV.12**. The adsorption capacity of solid materials is controlled by surface properties, in addition to their pore size and surface area. The surface water molecules (H_2O) and sulfate (SO_4^{2-}) groups on the surface of gypsum are possible adsorption sites [39].

Kinetic, isotherm, and pH studies indicate that CV adsorption onto gypsum involves both physical and chemical interactions. The pH_{pzc} of GS is 6.8; above this pH, the surface becomes negatively charged, while below it, the surface is positively charged. At alkaline pH (10), CV exists as positive cations (CV^+), leading to strong electrostatic attraction between CV^+ and negatively charged surface sites (such as SO_4^{2-} or $[Ca–O]^-$), which enhances removal efficiency [40].The PSO model confirms chemical interactions between dye molecules and active centers (oxygen, –OH), while hydrogen bonds and van der Waals forces further stabilize adsorption [40]. Freundlich model confirms a heterogeneous surface with multienergy sites, allowing multilayered adsorption and pore diffusion, increasing capacity over time [41]. Furthermore, hydrogen bonds are created between the N atoms of the CV dye and the H atoms of water molecules (H_2O) present on the surface of GS [42]. An n–π interaction can also occur by delocalizing the lone pair electrons of O atoms into the π orbital of the dye rings. Thus, GS and CV dye may interact via n–π interaction, hydrogen bonding, and electrostatic attraction, which would efficiently reinforce the uptake process. Collectively, these interactions enhance the adsorption efficiency of CV dye onto the GS surface, making it an effective material for the removal of cationic dyes from aqueous solutions [43].

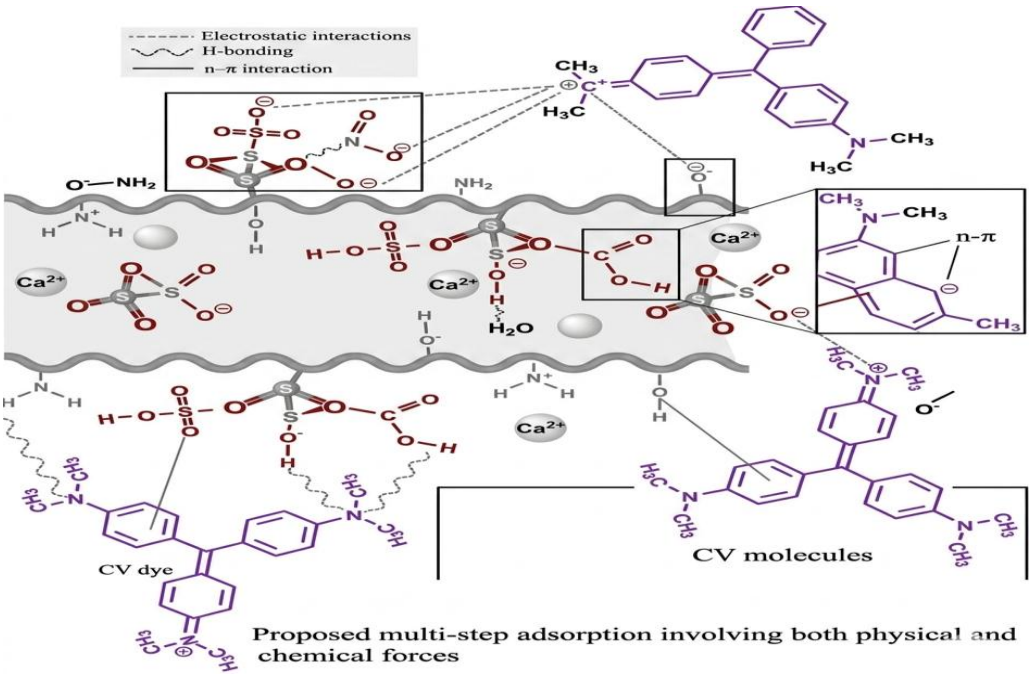

Figure IV.12. Proposed adsorption mechanism of CV dye onto the GS surface

IV.9 Regeneration studies of the adsorbent

The regenerability and reusability of the adsorbent are fundamental pillars in assessing the economic feasibility and environmental sustainability of any treatment process, as they help reduce operational costs and generated waste [44].

In this study, the possibility of recovering GS after adsorption of CV dye was evaluated by performing two consecutive cycles of adsorption and regeneration under optimal conditions (mass 2 g, concentration 25 ppm, pH = 10, temperature 45 °C).

Regeneration was carried out using a 1 M hydrochloric acid solution, which acts as a desorbing agent to break the bonds between the dye and the active surface of the gypsum, followed by a thorough washing with distilled water until neutrality (pH ≈ 7) was reached, a necessary procedure to ensure that the subsequent adsorption process is not affected by changes in surface acidity [41].

The results showed in **Figure IV.13** a slight decrease in removal efficiency from 95.30% in the first cycle to 88.87% in the second cycle. This decline is attributed to three main factors:

- Partial pore clogging: dye molecules trapped inside micropores that were not reached by the washing process [45].
- Inactivation of active sites: possible permanent saturation of some high-energy active sites.

- Surface alteration: possible slight chemical erosion or modification of the surface structure due to repeated acid treatment.

Despite this decline, the results are very promising; the retention of a removal efficiency exceeding 88% indicates that GS surface is not only a low-cost adsorbent, but also a material with good ” regenerative flexibility ”, strengthening its position as an

environmentally friendly and sustainable option for treating water polluted with industrial dyes.

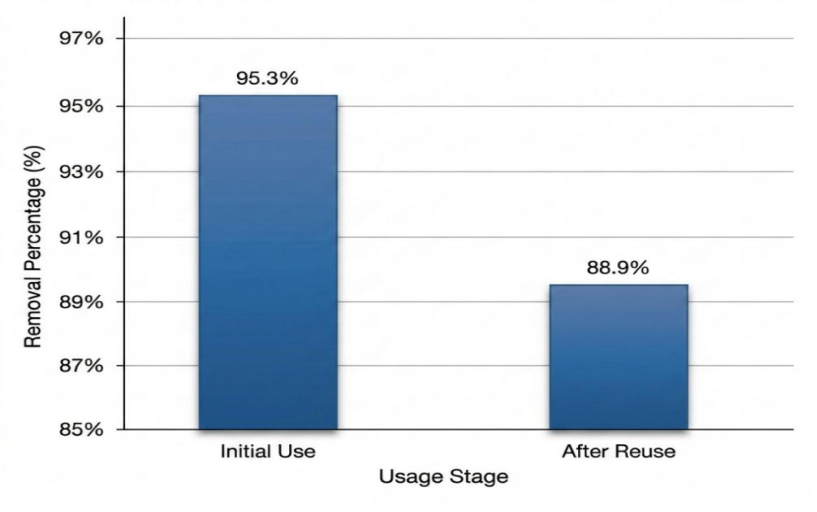

Figure IV.13. Removal Efficiency of the Dye During Reuse Cycles

Bibliography

[1] H. P. Klug and L. E. Alexander, X-raydiffraction procedures: for polycrystalline and amorphous materials, 1974.

[2] F. JCPDS, "Joint committee on powderdiffraction standards," International Centre for Diffraction Data,Philadelph ia, 1977.

[3] W. A. Deer, R. A. Howie, and J. Zussman,"Rock-forming Minerals: Feldspars, Vol ume 4A," 1978.

[4] J. Coates, "Interpretation ofinfrared spectra, a practical approach," Encyclopedia of analyticalchemistry, vol. 12, pp. 10815-10837, 2000.

[5] B. H. Stuart, Infrared spectroscopy:fundamentals and applications: J ohn Wiley & Sons, 2004.

[6] R. M. Silverstein and G. C. Bassler,"Spectrometric identification of organic compounds," Journal ofChemical Educat ion, vol. 39, p. 546, 1962.

[7] G. Socrates, Infrared and Ramancharacteristic group frequencies: tables and charts: John Wiley & Sons,2004.

[8] D. L. Pavia, G. M. Lampman, G. S. Kriz,and J. R. Vyvyan, "Introduction to spectro scopy," Belmont, USA, vol.13, 2001.

[9] X. Wang, Y. Zhang, R. Shan, and H. Hu,"Polydopamine interface encapsulating graphene and immobilizingultra-small, active Fe3O4 nanoparticles for organic dye adsorption,"Ceramics Intern ational, vol. 47, pp. 3219-3231, 2021.

[10] M. J. Hassan, M. F. Islam, N. Akter, M. N.Uddin, A. Y. Abir, S. B. Aoun, et al., "Applicability of gypsum inselective removal of anionic dye molecules from aqueous medium," App liedWater Science, vol. 11, p. 7, 2021.

[11] V. Danielik, P. Fellner, M. Králik, B.Baďurová, J. Gabčová, J. Jurišová, et al., "Relation between thereactivity and surface area of gypsum," Journal of Molecu lar Liquids, vol.283, pp. 763-771, 2019.

[12] M. Kosmulski, Surface charging and pointsof zero charge: CRC press, 2009.

[13] D. M. Ruthven, Principles of adsorption and adsorption processes: John Wiley & Sons, 1984.

[14] D. C. Montgomery, Design and Analysis of Experiments. John Wiley & Sons, 2017.

[15] R. H. Myers and D. C. Montgomery, Response Surface Methodology. Taylor & Francis, 1996.

[16] İ. Bayram and A. Günay, "Optimization of a Reaction Distillation Column by Design Expert Method and Statistical Analysis of the Process," Journal of the Turkish Chemical Society Section B: Chemical Engineering, vol. 8, pp. 111–122, 2025.

[17] V. K. Gupta, "Application of Low-Cost Adsorbents for Dye Removal: A Review," Journal of Environmental Management, vol. 90, pp. 2313–2342, 2009.

[18] Y.-S. Ho and G. McKay, "Pseudo-Second-Order Model for Sorption Processes," Process Biochemistry, vol. 34, pp. 451–465, 1999.

[19] O. Hamdaoui, "Batch Study of Liquid-Phase Adsorption of Methylene Blue Using Cedar Sawdust and Crushed Brick," Journal of Hazardous Materials, vol. 135, pp. 264–273, 2006.

[20] Y.-S. Ho and G. McKay, "The Kinetics of Sorption of Basic Dyes from Aqueous Solution by Sphagnum Moss Peat," The Canadian Journal of Chemical Engineering, vol. 76, pp. 822–827, 1998.

[21] M. N. Rashed, "Adsorption Technique for the Removal of Organic Pollutants from Water and Wastewater," in Organic Pollutants—Monitoring, Risk and Treatment. IntechOpen, 2013.

[22] B. Hameed, A. Ahmad, and N. Aziz, "Isotherms, Kinetics and Thermodynamics of Acid Dye Adsorption on Activated Palm Ash," Chemical Engineering Journal, vol. 133, pp. 195–203, 2007.

[23] S. Patil, V. Deshmukh, S. Renukdas, and N. Patel, "Kinetics of Adsorption of Crystal Violet from Aqueous Solutions Using Different Natural Materials," International Journal of Environmental Sciences, vol. 1, p. 1116, 2011.

[24] E. D. Revellame, D. L. Fortela, W. Sharp, R. Hernandez, and M. E. Zappi, "Adsorption Kinetic Modeling Using Pseudo-First-Order and Pseudo-Second-Order Rate Laws: A Review," Cleaner Engineering and Technology, vol. 1, p. 100032, 2020.

[25] S. Lagergren, "Zur Theorie der Sogenannten Adsorption Gelöster Stoffe," 1898.

[26] W. Plazinski, W. Rudzinski, and A. Plazinska, "Theoretical Models of Sorption Kinetics Including a Surface Reaction Mechanism: A Review," Advances in Colloid and Interface Science, vol. 152, pp. 2–13, 2009.

[27] D. Chattoraj and H. Freundlich, "On the Adsorption in Solution," Journal of Physical Chemistry A, vol. 57, pp. 385–470, 1906.

[28] I. Langmuir, "The Adsorption of Gases on Plane Surfaces of Glass, Mica and Platinum," Journal of the American Chemical Society, vol. 40, pp. 1361–1403, 1918.

[29] M. Temkin, "Kinetics of Ammonia Synthesis on Promoted Iron Catalysts," Acta Physiochimica URSS, vol. 12, pp. 327–356, 1940.

[30] K. Y. Foo and B. H. Hameed, "Insights into the Modeling of Adsorption Isotherm Systems," Chemical Engineering Journal, vol. 156, pp. 2–10, 2010.

[31] N. Ayawei, A. N. Ebelegi, and D. Wankasi, "Modelling and Interpretation of Adsorption Isotherms," Journal of Chemistry, vol. 2017, p. 3039817, 2017.

[32] S. Abbas, T. Javeed, S. Zafar, M. B. Taj, A. R. Ashraf, and M. I. Din, "Adsorption of Crystal Violet Dye by Using a Low-Cost Adsorbent–Peanut Husk," Desalination and Water Treatment, vol. 233, pp. 387–398, 2021.

[33] A. M. Alotaibi, A. A. Aljabbab, M. S. Alajmi, A. N. Qadrouh, M. Farahat, M. A. Abdel Khalek, et al., "Utilization of Phosphogypsum as Sustainable Adsorbent for Removal of Crystal Violet Dye from Wastewater: Kinetics, Thermodynamics, and Applications in Textile Effluent Treatment," Sustainability, vol. 17, p. 3320, 2025.

[34] M. Sadoq, H. Atlas, S. Imame, A. Kali, A. Amar, I. Loulidi, et al., "Elimination of Crystal Violet from Aqueous Solution by Adsorption on Natural Polysaccharide: Kinetic, Isotherm, Thermodynamic Studies and Mechanism Analysis," Arabian Journal of Chemistry, vol. 17, p. 105453, 2024.

[35] F. Bibi, A. Sattar, S. Hussain, and M. Waseem, "Tailoring the Sorption Properties of Crystal Violet by Activated Carbon Extracted from Waste Onion," Chemical Papers, vol. 77, pp. 3957–3966, 2023.

[36] S. Khattri and M. Singh, "Colour Removal from Synthetic Dye Wastewater Using a Bioadsorbent," Water, Air, and Soil Pollution, vol. 120, pp. 283–294, 2000.

[37] H. N. Tran, S.-J. You, and H.-P. Chao, "Thermodynamic Parameters of Cadmium Adsorption onto Orange Peel Calculated from Various Methods: A Comparison Study," Journal of Environmental Chemical Engineering, vol. 4, pp. 2671-2682, 2016.

[38] Y. Liu, "Is the Free Energy Change of Adsorption Correctly Calculated?," Journal of Chemical & Engineering Data, vol. 54, pp. 1981-1985, 2009.

[39] G. Yiyen, K. V. Duck, and R. A. Walker, "Surfactant Adsorption to Gypsum Surfaces and the Effects on Solubility in Aqueous Solutions," Langmuir, vol. 38, pp. 2804-2810, 2022.

[40] L. Luo, T. Liu, J. He, J. Ma, and H.-Q. Yu, "Interface Gypsum Deposition in Flow-Electrode CDI Treating Brackish Water: Impacts and Mechanisms," Water Research, vol. 272, p. 122920, 2025.

[41] M. T. Yagub, T. K. Sen, S. Afroze, and H. M. Ang, "Dye and Its Removal from Aqueous Solution by Adsorption: A Review," Advances in Colloid and Interface Science, vol. 209, pp. 172-184, 2014.

[42] D. Silva, N. Lima, J. Soares, S. Jesus, B. Teti, R. Manta, et al., "Thermodynamic Characteristics of Hydrogen Bonding Formation in Gypsum-Based Materials and Its Effects on Mechanical Performance," Construction and Building Materials, vol. 470, p. 140666, 2025.

[43] N. N. Abd Malek, A. H. Jawad, A. S. Abdulhameed, K. Ismail, and B. Hameed, "New Magnetic Schiff's Base-Chitosan-Glyoxal/Fly Ash/Fe3O4 Biocomposite for the Removal of Anionic Azo Dye: An Optimized Process," International Journal of Biological Macromolecules, vol. 146, pp. 530-539, 2020.

[44] D. A. Gkika and G. Z. Kyzas, "Reusability of Spent Adsorbents for a Circular Materials Economy in the Sustainable Chemical Industry," RSC Sustainability, vol. 4, pp. 1023-1048, 2026.

[45] H. N. T. Hai Nguyen Tran, Y. S. YouShengJie, A. Hosseini-Bandegharaei, and C. H. Chao HuanPing, "Mistakes and Inconsistencies Regarding Adsorption of Contaminants from Aqueous Solutions: A Critical Review," 2017.

General Conclusion

Conclusion General:

Synthetic dyes represent one of the major sources of water pollution, which necessitates the search for effective and environmentally friendly natural adsorbents for the treatment of such contaminants. In this context, the present study aimed to evaluate the applicability of waste gypsum (GS) as a low-cost and eco-friendly adsorbent for the removal of CV dye from aqueous solutions.

The physicochemical characterization results obtained using XRD, FTIR, and SEM–EDX revealed that natural gypsum possesses suitable structural and surface properties for the adsorption process. The analyses also confirmed the attachment of dye molecules onto the GS surface and the occurrence of interactions responsible for the removal process.

The optimum conditions for CV reduction obtained by BBD-RSM were recorded at adsorbent dosage of 2 g, pH 10, a temperature of 45 °C, and a contact time of 25 min. The results indicate that the highest CV dye decolourization (99.5 %) was noticed by significant interaction effect between AB (adsorbent dose x pH) and AD (adsorbent dose x time).

The results of kinetics and isotherms models indicate that the adsorption was affected by chemisorption and heterogeneous mode of adsorption. The qmax of GS surface for CV dye was 8.31 mg/g at 45 °C.

Furthermore, thermodynamic analysis showed that the adsorption process is spontaneous and endothermic, with adsorption efficiency increasing as temperature rises. The regeneration and reuse experiments demonstrated that natural gypsum maintained a high removal efficiency of 88.87%. Based on the obtained results, it can be concluded that natural gypsum is a promising and efficient adsorbent for the removal of Crystal Violet dye from aqueous solutions due to its natural availability, low cost, high removal efficiency, and reusability. These findings suggest that natural gypsum could be successfully applied in the treatment of dye-contaminated wastewater, making it a sustainable and attractive material for future environmental applications.

Future Recommendations

Based on the findings of the present study, the following recommendations are proposed:

- Investigate the modification of natural gypsum through physical or chemical treatments in order to enhance its adsorption properties and increase the number of active sites on its surface.
- Evaluate the effectiveness of waste gypsum for the removal of other types of pollutants, including anionic dyes, heavy metals, and emerging organic contaminants.

- Assess the performance of waste gypsum in continuous systems to simulate real industrial wastewater treatment conditions and evaluate its large-scale applicability.
- Improve regeneration and reuse procedures and examine a greater number of regeneration cycles to evaluate the longterm stability and efficiency of the adsorbent.
- Develop composite adsorbent materials based on waste gypsum by combining it with other natural or nanostructured materials to enhance adsorption capacity and removal efficiency.
- Conduct more in-depth investigations of the adsorption mechanism using advanced characterization techniques in order to better understand the interactions responsible for pollutant retention on the gypsum surface.
- Encourage the application of statistical experimental design approaches, such as BBD-RSM, due to their effectiveness in determining optimum operating conditions while reducing experimental time, effort, and cost.
- Promote the utilization of locally available and low-cost natural materials for wastewater treatment, thereby contributing to the development of sustainable and economically viable environmental solutions.


تم بحمد الله